1992

# Development length of fiber-composite concrete reinforcement

Kent E. Fish
*Iowa State University*

# Development length of fiber-composite concrete reinforcement

by

Kent E. Fish

A Thesis Submitted to the

Graduate Faculty in Partial Fulfillment of the

Requirements for the Degree of

MASTER OF SCIENCE

Department: Civil and Construction Engineering
Major: Civil Engineeering (Structural Engineering)



Iowa State University
Ames, Iowa

1992

## TABLE OF CONTENTS

## LIST OF FIGURES

## LIST OF TABLES

## ACKNOWLEDGEMENTS

At this time I would like to acknowledge those who have helped and encouraged me as I worked towards my master's degree. I would especially like to thank my parents, Darwin and Joan Fish, for all of their patience, love, and encouragement. They made my degree possible. Thanks must also be made to my fiancee, Tammy Behm, for putting up with me being gone for the past year and a half. Special thanks must be made to Dr. Porter for his guidance and help throughout my graduate education. I would also like to thank the other members of my committee, Dr. Klaiber and Dr. Zachary.

I would also like to thank Bruce Barnes, assistant project supervisor, for his help with computer work and proof reading of my reports. Thanks should also be made to Doug Wood, lab supervisor, who helped lab operations to run smoothly. In addition to Doug, I would like to thank all of the hourly employees for their time and efforts. Thanks should be made to Brad Lehr, my roommate and fellow graduate student, for his help and advice when I had problems with my research. Also thanks must be made to the Center for Applied Technology and Development (Richard F. Gaertner, Director) for sponsoring this research project. The project was directed under Max L. Porter, P.E., as principal

investigator. Appreciation is given to Composite Technologies Corporation, Sika Corporation, and Florida Wire and Cable for their material sample contributions.

Without all of these people, my degree program would have been impossible. Thank you one and all.

# 1 INTRODUCTION

## 1.1 Background

For many years mild steel and the more expensive epoxy-coated steel have been used as the principal reinforcement in reinforced concrete structures. Steel was a very good material because of its high strength and modulus of elasticity. Steel does, however, rust and corrode which causes millions of dollars of damage to reinforced concrete structures.

Because of the corrosion problems associated with steel reinforcement, a new material has been developed which is more resistant to corrosion than steel. This material is made of fibers and resins which form a fiber-composite rod (FCR). The shape of FCR was very different from that of deformed bars. The profile was more like a prestressing strand or a plain steel bar without deformation. FCR is more resistant to corrosion than steel but has a lower modulus of elasticity and requires a longer development length for similar bar configurations.

Steel has the ability to be molded and deformed which allows it to be made with deformations throughout the bar. These deformations are then used to produce a mechanical bond between the steel and the concrete which reduces the development length of the reinforcement. Fiber-composite

materials are usually harder to deform and thus FCR would usually possess less mechanical anchorage than steel, unless other mechanical means or shapes are used to provide necessary interlock with the concrete. A lower mechanical anchorage increases the embedment length required to fully develop the reinforcement. The FCR for this investigation utilized a spiral configurative shape for providing a means of mechanical interlock in concrete structures. A more detailed description of the rod can be found in Section 2.0.

## 1.2 Objective

The objective of this research project was to: (1) determine the feasibility of FCR as reinforcement for concrete structures, (2) formulate an expression for the development length of both three-eighths-inch and one-half-inch diameter fiber-composite reinforcement rods, and (3) develop the test procedure and test apparatus for FCR-reinforced concrete.

The development length expressions were analyzed and compared with experimental data. Other engineering properties such as tensile strength and modulus of elasticity were also determined.

## 1.3 Scope

To study the reinforced concrete flexural behavior and the effect of various parameters on the bond values of the FCR, a beam specimen and test procedure have been developed which represent a considerable departure from conventional testing procedures [21]. A new method of beam loading was designed to eliminate the restraint at loading points thus reducing confinement of the reinforcing rod. This test method was developed at Iowa State University and will be discussed further in Section 3.1 of this report.

Tensile strength of FCR was determined in three ways: theoretically, directly, and flexurally. Theoretical tensile strength was determined by comparing the composition of the rod with the tensile strength of each of the components. Direct tensile strength was determined by simply placing the rods in direct tension then loading the bar to failure. Flexural tensile strength was determined by using the ultimate load applied to a cantilever section to calculate the tensile capacity under flexural loads.

The modulus of elasticity of the FCR was also determined. These modulus values were determined simultaneously with the direct tensile strength tests.

A total of 127 beams were tested. Six of the beams were simply supported beams. The rest of the beams were cast in

the ISU beam configuration. The ISU beam is described in Section 3.1 of this report.

## 1.4 Parameters

Embedment lengths between twenty and forty-eight inches were tested. Beams were cast with concrete strengths between 3000 pounds-per-square inch (psi) and 7000 psi. The concrete strengths were selected to encompass most of the concrete in use at the present time. However, additional testing should be performed to check the bond characteristics of the reinforcement in high strength concrete.

Cover varied depending on the diameter of the rods. The distance between the edge of the concrete and the center of the bar was one-and-one-half inches.

The majority of the beams were cast with three-eighths and one-half-inch FCR reinforcement. Two of the beams however, were cast with three-eighths-inch steel reinforcement (rebar) and five were cast with five-eighths-inch epoxy-coated and non-epoxy-coated prestressing strands. Also, two of the epoxy-coated prestressing strands had a sand coating.

## 1.5 Literature Review

An extensive literature review was performed on bond strength and development length calculations. There is a large amount of material available on bond but there is little or no material that deals with the relationship between bond and fiber-composite materials. For this reason material was reviewed that dealt with deformed bars, plain steel bars, and prestressing strands. The theory behind the development length of these materials was then modified to work with the FCR. Some of the material will be discussed briefly in this section of the report. A more detailed discussion can be found elsewhere in the report.

The shape of FCR was very different from that of deformed bars. The profile was more like a prestressing strand or a plain steel bar without deformations. Literature which dealt with bond in prestressing strands or plain steel bars was found in References 3, 14, 15, and 16. The material in these references was used to determine the nature of bond in beams cast with FCR.

Bond strength consists of three components; adhesion, friction, and mechanical anchorage. These three components of bond are discussed further in Section 4.2 of this report. Descriptions of each of the three components can be found in References 3, 7, 12, 13, 14, 15, and 16.

Bond stress distribution throughout the length of the bar has been documented in most of the articles that were reviewed. The most applicable literature on bond stress distribution in deformed bars, plain bars and prestressing strands can be found in References 1, 3, 7, 9, 10, and 19.

Many different methods of researching bond stress have been explored in the past. The procedure most often used was the pullout specimen. Literature on pullout testing can be found in References 1, 3, 9, 10, and 13. Pullout specimens do not provide an accurate means of determining bond stress because the reinforcement is not being developed in a region of shear or moment. Also, the reaction point in pullout specimens causes confinement of the reinforcement and also reduces splitting of the concrete surrounding the bar.

Test specimens which were used to test bond stress in areas of shear and moment were developed because of the problems associated with the pullout tests. One test method, which was developed by Ferguson and Thompson [6], incorporated the use of a cantilever beam. This test method is discussed further in Section 3 of this report. Information on the cantilever beam tests can be found in References 3 and 6. While the cantilever beam provided bond stress data in a region of shear and moment, it did not eliminate the confinement problem associated with applying loads near the reinforcement.

A test method was developed by Mathey and Watstein [4] which incorporated concrete outcroppings on the sides of the beam. The reaction points on the simply supported span could then be moved away from the reinforcement thus reducing the confinement problem. This test procedure is discussed further in Section 3 of this report. Information on this test configuration can be found in References 3, 4, and 5.

The Mathey and Watstein beam and the Ferguson and Thompson beam were combined to make the ISU beam. The ISU beam incorporates both the cantilever section and the concrete outcroppings to form an efficient tool for measuring bond and development length. A more detailed discussion of the ISU beam configuration can be found in Section 3.1 of this report.

The derivation of the bond stress and development length equations for FCR was similar to the derivations for deformed bars and prestressing strands. Literature on the derivation of the bond stress and development length equations can be found in References 1, 9, 11, 14, and 15. A history of bond stress and development length can be found in Reference 1.

Bond stress and development length vary based on many factors. The type and strength of the concrete are important parameters. In general, as concrete strength increases, the bond strength will increase. Literature on these properties can be found in References 9, 14, 15, and 16. The condition

of the surface of the bar is also an important factor. References 15 and 27 discuss the change in bond stress based on the surface condition of the rods. The amount of curing time was found to effect mechanical bond strength much more than frictional or adhesive bond strength. Literature on the effect of curing time on bond strength can be found in Reference 13. Normal pressure confines the reinforcement and reduces splitting. Literature on normal pressure and confinement can be found in References 12 and 20.

As tensile stress in a rod increases, radial contraction takes place, and as the diameter of the rod gets smaller, the bond stress declines because the smaller diameter reduces the frictional bond strength. Literature on radial contraction can be found in References 15 and 16. Also, this subject is discussed in more detail in Section 4.2 of this report.

Little information can be found that deals with bond strength of fiber-composite reinforcement. Researchers at Iowa State University however, have performed testing on bond strength of ties for sandwich wall construction as well as other fiber-composite products. Literature on these topics can be found in References 21, 24, and 25.

# 2 Materials

The material used in this study was three-eighths-inch and one-half-inch diameter rods produced by Composite Technologies Corporation (CTC) of Ames, Iowa.

The rod was made in two stages. The first stage involved the pultruding of strands which were made of E-glass fibers and a vinyl-ester resin [23]. The second stage required winding seven strands into a spiral and connecting them with an epoxy. The final product looked similar to a prestressing strand as shown in Figure 1.1.

Two different types of FCR were made based on the type of resin used. Thermoset FCRs were made with a vinyl-ester resin. Once the resin had cured with the thermoset FCR, the rod could no longer be deformed. Most of the beams that were tested were reinforced with thermoset FCR.

Thermoplastic FCRs were made with a polycarbonate resin. When the resin cured with the thermoplastic FCR, the rod could be deformed by applying heat. The ability to be deformed was a significant improvement in the FCR but unfortunately, the polycarbonate resin allowed the rod to contract radially which allowed the rod to be pulled out of the concrete. Six thermoplastic rods were tested and none of the rods could be failed in the concrete because the rods pulled out. For this reason, testing was discontinued for

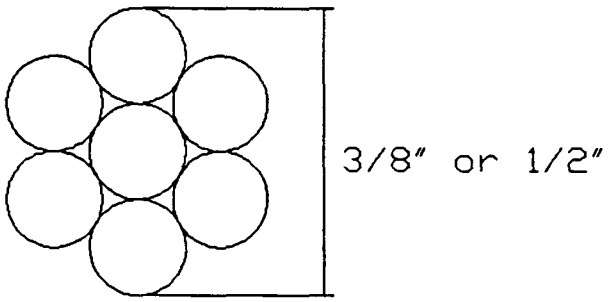


Figure 1.1. Cross-section of a FCR

the thermoplastic FCR. The longest embedment tested with thermoplastic FCR was thirty-eight inches.

The cross-sectional area, rod circumference, modulus of elasticity, tensile strength, and rod composition were determined and will be presented in this section. Tensile strength was calculated both theoretically and experimentally.

## 2.1 Areas and Rod Composition

The cross-sectional area of the rods was determined by immersing short pieces of the rod in water and measuring the volume displaced. This number was then divided by the length of the specimen. The area of the individual strands was also found in this manner. Using the values found in these tests, and the known properties and mixture proportions, the

composition of the rods were found. A listing of the test data is shown in Table 2.1.

The same procedure was used for the three-eighths-inch rod specimens. Two different size rods were used for the three-eighths-inch specimens. The tooling at the manufacturer was changed during through the test series thus producing a variation in the rod cross-section. Calculation of properties based on three-eighths-inch FCR utilized the latest rod dimensions because material was unavailable for the determination of the individual strand sizes for the first set of rods. The areas are shown in Tables 2.2 and 2.3.

The areas of the individual strands were calculated in the same manner. The areas of the strand specimens are shown in Tables 2.4 and 2.5.

Rod composition was then determined by calculating the percentages of each component relative to the entire rod. The composition of the individual strands was known to be 76% fibers and 24% resin. This information was supplied by CTC. Therefore the percentages of each could be found with respect to the rod as a whole. These calculations are shown in Tables 2.6 and 2.7.

Table 2.1. Areas of one-half-inch test specimens

| Sample 1/2 in. | Length (in) | Weight Disp (lb) | Volume Disp ($in^3$) | Area ($in^2$) |
|---|---|---|---|---|
| 1 | 3.98 | 0.0268 | 0.61 | 0.15 |
| 2 | 3.98 | 0.0226 | 0.52 | 0.13 |
| 3 | 3.99 | 0.0231 | 0.53 | 0.13 |
| 4 | 3.99 | 0.0214 | 0.49 | 0.12 |
| 5 | 3.00 | 0.0227 | 0.52 | 0.17 |
| 6 | 3.99 | 0.0247 | 0.56 | 0.14 |
| 7 | 3.98 | 0.0241 | 0.55 | 0.14 |
| 8 | 4.00 | 0.0255 | 0.58 | 0.15 |
| 9 | 3.97 | 0.0245 | 0.56 | 0.14 |
| 10 | 4.00 | 0.0247 | 0.56 | 0.14 |

Average Area = 0.14 $in^2$

Table 2.2. Areas of three-eighths-inch FCR specimens

| Sample 3/8 in. | Length (in) | Weight Disp (lb) | Volume Disp ($in^3$) | Area ($in^2$) |
|---|---|---|---|---|
| 1 | 3.99 | 0.0163 | 0.37 | 0.09 |
| 2 | 3.99 | 0.0162 | 0.37 | 0.09 |
| 3 | 3.99 | 0.0167 | 0.38 | 0.10 |
| 4 | 3.99 | 0.0146 | 0.33 | 0.08 |
| 5 | 3.98 | 0.0148 | 0.34 | 0.08 |

Average Area = 0.09 $in^2$

Table 2.3. Areas of three-eighths-inch FCR specimens

| Sample 3/8 in. | Length (in) | Weight Disp (lb) | Volume Disp ($in^3$) | Area ($in^2$) |
|---|---|---|---|---|
| 1 | 3.99 | 0.0211 | 0.48 | 0.12 |
| 2 | 4.00 | 0.0202 | 0.46 | 0.12 |
| 3 | 3.99 | 0.0225 | 0.51 | 0.13 |
| 4 | 4.00 | 0.0229 | 0.52 | 0.13 |
| 5 | 4.00 | 0.0216 | 0.49 | 0.12 |

Average Area = 0.12 $in^2$

Table 2.4. Areas of the individual strands for one-half-inch FCR

| Sample 1/2 in. | Length (in) | Weight Disp (lb) | Volume Disp ($in^3$) | Area ($in^2$) |
|---|---|---|---|---|
| 1 | 4.08 | 0.0031 | 0.071 | 0.017 |
| 2 | 4.07 | 0.0035 | 0.080 | 0.020 |
| 3 | 4.01 | 0.0032 | 0.073 | 0.019 |
| 4 | 4.18 | 0.0031 | 0.070 | 0.017 |
| 5 | 3.95 | 0.0030 | 0.067 | 0.017 |
| 6 | 4.15 | 0.0030 | 0.069 | 0.017 |
| 7 | 3.98 | 0.0034 | 0.077 | 0.019 |
| 8 | 4.11 | 0.0033 | 0.075 | 0.018 |
| 9 | 4.11 | 0.0035 | 0.081 | 0.020 |
| 10 | 4.07 | 0.0033 | 0.075 | 0.019 |

Average Area = 0.018 $in^2$

Table 2.5. Areas of individual strands for three-eighths-inch FCR

| Sample 3/8 in. | Length (in) | Weight Disp (lb) | Volume Disp ($in^3$) | Area ($in^2$) |
|---|---|---|---|---|
| 1 | 4.21 | 0.0015 | 0.034 | 0.008 |
| 2 | 3.99 | 0.0016 | 0.037 | 0.009 |
| 3 | 4.20 | 0.0014 | 0.032 | 0.008 |
| 4 | 4.09 | 0.0017 | 0.040 | 0.010 |
| 5 | 3.89 | 0.0015 | 0.035 | 0.009 |
| 6 | 4.07 | 0.0017 | 0.040 | 0.010 |
| 7 | 4.07 | 0.0017 | 0.039 | 0.010 |
| 8 | 4.07 | 0.0019 | 0.043 | 0.011 |
| 9 | 4.17 | 0.0017 | 0.039 | 0.009 |
| 10 | 4.01 | 0.0018 | 0.040 | 0.010 |

Average Area = 0.0093 $in^2$

Table 2.6. Calculations of composition for one-half-inch FCR

| | |
|---|---|
| Average Area of Rods ($A_r$) | 0.14 $in^2$ |
| Average Area of Strands ($A_s$) | 0.018 $in^2$ |
| Area of Fibers = ($A_s$)*0.76 | 0.014 $in^2$ |
| Area of Resin = ($A_s$)*0.24 | 0.004 $in^2$ |
| 7*($A_s$) | 0.127 $in^2$ |
| 7*Area of Fibers | 0.096 $in^2$ |
| 7*Area of Resin | 0.031 $in^2$ |
| % Fibers = 0.096/0.14*100 | 68.2% |
| % Resin = 0.031/0.14*100 | 21.5% |
| % Epoxy = 100-68.2-21.5 | 10.3% |

Table 2.7. Calculations of composition for three-eighths-inch FCR

| | |
|---|---|
| Average Area of Rods ($A_r$) | 0.12 $in^2$ |
| Average Area of Strands ($A_s$) | 0.0093 $in^2$ |
| Area of Fibers = ($A_s$)*0.76 | 0.0070 $in^2$ |
| Area of Resin = ($A_s$)*0.24 | 0.0023 $in^2$ |
| 7*($A_s$) | 0.0648 $in^2$ |
| 7*Area of Fibers | 0.0493 $in^2$ |
| 7*Area of Resin | 0.0161 $in^2$ |
| % Fibers = 0.0493/0.123*100 | 40.0% |
| % Resin = 0.0161/0.123*100 | 12.6% |
| % Epoxy = 100-40.0-12.6 | 47.4% |

## 2.2 Tensile Strength

### 2.2.1 Theoretical Tensile Strength

The theoretical tensile strength of the FCR was found by using the known tensile capacity of both the fibers and the resin and assuming that the epoxy added minimal tensile strength. The strands contained 76% glass and 24% resin, therefore the theoretical tensile capacity of the rods could be found. The glass was assumed to have a tensile capacity of 200-kips-per-square inch (ksi) and the epoxy was assumed to have a tensile capacity of 11.5 ksi [23, 25]. Seven strands were used to make one rod. The composition of the rods are shown in Table 2.8.

Table 2.8. Composition of one-half-inch FCR

| Rod Size | % Fibers | %Epoxy Rod | % Resin Strand |
|---|---|---|---|
| 3/8 Inch | 40.0 | 47.4 | 12.6 |
| 1/2 Inch | 68.2 | 10.3 | 21.5 |

Using this data the theoretical tensile strength of the rod can be found by using Equation 2.1.

$$T = T_g\left(\frac{A_g}{A_T}\right)+T_r\left(\frac{A_r}{A_T}\right) \qquad \text{Eqn. 2.1}$$

Where:

T = Theoretical tensile strength of FCR

$T_g$ = Tensile strength of glass fibers (200 ksi)

$T_r$ = Tensile strength of resin (11.5 ksi)

$A_g/A_T$ = Area of glass divided by the total area of the rod

$A_r/A_T$ = Area of resin divided by the total area of the rod

Therefore, the theoretical tensile strength of the one-half-inch FCR was determined to be 139 ksi and the

theoretical tensile strength of three-eighths-inch FCR was determined to be 81 ksi.

### 2.2.2 Direct Tensile Strength

The tensile capacity was also determined experimentally using a procedure developed at Iowa State University. The rod was placed in specially fabricated end connections which were used to protect the rod from being crushed by the wedge action grips of the hydraulic testing machine. Because glass fiber based composites possess a low capacity to loads applied normal to the fiber direction, the portion of the rod in the grip had to be protected from crushing. The following test, developed in References 21, 23, and 24, was developed to solve this problem.

The FCR was epoxied into a ten-inch section of copper pipe. The inside of the copper pipe was sandblasted to help the epoxy adhere to the copper surface. The bearing stress of the wedge action grips could then be transferred from the copper pipe to the rod without crushing the rod. The copper pipe that was used was a seven-eighths-inch outside diameter pipe and the epoxy that was used was Sikadure-33 epoxy.

Five specimens of both the three-eighths-inch and one-half-inch FCRs were tested. The results of the testing are shown in Table 2.9.

Table 2.9. Direct tensile strength

| Specimen | 3/8 in. (ksi) | 1/2 in. (ksi) |
|---|---|---|
| Test 1 | 82.5 | 140.2 |
| Test 2 | NA[a] | 96.5 |
| Test 3 | 79.8 | 102.2 |
| Test 4 | 79.9 | 132.3 |
| Test 5 | NA[a] | 128.3 |
| Average | 80.7 | 119.9 |
| Standard Dev. | 1.53 | 19.33 |

[a] Incomplete data due to epoxy failure in gripping hardware.

### 2.2.3 Flexural Tensile Strength

The tensile capacity of the rod was also determined using the flexural test data. Figure 2.1 shows a cutaway of the cantilever section of the beam.

By using statics, the sum of the forces and the sum of the moments must be equal to zero for the beam to be in equilibrium. Therefore, the internal tensile forces must be equal to the internal compressive forces. Before the concrete cracks the stress distribution will be similar to the diagram shown in Figure 2.2. After the first major crack occurs, the concrete no longer possesses any tensile capacity, therefore the FCR will carry all of the tensile forces in the post cracking region as shown in Figure 2.3.

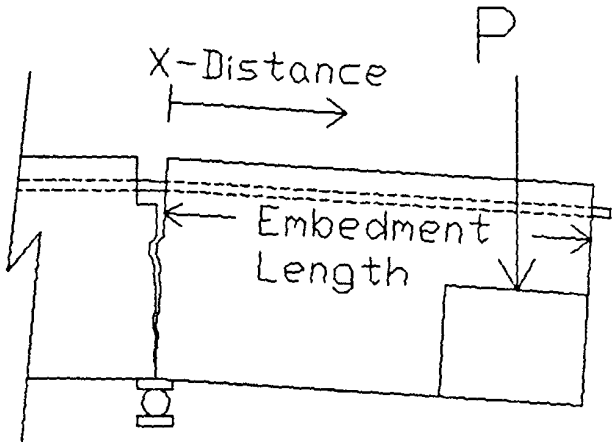


Figure 2.1. Cantilever section of the ISU Beam

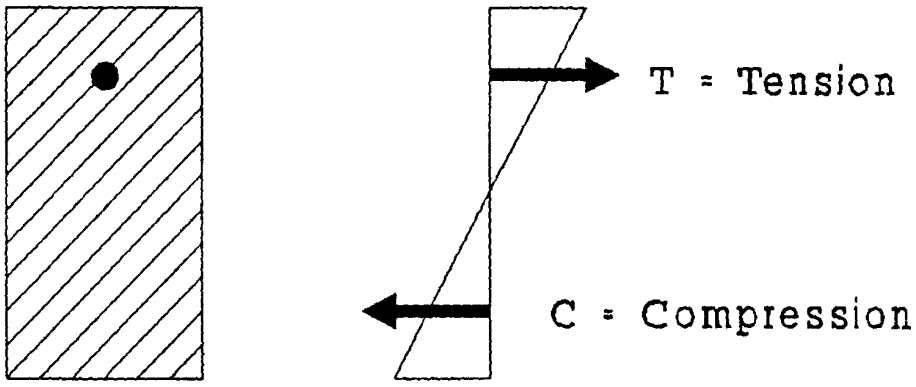


Figure 2.2. Stress distribution of an uncracked section

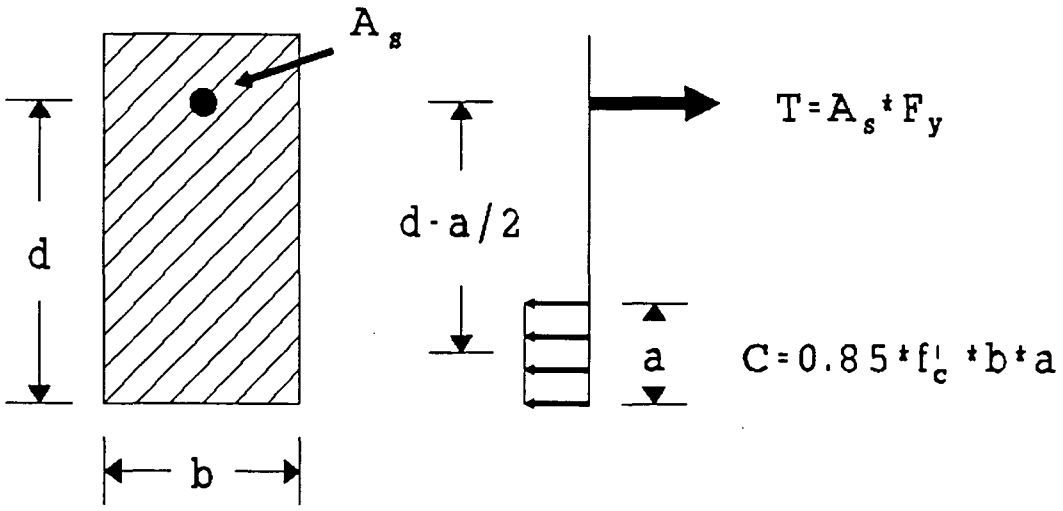


Figure 2.3. Stress distribution of a cracked section at ultimate load

The compressive force in the cracked section was assumed to be 85% of the compressive strength of the concrete multiplied by the area that is being compressed. The width of this area was six-inches and the height was approximated by using the Whitney stress block [1]. The Whitney stress block is not the most precise method for estimating the tensile stress in the rods. A more precise method would incorporate the use of an approximated compressive stress distribution [28]. An analysis using the approximated stress distribution was more difficult than the Whitney stress block method. Also, the difference in tensile strengths that were

obtained by each of the two methods proved to be minimal, therefore the Whitney stress block method was used to solve for the tensile stress in the rods.

By summing forces in the horizontal direction, Equation 2.2 is formed then solved for the variable a as shown in Equation 2.3. Next the moments are summed around the center of the stress block which yields Equation 2.4. This equation is then solved for $F_y$, which is the tensile stress in the rod.

$$A_s F_y = 0.85 f'_c b a \qquad \text{Eqn. 2.2}$$

$$a = \frac{A_s F_y}{0.85 f'_c b} \qquad \text{Eqn. 2.3}$$

$$\sum M = 0 = A_s F_y \left(d - \frac{a}{2}\right) - M_{max} \qquad \text{Eqn. 2.4}$$

$$F_y = \frac{M_{max}}{A_s \left(d - \frac{a}{2}\right)} \qquad \text{Eqn. 2.5}$$

Where:

$A_s$ = Area of the reinforcing rod

$F_y$ = Tensile strength of the rod

$f'_c$ = Compressive strength of the concrete

b = Width of the beam

a = Height of the Whitney stress block

d = Depth to centroid of reinforcement

$M_{max}$ = Moment resisted by section

The ultimate tensile stress of the rods was found for each test beam and the averages are presented in Table 2.10. The flexural tensile strength of the FCR is less than the experimental tensile strength. This reduction in strength is caused by the transverse reactive force applied to the FCR when the beam deflects. FCR was strong in tension but was considered to be weak in shear and transverse bearing and therefore the transverse bearing force applied to the rod by bearing on the concrete could reduce the tensile strength. Also, some of the reduction in strength could be attributed to the crushing of some of the fibers at the interface of the FCR with the concrete.

The theoretical tensile strength was similar to the direct tensile strength for the three-eighths-inch FCR but was somewhat higher for one-half-inch FCR. A slightly different rod composition than the actual composition could be the cause of the difference.

Table 2.10. Average tensile stress (flexure tests)

| Rod Size | 3/8 in. (ksi) | 1/2 in. (ksi) |
|---|---|---|
| Tensile Strength | 68 | 75 |

## 2.3 Modulus of Elasticity

The modulus of elasticity was determined experimentally using an extensiometer. The modulus tests were conducted concurrently with the tensile tests. The extensiometer was removed at seventy-five percent of the predicted ultimate load to protect the sensitive equipment.

The elongation of the rod along a two-inch gage length was found using this device. This data, along with the tensile stress in the rod, was used to calculate the modulus of elasticity. The results of these tests are shown in Table 2.11 and Figures 2.4 and 2.5. The discontinuity of Test 2 in Figure 2.4 is a result of the rod slipping in the epoxy. The equation used to calculate the modulus of elasticity is shown in Equation 2.5.

$$E = \frac{f_{FCR}}{e * l_g} \qquad \text{Eqn. 2.6}$$

Where:

$f_{FCR}$ = Tensile stress in the FCR

e = Elongation recorded in two-inch gage length

$l_g$ = Gage Length (two inches)

E = Modulus of elasticity

Table 2.11. Experimental modulus of elasticity

| Test | 3/8 in. (psi) | 1/2 in. (psi) |
|---|---|---|
| Test 1 | $3.66 \times 10^6$ | $4.78 \times 10^6$ |
| Test 2 | $3.55 \times 10^6$ | $4.73 \times 10^6$ |
| Test 3 | $3.48 \times 10^6$ | $5.09 \times 10^6$ |
| Test 4 | $3.33 \times 10^6$ | $5.02 \times 10^6$ |
| Test 5 | $3.17 \times 10^6$ | $4.93 \times 10^6$ |
| Average | $3.43 \times 10^6$ | $4.91 \times 10^6$ |
| Standard Dev. | $0.19 \times 10^6$ | $0.15 \times 10^6$ |

## 2.4 Surface Area of the Rod

The surface area of the rod proved to be difficult to determine by any method of measurement. For this reason the circumference was approximated using a computer aided drawing (CAD) by assuming the amount of excess epoxy which ran into the cracks between the bars as shown in Figure 2.6. The program was then used to determine the length of the line used to generate the circumference of the rod. From this property, the surface area is simply the length of the embedment multiplied by the circumference of the rod. The calculated values are listed in Table 2.12.

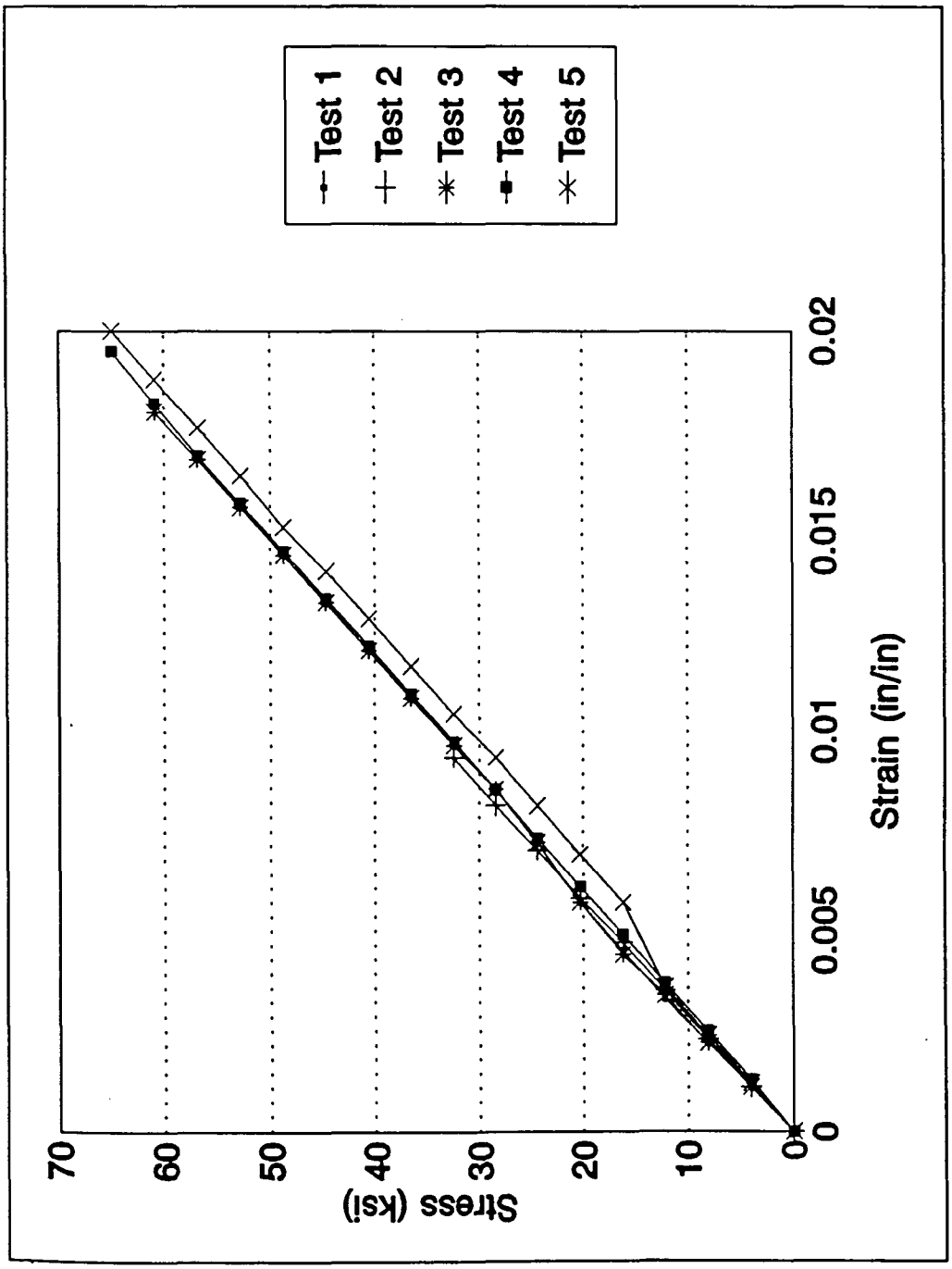


Figure 2.4. Stress versus strain for three-eighths-inch FCR

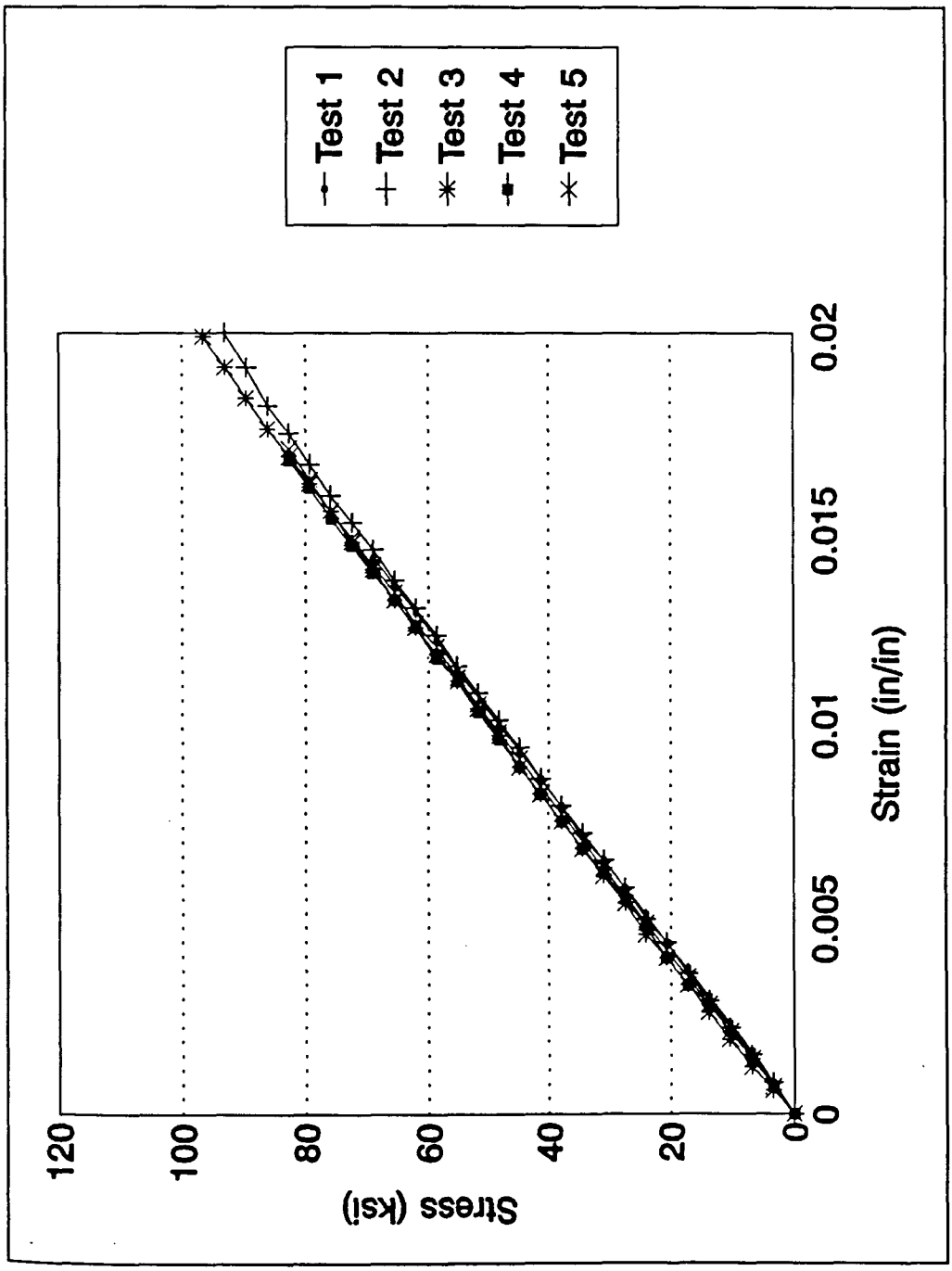


Figure 2.5. Stress versus strain for one-half-inch FCR

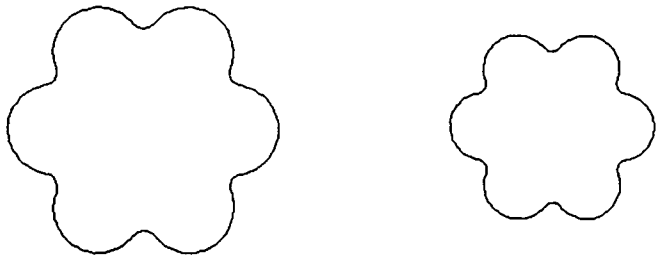

Figure 2.6. Diagrams used for determination of rod circumference

Table 2.12. Circumference values of FCR

| Rod Size | 1/2 inch | 3/8 inch |
|---|---|---|
| Circumference (in) | 1.569 | 1.451 |

## 2.5 Development Length Properties

Two different criteria were used to calculate development length. Development length, in this report, is defined as the length that the FCR had to be embedded to achieve a given end slip. End slip is defined as the distance that the end of the FCR moves when the rod is at its ultimate load. The first criteria used for determining development length was zero end slip. When the beams were cast, the FCR was allowed to extend out of the beam

approximately one inch. The end slip was then measured as the beams were tested. When no end slip was recorded at ultimate load the rod was assumed to be fully developed.

This criteria is somewhat conservative because the FCR will fracture even though there is end slip but because of the limited experience with the performance of this product, a more conservative approach was taken.

The second criteria used was one-tenth-inch end slip. Bond strength, in most of the beams tested, was much higher than the tensile strength of the rod. Bond stress was determined in some of the beams with the use of slip wiring techniques and was shown to be a maximum at around ten inches from the loaded end of the bar for that concrete strength. Soon after this point, the bond stress dropped to almost zero which indicates that the bar was fully developed in only ten inches. For this reason, the zero end slip criteria was deemed overly conservative and an alternative approach to designing for development length was desired.

Slip wires were installed on some of the beams. Slip wires show the differential movement of the FCR inside the concrete and are discussed in Section 4.7 of this report. The bar slippage just after the point of maximum bond stress was around 0.075 inches. The remaining length of the rod will reduce the slippage at this point but the bond stress was small enough along the rest of the bar that the reduction

in slip was neglected. The slippage listed above and the fact that the deflections would become excessive if large end slips were allowed, prompted the use of the one-tenth-inch end slip criteria.

Reinforcement in the ISU beams was cast as top bar reinforcement. The ACI code [2] increases the development length by a factor of 1.3 for bars cast as top bar reinforcement. For this reason a smaller development could possibly be used for FCR cast as bottom bars. More research needs to be performed to determine the magnitude of reduction that could be allowed. Chapter 5 dwells further into the more detailed aspects of development length.

# 3 TEST SPECIMENS

For many years the concrete industry has used simply supported beams or pullout specimens to determine the development length of reinforcing rods. A list of the advantages of the standard pullout test is provided below [3]:

1. Pullout tests give a reasonable measure of the necessary anchorage length of a bar when it is embedded in a pier or an inactive piece of concrete.
2. Pullout tests represent the basic idea of anchorage, even if that anchorage length is not in a region of shear or moment.
3. Pullout tests vaguely represents what happens adjacent to any concrete crack where a bar always carries more tension than exists at nearby sections.
4. The bar slip at the loaded end of a pullout specimen is considered to be half the crack width which would result in the same steel stress. This crack estimate however, has been proven to be too large [3].
5. The effect of reduced cover over the bar can be simulated by adaptations of the pullout test which place the bar off center and nearer one face.

6. The pullout specimens are easy to cast and test requiring only simple formwork and hardware.

The standard pullout test does however, have many weaknesses. The disadvantages are listed below:

1. Pullout tests do not properly model the combined shear and flexural action of a beam type member because bond and anchorage are not being tested in a region of shear or moment.
2. The pullout test places the concrete in compression which eliminates transverse tension cracking and provides normal compressive stresses on the reinforcing bar.
3. Friction on a loaded end bearing reduces local splitting and confines the reinforcement thus increasing the friction portion of bond.
4. As the concrete is confined, the results may provide data concerning anchorage but probably little about the factors that relate to splitting.
5. The computed, or nominal maximum bond resistance in ordinary beams is less than that in pullout specimens; thus, pullout tests tend to yield unconservative results [9].

Many attempts have been made to find a better standard test method. One such attempt was tried by Mathey and Watstein [4,5]. In this test, simply supported beams were cast with concrete outcroppings on the sides of the beams at the loaded ends as shown in Figure 3.1. The beams were cast

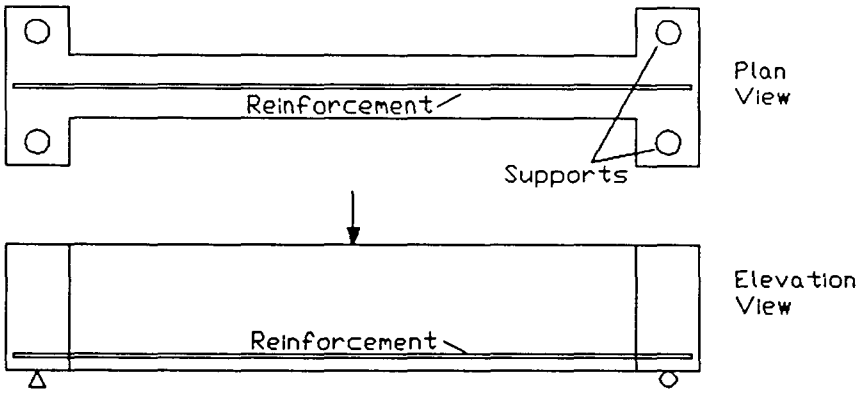


Figure 3.1. Mathey and Watstein beam

this way in an effort to reduce the confinement effects around the simple supports.

Another test method was attempted by the University of Texas by Ferguson and Thompson [3,6] and at Iowa State University by Warren [20]. This test method involved casting a simply supported beam with a cantilever section at one end as shown in Figure 3.2. The development length is tested in

the cantilever section. This method worked well but the cantilever section was still being loaded above the reinforcement which produced confinement effects on the reinforcement.

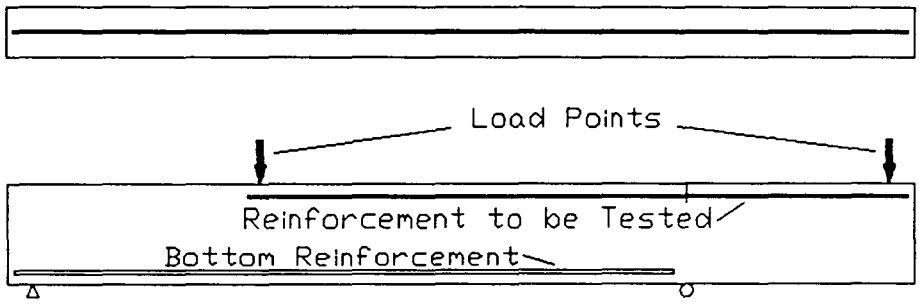


Figure 3.2. Ferguson and Thompson beam

### 3.1 New Test Configuration

Researchers at Iowa State University have developed a new technique which combines both of these test methods. Beams were cast with the cantilever section similar to the Ferguson and Thompson test [3,6], but they also included the concrete outcroppings extending from the side of the beam, similar to those used by Mathey and Watstein [4,5]. These outcroppings are called dogbones and are shown in Figure 3.3. By loading the ISU beams on the dogbones, the compressive

effects of the load no longer confine the reinforcing and effect the bond characteristics of the reinforcement.

The cantilever section is variable and can be adjusted by moving the reaction point. To get a more precise length of the cantilever section, a styrofoam bond breaker was inserted around the rod and attached to the forms during the casting of the beams. This bond breaker was located above the cantilever reaction point.

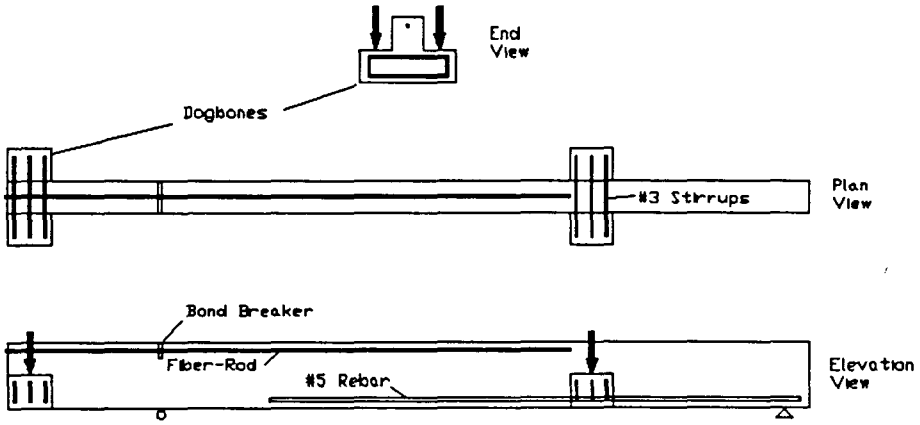


Figure 3.3. ISU Beam test setup

### 3.2 Casting

The ISU beams proved to be efficient from a testing standpoint but were more difficult to cast than simply

supported beams or pullout specimens. Steel forms, provided by Economy Forms of Des Moines, Iowa, were used to form the bottom and most of the sides of the beams. The dogbone forms were made of wood. These forms were coated with used motor oil to allow for ease of stripping.

The forms were stripped after a three-day curing period. The beams were covered with plastic until the forms were stripped. The beams were then allowed to cure for a minimum of seventeen days.

The reinforcement used in the bottom of the beam consisted of one number-five reinforcing bar. This reinforcement started at the back of the beam (opposite the cantilever section) and had a length of nine feet. The top reinforcement was the reinforcement that was being tested. When the beams were cast, this part of the reinforcement was allowed to extend past the end of the beam approximately one inch so that the end slip could be measured. The length of the top reinforcement was also nine feet.

The dogbones were reinforced with three, number-three stirrups bent into a three-inch by fifteen-inch rectangle. The three stirrups were then joined together by welding two, seven-inch pieces of number-three bar across the top of the stirrups. The stirrups started in one of the dogbones, extended through the beam, then terminated in the opposite dogbone as shown in Figure 3.3. If the shear stress in the

beam was expected to exceed the shear capacity of the concrete used in the beams, U-shaped stirrups were inserted at six-inch intervals throughout the beam and two stirrups were inserted vertically in each dogbone to keep the dogbone from breaking away from the rest of the beam.

The overall length of the beams was approximately twelve-feet long with the cross-sectional dimensions being six-inches wide by twelve-inches high. The dogbones were eight-inches long by six-inches high by six-inches wide. A diagram of the beam dimensions and reinforcement locations is shown in Figure 3.4.

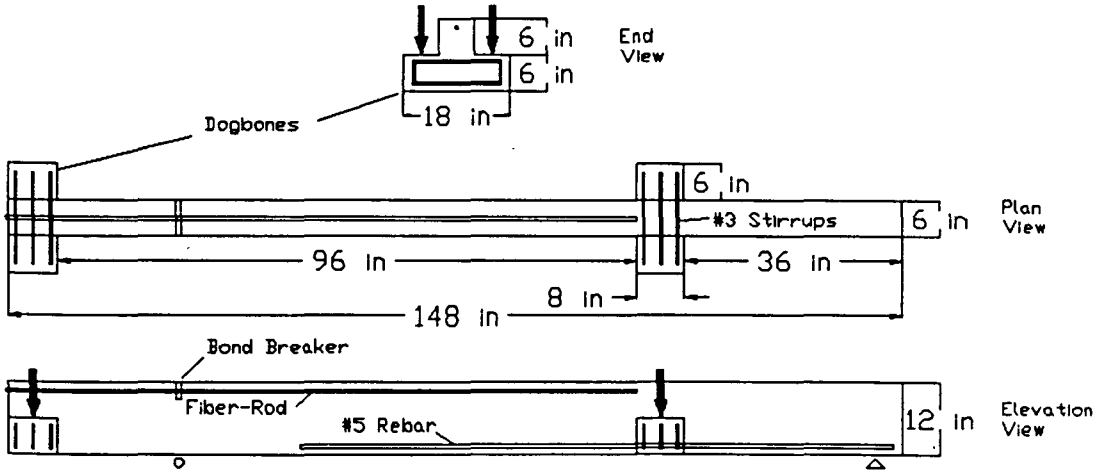


Figure 3.4. Dimensions of the ISU Beam

### 3.3 Concrete Strengths

Concrete strengths ranged from 2500 to 7000 psi based on the average of six test cylinders for each set of six beams. These cylinders were the standard six-inch diameter by twelve-inch high type. The concrete was placed in the beams in two layers and was consolidated with a vibrator.

Slumps between five and seven inches were needed to allow the concrete to flow into the dogbones. All concrete was cast and tested according to ASTM specifications [22]. The concrete did not contain any air entrainment, plasticizers, or other additives. Concrete was supplied by Manatts Ready-Mix of Ames, Iowa.

# 4 BOND THEORY

## 4.1 Flexural Bond and Anchorage Bond

As moment varies along a span, the tensile force in the steel also varies; this induces a longitudinal interaction between the bars and the surrounding concrete. This phenomena is known as flexural bond. Flexural bond is defined as the bond stress induced in the concrete by the flexural stresses, shear and moment. High flexural bond is required at locations along the span where the rate of change of tensile force in the reinforcing bars is high, such as points of inflection within continuous spans and at simply supported ends of beams, even though the tensile force to be developed is zero.

Flexural bond is determined locally by the shear or the change in moment. Flexural cracking reduces flexural bond to a local average stress.

Anchorage bond is defined as the bond strength required to reach the yield strength of the rod. If flexural bond exceeds anchorage bond the bar will pull out of the concrete. For this reason, the magnitudes of both the flexural bond and anchorage bond should be determined.

## 4.2 Bond in General

A basic requirement in reinforced concrete construction is that there is bond between reinforcement and the surrounding concrete. This bond is the major focus of the theoretical portion of this report.

Anchorage bond stress is defined as the unit shear force acting parallel to the bar on the interface between the bar and the concrete, or more simply, the stress per unit area of the bar surface. Bond stress is the complex system by which stress is transferred between concrete and reinforcement in making an integral structural member. Bond is made up of three components. These are:

1. Chemical Adhesion
2. Friction
3. Mechanical interaction between the concrete and reinforcement.

Chemical adhesion is the gluing action between the reinforcing rod and the concrete paste. Concrete strain and the radial contraction from the tension in the rod are the criterion for rupture of adhesion. In the adhesive stage of bond, the two materials deform together without movement relative to each other. As soon as the reinforcement moves

relative to the concrete, all adhesive bond is lost at this point on the rod.

When adhesive bond is lost, friction becomes the largest source of bond strength for undeformed bars. The coefficient of friction is dependent on the surface characteristics of the reinforcement and with the character of the concrete paste. Frictional bond is believed to be the largest source of bond in plain steel bars without deformations and in prestressing strands. Therefore, frictional bond is of major concern when dealing with the FCR since the FCR cross-section is similar to both the plain steel bar and the prestressing strand.

Frictional bond is assumed to vary along the length of the bar. The variation is caused by the fact that the relative movement between the materials is greater toward the loaded end of the bar. This movement produces a greater polishing action on the touching surfaces of the materials with a consequent reduction in frictional force.

Once a plain bar has moved through the concrete a sufficient distance, the frictional bond stress is all but destroyed and the system fails unless mechanical anchorage is provided. With a prestressing strand the helical shape of the individual wires will provide sufficient friction and mechanical resistance so that anchorage bond can result [19]. FCR however, theoretically, exhibits more radial contraction

than a prestressing strand with a corresponding reduction in mechanical resistance when compared to prestressing strands.

Mechanical bond is the mechanical interlocking between the concrete and the deformations on the reinforcement. In plain steel bars the mechanical bond is small and is considered negligible. For this reason deformed bars were developed to increase mechanical bond strength. Both adhesion and friction play a smaller role in deformed bars with mechanical anchorage being the largest component of anchorage bond strength. Prestressing strands have some mechanical bond characteristics but the largest source of anchorage bond is friction.

FCR has a cross-section that is a variation between a plain steel bar and a prestressing strand. FCR is made up of the same geometrical shapes as the prestressing cable but when the individual strands are epoxied together, epoxy fills in some of the spiraling grooved surfaces which run longitudinally with the rod. The excess epoxy reduces the surface area for frictional and adhesive bond to apply.

Mechanical anchorage in FCR is thus similar to both the plain steel rod and the prestressing strand with some variations. When prestressing strands are pulled through the concrete the smooth helical texture of the strands does not provide a positive means of mechanical interlocking since the strand tends to unscrew as it slips through the concrete.

However, as a strand elongates, the pitch of the strand changes with respect to the surrounding impression in the concrete. This effect causes increased normal and frictional forces which more than compensate for the effect of radial contraction associated with the strand at elongation [16].

The Poisson's shrinking effect on FCR is more pronounced than with steel because of the smaller Young's modulus of FCR. Equation 4.1 demonstrates that the change in bar radius is inversely proportional to the modulus of elasticity of the specimen [15]. Using a Young's modulus of thirty-million psi for steel versus four-million psi for FCR and if the Poisson's ratio for steel and FCR were considered to be similar, the radial shrinkage of the FCR can be shown to be as much as eight times that of the prestressing strand.

$$\Delta r = r(\Delta f)\frac{\mu_s}{E} \qquad \text{Eqn. 4.1}$$

Where:

$\Delta r$ = Change in radius (in)

$r$ = radius of the rod (in)

$\Delta f$ = Change in the tensile stress in the rod (psi)

$\mu_s$ = Poisson's ratio

E = Modulus of elasticity (psi)

For these reasons, anchorage bond in FCR is assumed to be composed mostly of adhesive bond and friction and that mechanical anchorage plays a smaller role. The percentages of frictional and mechanical bond strength were determined analytically by trial and error procedures and are presented in Section 5.0.

### 4.3 Bond Stress Distribution

In both pullout specimens and beams, bond stress is not uniformly distributed over the length of the bar. The magnitude of bond stress is equal to zero at the end of a bar and where the concrete is cracked. From these points, bond stress increases until sufficient anchorage is provided to resist the tensile force in the rod. If the total bond force capacity is lower than the ultimate tensile strength of the rod the bar will pull out of the concrete.

Small amounts of slipping will occur along the bar as adhesive bond is lost. After slipping begins, the bond stress at any point along the bar increases with the movement of the bar, very rapidly at first, then more slowly until the maximum bond resistance is achieved. After this point, bond stress gradually declines as slipping progresses.

Figures 4.1a and 4.1b show the bond stress distribution as the bar is being loaded. The bond stress will increase

proportionally until the maximum bond stress is achieved. Figures 4.1c and 4.1d show the point of maximum bond being achieved and propagating towards the free end of the bar. When the maximum bond stress reaches the end of the bar the system exhibits the maximum bond stress that can be obtained as shown in Figure 4.1d. Figures 4.1e and 4.1f show the bond stress being overcome by the tensile force in the bar. At this point the bar will start to pull out of the concrete.

The differential movement of the FCR was monitored in some of the beams with slip wires. The results of these tests are presented in Section 4.6 of this report. A plot of an actual bond stress distribution of one beam is presented in Section 4.7.2.

### 4.4 Time and Shrinkage Effects on Bond

Frictional bond resistance is primarily caused by shrinkage of the concrete closely adjacent to the reinforcement [13]. For this reason frictional bond strength can be expected to have the same time relationship as shrinkage. Although initially, shrinkage is very rapid, it does continue appreciably up to ages of 28 or 56 days. Based on the results of Reference 13, the 17-day curing period was assumed to be sufficient.

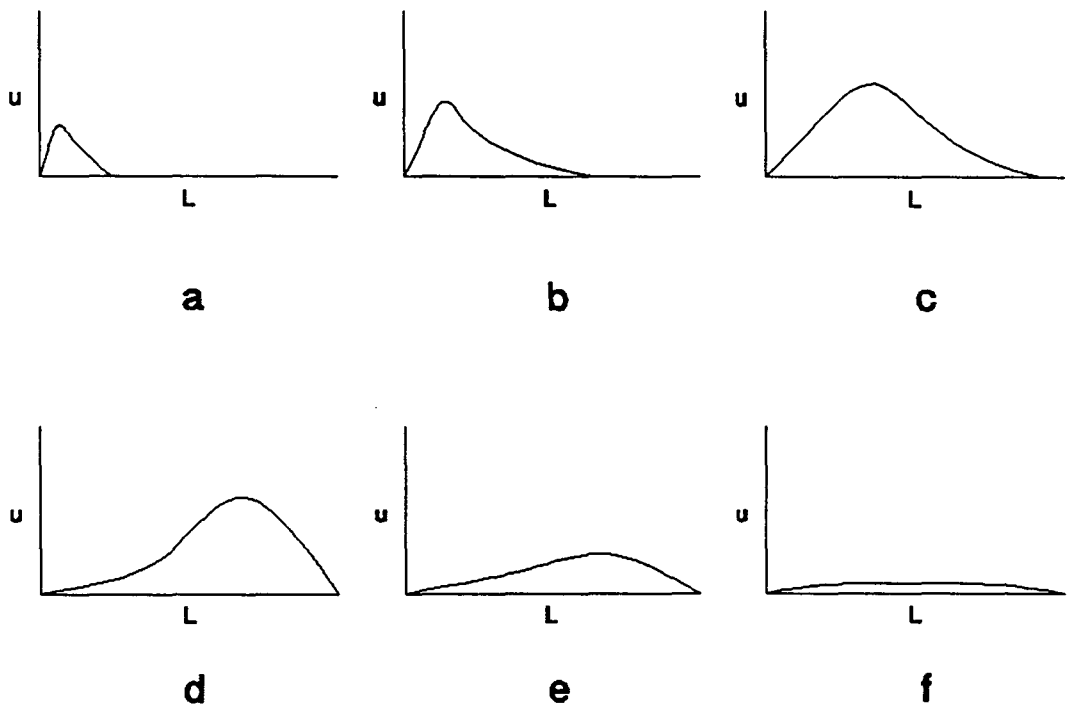


Figure 4.1. Propagation of stress distribution

Growth of adhesive and frictional bond resistance is much more rapid than that of concrete strength [13]. Mechanical bond strength however, is related more to the tensile strength of the concrete which increases at a much slower rate with time. Because FCR possesses only small deformations, the normal force exerted on the concrete is smaller than the normal force exerted by deformed steel and

the tensile strength of the concrete does not have as much of an effect on the development of the FCR.

In an article by J. R. Salmons and T. E. McCrate [16] which dealt with the bond characteristics of untensioned prestressing strands, concrete strengths from 3750 psi to 6900 psi were shown to have no apparent effect on the bonding characteristics of embedded strands prior to general slip. Therefore, adhesive and frictional bond effects will depend mainly on the shrinkage of the concrete or more importantly the concrete which is closest to the reinforcement.

The majority of the bond strength is achieved in only four days for rods which are cast in the center of the concrete such as pullout specimens [13]. Because the hardening of concrete is an exothermic reaction and the concrete surrounding the bar provides thermal insulation, the concrete inside the specimen will reach a higher temperature than that at the outside of the beam. This higher temperature would result in more rapid hardening and contraction effects in that section of the concrete which would account for the rapid development of bond. The FCR is not however, located in the center of the concrete specimen. Therefore a longer curing time was allowed to provide more bond between the rod and the concrete. The minimum curing time allowed for the FCR specimens was seventeen days with

most of the rods having a curing time greater than twenty-eight days.

### 4.5 Surface Conditions of the Rod

The coefficient of friction in the concrete will vary with the surface condition of the rod and possibly with the character of the cement paste [15]. Bond strength in both prestressing strands and plain steel has been proven to increase with bars and strands that are slightly rusted [3, 15, 27]. From this knowledge, bond strength can be assumed to be greatly effected by even minor deformations in the rod. Mixing sand with the epoxy is a possible source of deformations. This practice has been used in the epoxy coated steel industry for many years.

The surface characteristics of the FCR varied from one rod to the other because of the manufacturing process. The individual strands were pultruded, then after they had cured the strands were hung from the ceiling, wrapped, and then painted with epoxy. This process resulted in runs in the epoxy and some discontinuity of the rod. While the discontinuity produced small undulations in the surface of the rod, the shape of the rod became more rounded and the surface area decreased and thus the anchorage bond strength declined.

## 4.6 Splitting Effects

A plain bar will pull loose either by longitudinal splitting of the concrete or by pulling out leaving a slick bore or hole. Most plain bars however, will not develop sufficient bond strength to split the surrounding concrete [3].

When deformations were introduced to steel reinforcement, the largest source of bond strength came from the lugs of the bar bearing on the surrounding concrete and the shearing strength of the concrete between the lugs. This bearing changed the major source of failure from pullout to longitudinal splitting. Splitting is directly related to the tensile strength of the concrete. Bond failure in deformed bars is almost always a splitting failure [1].

Adhesion and frictional bond still assist in the bond strength of deformed bars but the combined effect of the adhesion and friction is much smaller than mechanical bond. This fact is why the tensile strength of the concrete is the major contributing factor in the development of deformed bars.

Splitting should be reduced with the FCR because there are no lugs present which comprise the majority of the outward force from the deformed bars. Because of this fact, more FCRs could be put in beams and slabs and the rods could

be put closer together without having adverse splitting of the concrete. Care should be taken by the designer though, not to over reinforce the beam.

### 4.7 Slip Wires

A knowledge of the differential movement of the FCR inside of the beam would help in the determination of the nature of the bond strength of the rod. For this reason slip wires were installed on the first thirty-seven beams. Slip wires were eventually terminated because of the decrease in bond strength and consequently, the increase in development length of the FCR when they were used.

The increase in development length was caused by the discontinuities in the concrete produced by the attachment of the slip wires to the FCR. Direct contact between the concrete and the rod was lost for an area of approximately two inches longitudinally and one-quarter of the circumference of the rod radially at each slip wire attachment point.

Initially the introduction of deformations on the FCR from the attachment points of the slip wires was thought to decrease the embedment required to develop the rod. Because of the low shear strength between the epoxy and the rod this idea was soon proven wrong. This proof was shown by tests

that indicated that beams which incorporated slip wires exhibited more slip than beams without slip wires.

There were many problems with attaching the slip wires to the FCR. Initially the wires were attached using an epoxy similar to the one used to bond the strands together in the FCR. This approach was quickly abandoned because the bond between the FCR and the epoxy did not have enough shearing strength to pull the wire, and the deformation due to the connection, through the concrete.

The slip wires were attached so that they would be pulled through the concrete as the rod moved. This action depressed a spring actuated plunger which was mounted on top of the beam. A dial gage was mounted to the plunger to measure the movement.

The next approach for slip wire attachment was to use Sikadure-33 epoxy to mount the slip wire to the rod. Also, the end of the wire and the mounting surface of the rod were roughed using coarse sandpaper. The tubing to move the wire to the top of the beam was also changed from plastic tubing to three-sixteenths-inch outside diameter metal brake lines. This procedure also failed because of the shearing force between the epoxy and the rod.

The testing arrangement that finally worked was to push the wire through the beams rather then pull the wire. Since the wire was spring loaded due to the plunger, there was no

slack in the wire. Also, the wire and epoxy were allowed to move through a small void which was made by putting silicone sealant over the wire for around one-inch along the length of the rod. A diagram of the slip wire configuration is shown in Figure 4.2.

This arrangement worked but continued to present problems. The slip wires revealed when the bar would start moving but most of the wires detached from the FCR soon after this point. Four of the thirty-seven slip wired beams produced complete bond stress distribution data. The slip wires on the rest of the beams detached before sufficient data of bond stress could be achieved.

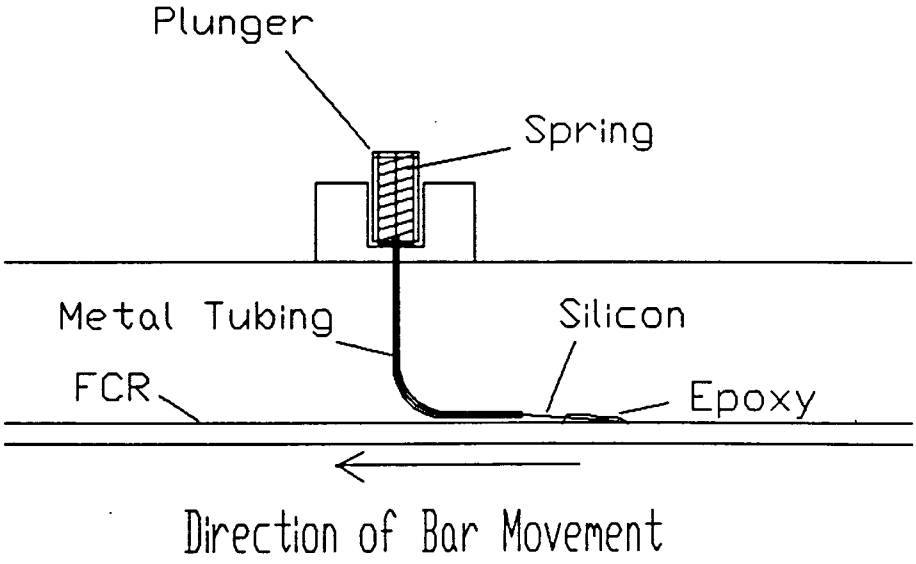


Figure 4.2. Diagram of slipwire apparatus

### 4.7.1 Loss of Adhesive Bond

The slip wire data provided knowledge of two facts; the point of loss of adhesive bond and the bond stress distribution. The loss of adhesive bond will be presented in this section. Bond stress distribution will be presented in Section 4.7.2.

When the bar moves, the adhesive bond is lost at that section of the rod. With this data, the loss of adhesive bond was proven to be a linear relationship when compared with the tension in the rod. R-squared values in excess of 0.9 were achieved when a linear regression was performed on the data. A sample plot of this data is shown in Figure 4.3. A diagram defining the embedment length can be found in Figure 2.1.

Using this knowledge, the loss of adhesive bond can be calculated by using the tension in the rod at the point of initial end slip and forming a line between this point and the point of zero load. The point of zero load corresponds to no loss of adhesion. Since the assumption has been made that the majority of the bond strength rests on the frictional bond, then frictional bond must comprise the largest part of the remaining anchorage bond after adhesive bond is lost.

### 4.7.2 Stress Distribution

Bond stress distribution was calculated on four of the beams tested. Some of the data presented had to be extrapolated because the slip wires detached from the FCR.

A typical bond stress distribution, as the FCR was loaded, is shown in Figure 4.4. The bond stress develops as expected but did not propagate towards the end of the bar. This fact proved that the bar is embedded well past the minimum development length of the FCR. Also, the zero end slip criteria used for the first derivation of the development length equation was shown to be overly conservative.

The differential movement in the bar was used to calculate the bond stress. The change in length of the rod was divided by the length of the rod to determine the experimental strain. The strain was then multiplied by the modulus of elasticity and cross-sectional area of FCR to obtain the tension in the rod. The tension in the rod was then divided by the surface area over the section where the bond stress was being calculated to determine the bond stress at that section of the rod.

Figure 4.5 shows the bond stress distribution at ultimate strength of FCR. The stress distributions are similar for all of the embedment lengths shown. This fact

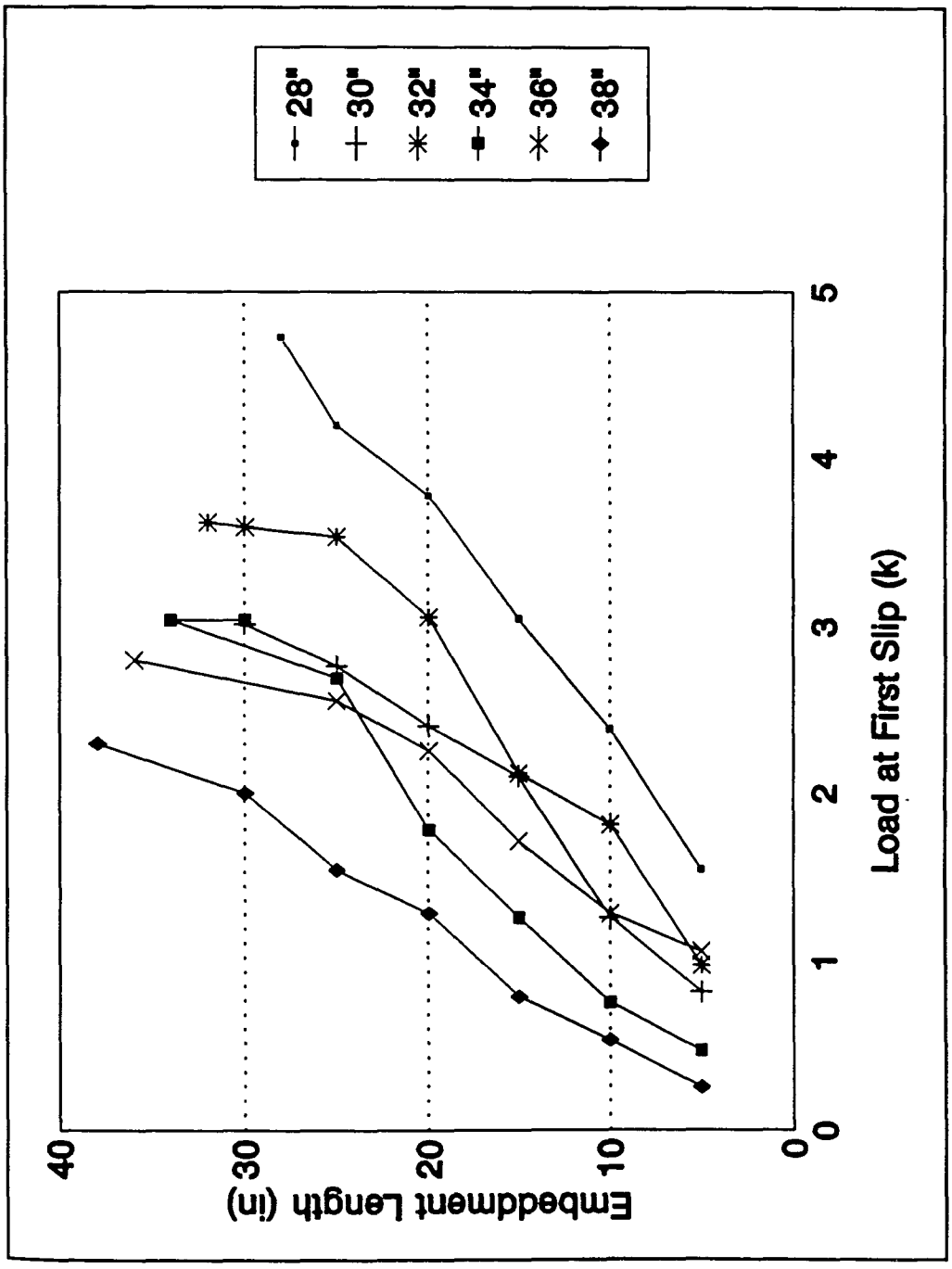


Figure 4.3. Embedment versus load at first slip, 28-38 inch embedment

demonstrates that the rod is embedded past the required development length of the FCR. Note that the addition of the slip wires reduced the bond stress, therefore bars tested without slip wires should have slightly higher bond stresses. A diagram defining the X-distance and embedment length can be found in Figure 2.1.

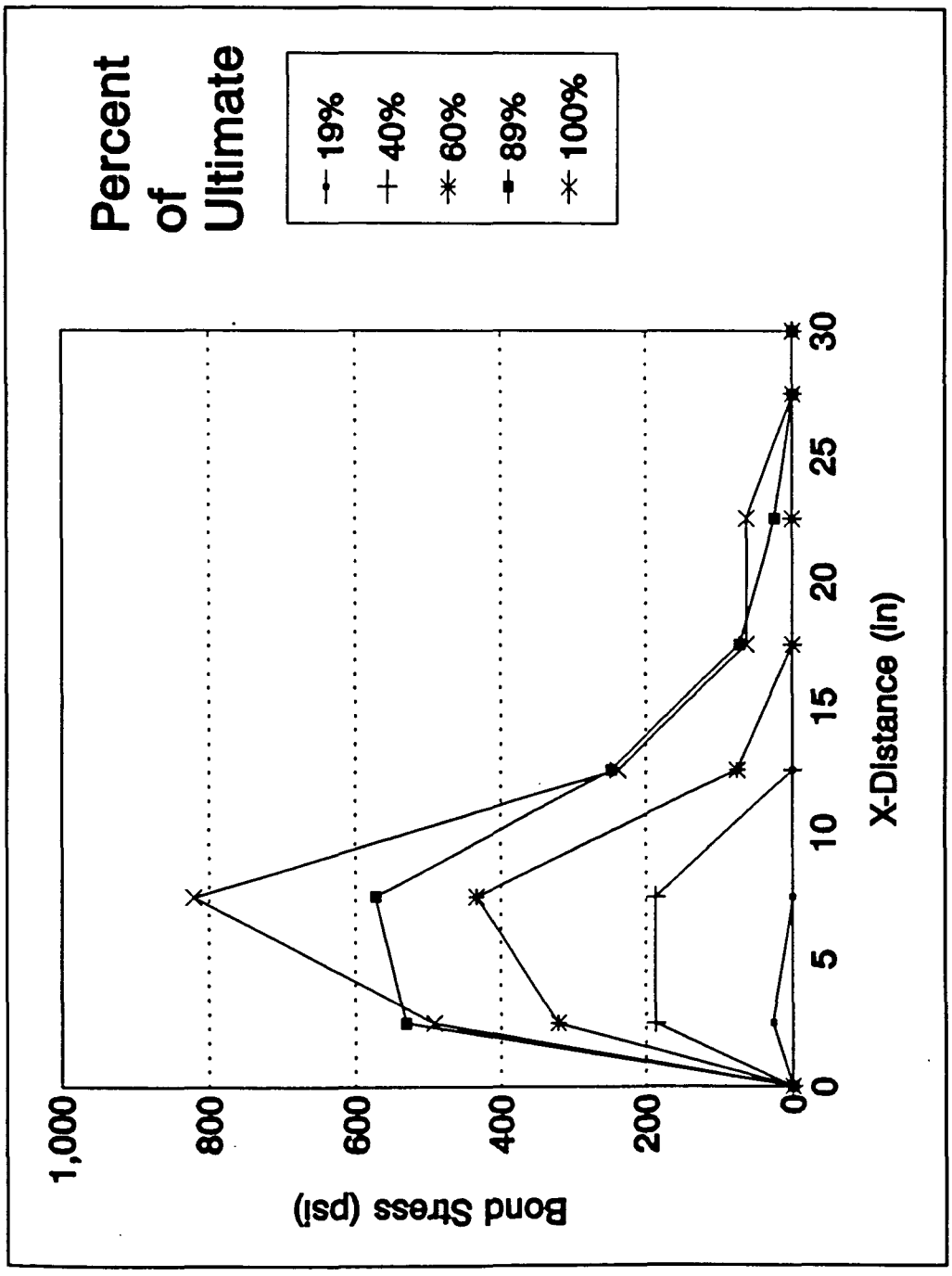


Figure 4.4. Bond stress distribution at different rod tensions

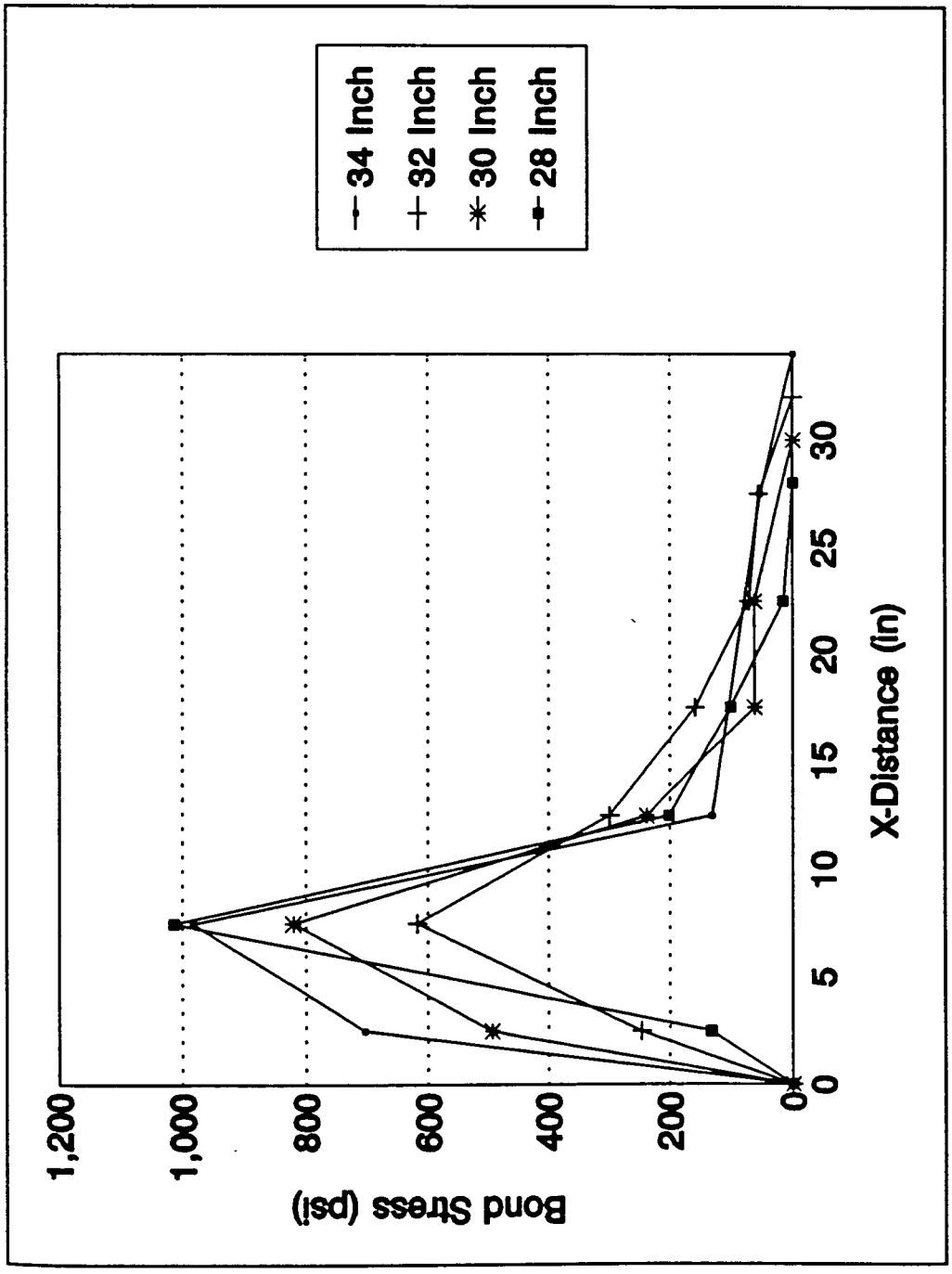


Figure 4.5. Bond stress distribution at ultimate load for four beams, 28-34 inch embedment

# 5 DEVELOPMENT LENGTH

## 5.1 Determination of Bond Stress

The theoretical determination of the bond strength is very similar to that used to determine the bond strength in deformed bars, therefore this procedure will be reviewed [1].

By examining the statics of the bar, Equation 5.1 shows that the bond strength (u) multiplied by the longitudinal surface area of the bar must be equal to the stress in the bar ($f_s$) multiplied by the cross-sectional area. From this equation, the average bond stress can be calculated by solving for u as shown in Equation 5.2. The ultimate bond strength can be determined by substituting the ultimate stress in the bar ($f_u$) for $f_s$, as shown in Equation 5.3. A free-body diagram of the rod is shown in Figure 5.1.

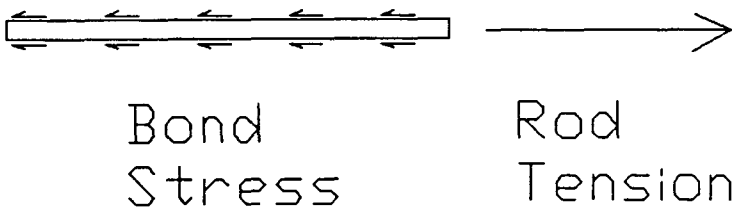


Figure 5.1. Free-body diagram of reinforcement in concrete

The surface area of the FCR was not as easily calculated as that in a round bar, therefore, it had to be calculated by alternate techniques which are presented in Section 2.4 of this report.

$$\sum F=0=u\pi d_b L-f_s\pi\frac{d_b^2}{4} \qquad \text{Eqn. 5.1}$$

$$u=\frac{f_s d_b}{4L} \qquad \text{Eqn. 5.2}$$

$$u_u=\frac{f_u d_b}{4L} \qquad \text{Eqn. 5.3}$$

$$L=\frac{f_u d_b}{4u_u} \qquad \text{Eqn. 5.4}$$

Where:

u = Average bond stress (psi)

$u_u$ = Ultimate average bond stress (psi)

$d_b$ = Diameter of the bar (in)

L = Embedment length (in)

$f_s$ = Tensile stress in the rod (psi)

$f_u$ = Ultimate tensile stress in the rod (psi)

From Equation 5.4 the development length can be calculated if the ultimate bond stress is known. The average ultimate bond stress was calculated by using the same basic equations as for steel, but with the dimensions of the FCR.

For the one-half-inch FCR, the cross-sectional area was 0.141-square inches ($in^2$), the circumference was 1.569 inches (in.), and the theoretical tensile strength of the rod was 139 ksi. The cross-sectional area of the three-eighths-inch FCR was 0.123 $in^2$, the circumference was 1.451 in., and the theoretical tensile strength was 81 ksi.

From these properties the theoretical ultimate bond stress was calculated. An average bond stress for each size of rod was calculated using the flexural test data. A free-body diagram of the rod is shown in Figure 5.1.

$$\sum F=0=u_u C_b L - f_u A_b \qquad \text{Eqn. 5.5}$$

$$u_u=\frac{f_u A_b}{C_b L} \qquad \text{Eqn. 5.6}$$

$$u_{u1/2}=\frac{f_{u1/2}(A_{b1/2})}{C_{b1/2}(L)}=\frac{12.491}{L} \qquad \text{Eqn. 5.7}$$

$$u_{u3/8}=\frac{f_{u3/8}(A_{b3/8})}{C_{b3/8}(L)}=\frac{6.866}{L}$$ Eqn. 5.8

Where:

$u_{u\ 1/2}$ = Ultimate average bond stress (ksi)

$u_{u\ 3/8}$ = Ultimate average bond stress (ksi)

$C_{b\ 1/2}$ = Circumference of the rod (1.569 in)

$C_{b\ 3/8}$ = Circumference of the rod (1.451 in)

L = Embedment Length (in)

$f_{u\ 1/2}$ = Ultimate tensile stress of FCR (139 ksi)

$f_{u\ 3/8}$ = Ultimate tensile stress of FCR (81 ksi)

$A_{b\ 1/2}$ = Area of the rod (0.141 $in^2$)

$A_{b\ 3/8}$ = Area of the rod (0.123 $in^2$)

The flexural test data was used to calculate an experimental average of the ultimate bond stress. The ultimate bond stress was calculated by substituting the experimental tension (T) in the FCR in place of the $f_u(A_b)$ term. A sample calculation is shown for a one-half-inch FCR with a 28-inch embedment that achieved a maximum tension of 14 Kips.

$$\sum F=0=u_u C_b L-T$$ Eqn. 5.9

$$u_u = \frac{T}{C_b L} = 319 \qquad \text{Eqn. 5.10}$$

Where:

$u_u$ = Ultimate average bond stress (psi)

$C_b$ = Circumference of the rod (1.569 in)

L = Embedment length (28 in)

T = Tension in the rod (14000 lbs)

The average experimental ultimate bond stress was calculated to be 262 psi for the one-half-inch FCR and 230 psi for the three-eighths-inch rod.

The average ultimate bond stress for plain steel bars is approximately 120 psi [3]. The average bond stress for clean prestressing strands is between 160 and 220 psi and for slightly rusted prestressing strands the average bond stress is between 500 and 800 psi [15].

A plot of the average ultimate bond stress versus development length is shown in Figure 5.1. The theoretical ultimate bond stress was calculated in Equation 5.7. When plotted with the experimental data the theoretical bond stress proved to be approximately twice the value of the experimental results. For this reason, the flexural tensile strength of the rod was substituted into Equation 5.7 rather than using the theoretical tensile strength. The plot which

used the flexural tensile strength fit the data better as shown in Figures 5.1 and 5.2.

The theoretical tensile strength of the FCR did not provide the correct theoretical bond stress. From this knowledge, the tensile strength of the rod was assumed to be smaller when the rod was tested in concrete than if the rod was tested in a direct tension test. One reason for the reduced strength was the fact that the rod was not in direct tension. As the beam deflected the rod was being forced to bend slightly, resulting in curvature effects. This action applied more load to the top fibers of the rod and also produced a normal force on the rod from bearing on the concrete [17]. Dowel shear, binding, and the destruction of some of the fibers at the bar/concrete interface could also reduce the flexural tensile strength. For this reason the flexural tensile strength was used in all calculations.

## 5.2 Derivation of the Development Length Equation Zero End Slip Criteria

The criteria used in this section of the report for development length was the point of zero end slip. At the point of zero end slip the rod had moved relative to the concrete at every point along the bar up to, but excluding this point. For this reason, the adhesive bond stress did

not apply in the calculations for the bond stress. The remaining components were friction and mechanical anchorage.

Equation 5.10 shows that the frictional bond strength is directly proportional to the tension in the rod divided by the surface area in contact with the concrete. The mechanical bond strength is directly proportional to the square-root of $f'_c$, to the circumference of the rod, to the angle of twist, and to the depth of the grooves in the FCR. The ultimate bond strength equation was derived from these two equations and each was modified by a factor which was used to fit the equation to the experimental data.

$$U_u = \frac{f_u A_b}{C_b L} X_1 + C_b \sqrt{f'_c} X_2 \qquad \text{Eqn. 5.11}$$

$$L = \frac{f_u A_b}{C_b U_u} \qquad \text{Eqn. 5.12}$$

$$L = \frac{f_u A_b}{C_b \left( \frac{f_u A_b X_1}{L} + C_b^2 \sqrt{f'_c} X_2 \right)} \qquad \text{Eqn. 5.13}$$

Equation 5.13 is then solved for L which yields Equation 5.14.

$$L=\frac{f_u A_b(1-X_1)}{C_b^2\sqrt{f'_c}X_2} \qquad \text{Eqn. 5.14}$$

Where:

L = Development length (in)

$f_u$ = Ultimate tensile stress of FCR (psi)

$f'_c$ = Compressive strength of the concrete (psi)

$A_b$ = Area of the rod ($in^2$)

$C_b$ = Circumference of the rod (in)

$X_1$ = Factor relating to the frictional bond strength

$X_2$ = Factor relating to the mechanical bond strength

Since frictional bond stress is thought to be the larger source of bond stress, the coefficient for frictional bond strength had a larger value than the coefficient for mechanical bond. Values of 0.80 and 0.34 were chosen for the calculations because they fit the data well. Using these coefficients, the development length of the FCR can be calculated as shown in Equations 5.15 and 5.16.

$$L=\frac{f_u A_b(1-0.8)}{C_b^2\sqrt{f'_c}(0.34)} \qquad \text{Eqn. 5.15}$$

$$L=\frac{0.59 f_u A_b}{C_b^2\sqrt{f'_c}} \qquad \text{Eqn. 5.16}$$

Where:

$f_u$ = Ultimate tensile strength of the rod (psi)

$A_b$ = Area of the rod ($in^2$)

$C_b$ = Circumference of the rod (in)

$f'_c$ = Compressive strength of the concrete (psi)

A plot of concrete strength versus development length for three-eights-inch FCR is shown in Figure 5.3 and a plot for the one-half-inch rods is shown in Figure 5.4. Equation 5.16 is used to calculate the theoretical development length and is plotted with the experimental data. The graph shows that the equation is accurate but slightly conservative.

Note that the FCR was cast as top bar reinforcement. The ACI code [2] increases the development length required for top bar reinforcement by a factor of 1.3. For this reason a smaller development length could possibly be used for FCR cast as bottom bars. However, more research should be performed to determine the magnitude of the reduction.

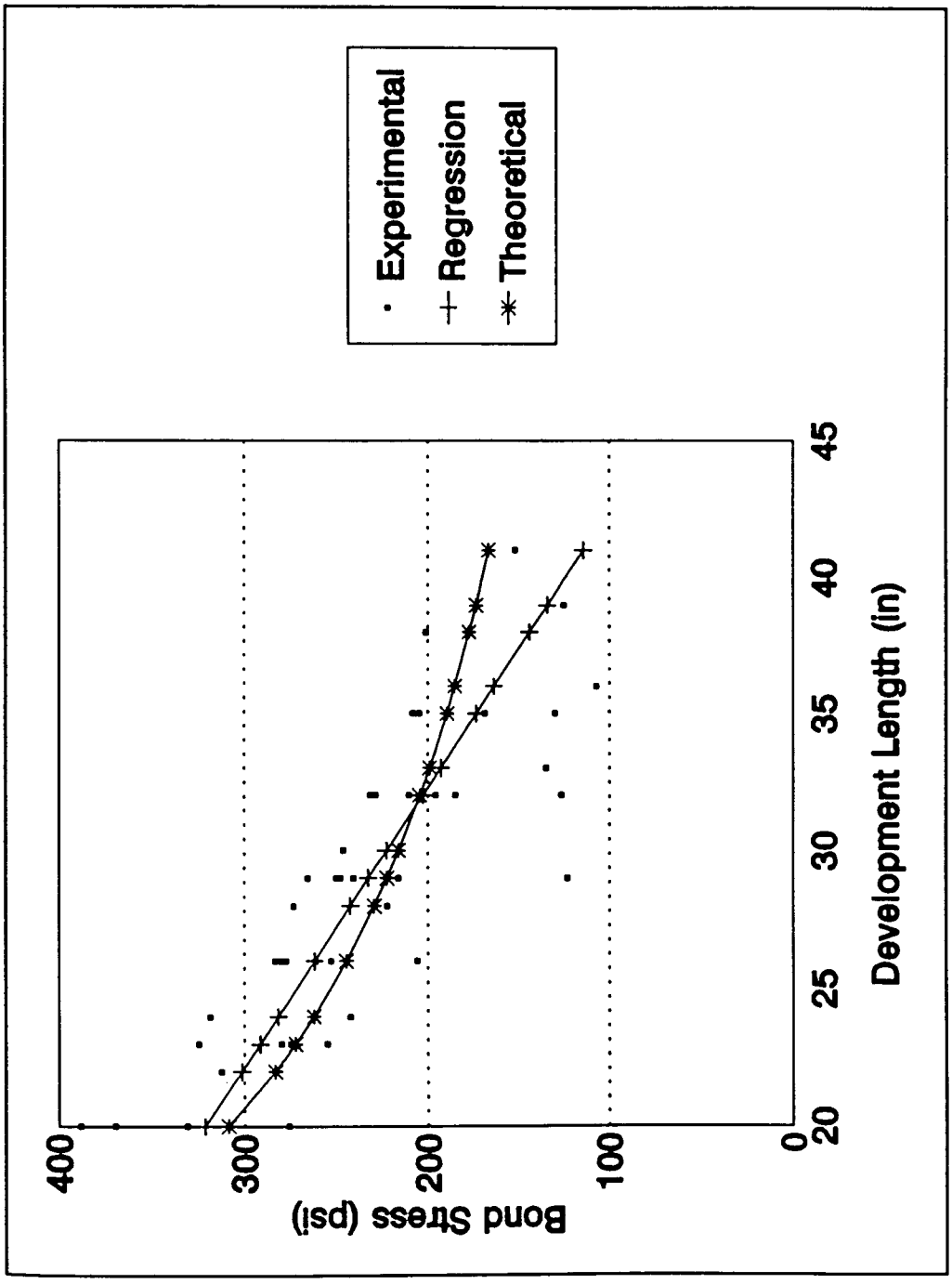


Figure 5.2. Development length versus bond stress, three-eighth-inch FCR, zero end slip criteria

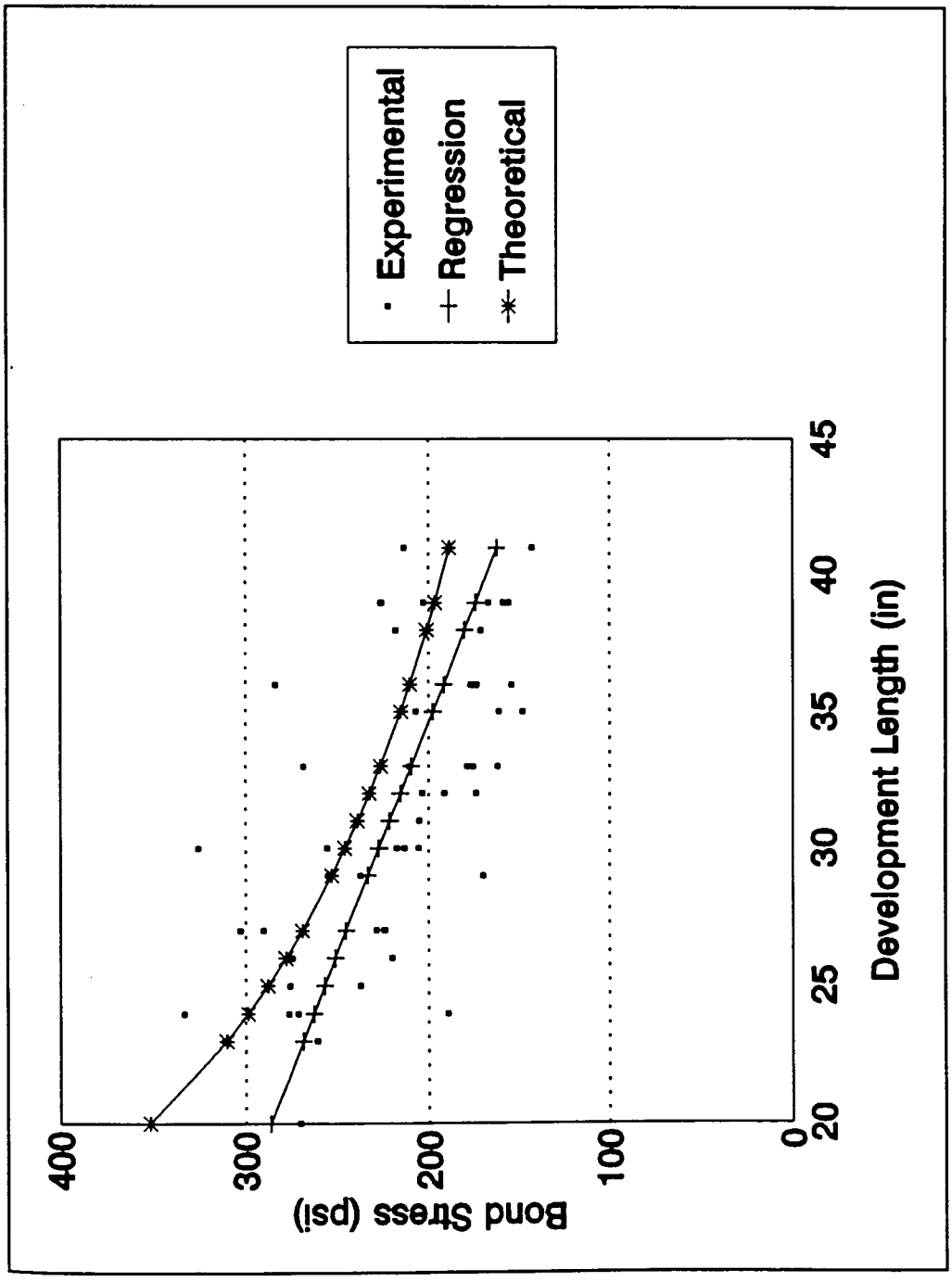


Figure 5.3. Development length versus bond stress, one-half-inch FCR, zero end slip criteria

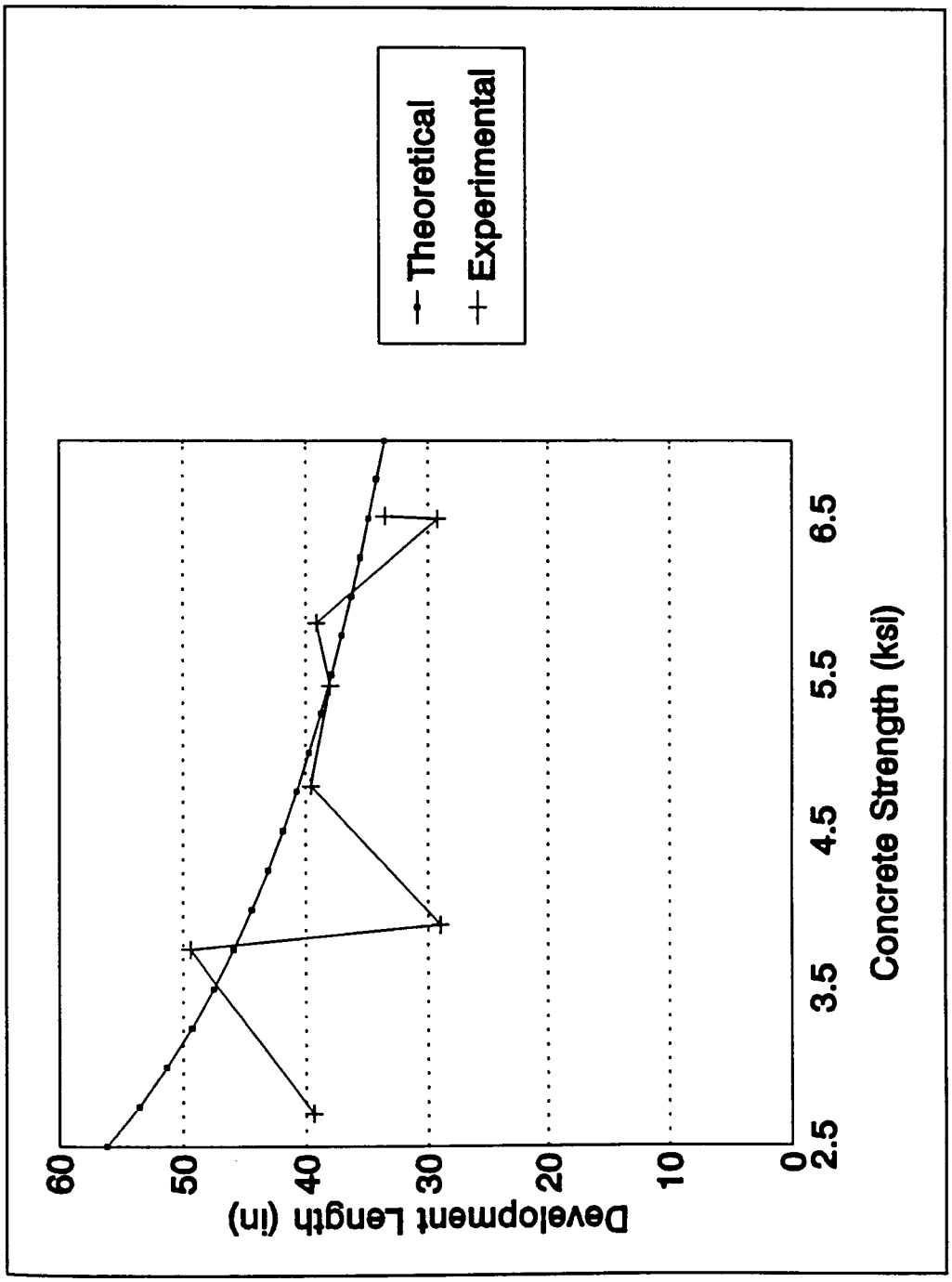


Figure 5.4. Concrete strength versus development length, three-eighths-inch FCR, zero end slip criteria

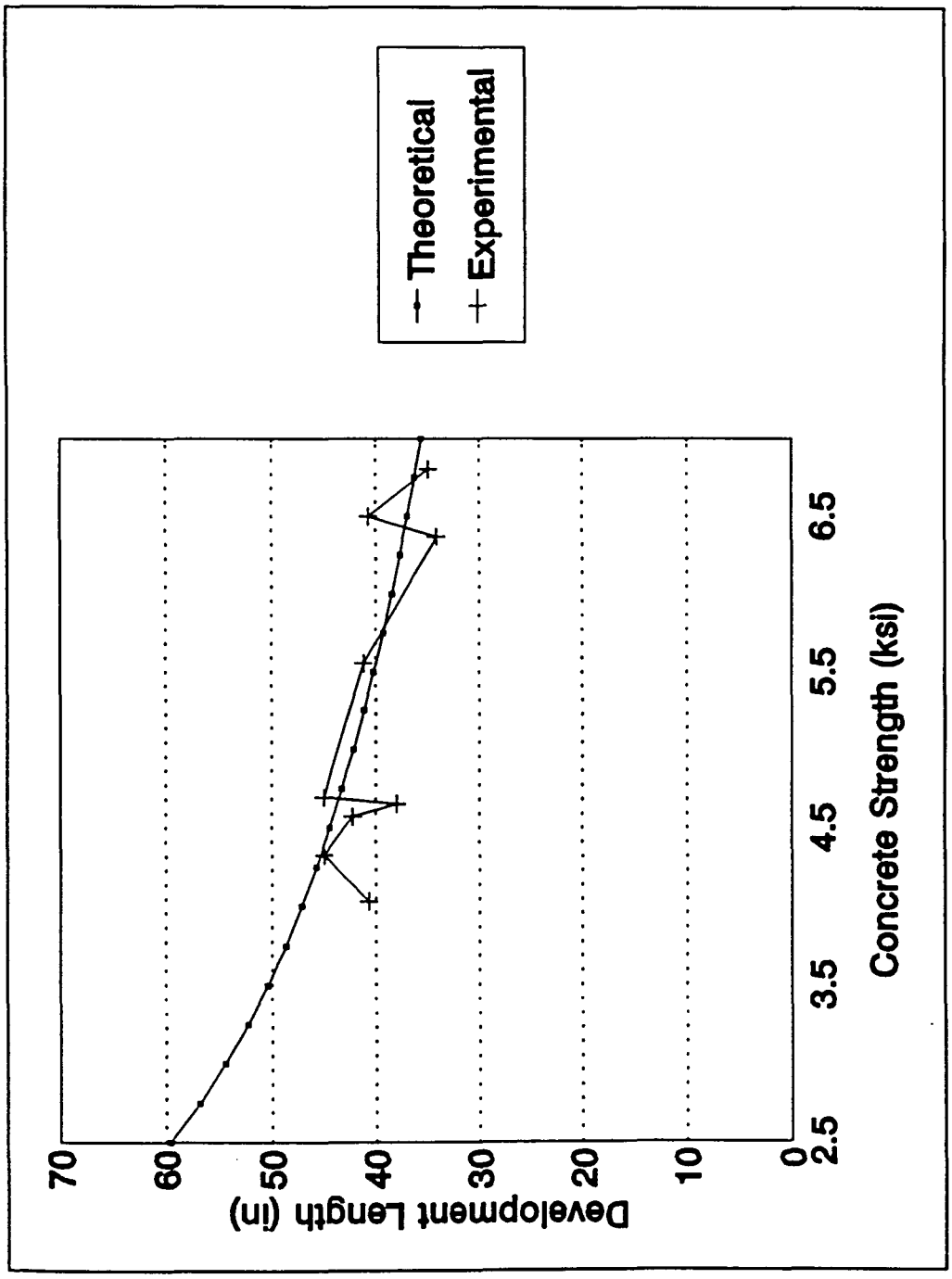


Figure 5.5. Concrete strength versus development length, one-half-inch FCR, zero end slip criteria

## 5.3 Derivation of the Development Length Equation One-Tenth-Inch End Slip Criteria

Derivation of a development length equation which allows end slip was a more difficult task than the deriving the zero end slip development length equation. Four of the beams tested with slip wires provided complete data for determining bond strength. These four beams were from the same test series, therefore they had similar concrete strengths. An equation for the bond stress of these beams could be derived but the equation would only be valid for one concrete strength. For this reason, bond strength had to be approximated by other methods.

At the beginning of the flexural testing, zero end slip was chosen as the criteria for development length. For this reason, all of the beams were cast with long embedment lengths to try to achieve zero end slip. FCR possesses a low adhesive bond strength, therefore the bars would slip slightly, even when a small load was applied. This fact caused the point of zero end slip to extend well past the point required to develop the bar. With the exception of the thermoplastic rods, the FCR was fractured in all of the beam specimens, even when end slips exceeded one-half of an inch.

If one-half-inch end slips were permitted, deflections would probably become excessive as well as result in larger

crack widths. For this reason a maximum end slip criteria of one-tenth inch was established. Also, each of the four slip wired beams that provided usable bond stress distribution data had internal slips less than one-tenth inch just past the point of maximum bond stress. Granted, the bar is being held by the section of the rod which extends to the end of the beam but the bond stress in this section of the beam is small enough that it was considered negligible from a standpoint of holding the bar from slipping.

From this point, derivation of the development length equation was similar to the derivation of the zero end slip development length equation. The derivation of bond stress for zero end slip incorporated the use of the average bond stress based on the tensile stress that the FCR obtained. The stress distribution plot shows that this criteria is very conservative since only a small section of the rod is exposed to high bond stresses. Figure 4.5 shows that the point of maximum bond stress occurs at around ten inches from the loaded end of the bar then drops off sharply after this point. On each of the four beams shown in Figure 4.5, the bond stress achieved most of the bond resistance at around one-half of the length of the bar. For this reason the bond stress was assumed to be acting on one-half of the length of the FCR. This criteria will double the bond stress which was available under the zero end slip criteria. New values for

the coefficients $X_1$ and $X_2$ used in Equation 5.14 were calculated based on this new bond stress.

Experimental development lengths were determined by checking when the beams achieved an end slip of one-tenth of an inch. Because of the lack of a large amount of data which corresponds to one-tenth-inch end slip, some of the data had to be extrapolated to reach one-tenth-inch end slip. This was done by performing a linear regression of embedment length versus maximum end slip for each set of data.

New values for $X_1$ and $X_2$ were calculated as being equal to 0.84 and 0.38, respectively. The ratio of $X_1$ to $X_2$ was held approximately equal to the ratio used for the zero end slip criteria. Solving Equation 5.14 with the new values of $X_1$ and $X_2$ produces Equation 5.17. The one-tenth-inch end slip criteria reduces the development length, $l_d$, required by twenty-eight percent.

$$L_d = \frac{0.42 f_u A_b}{C_b^2 \sqrt{f_c'}} \qquad \text{Eqn. 5.17}$$

Where:

$f_u$ = Ultimate bond stress in the FCR (psi)

$A_b$ = Cross-sectional area of the FCR ($in^2$)

$C_b$ = Circumference of the FCR (in)

$f_c'$ = Strength of the concrete (psi)

A plot of predicted bond stress versus experimental bond stress is shown in Figures 5.5 and 5.6 for three-eighths-inch FCR and one-half-inch FCR, respectively. Figures 5.7 and 5.8 show a plot of concrete strength versus development length for the two bar sizes.

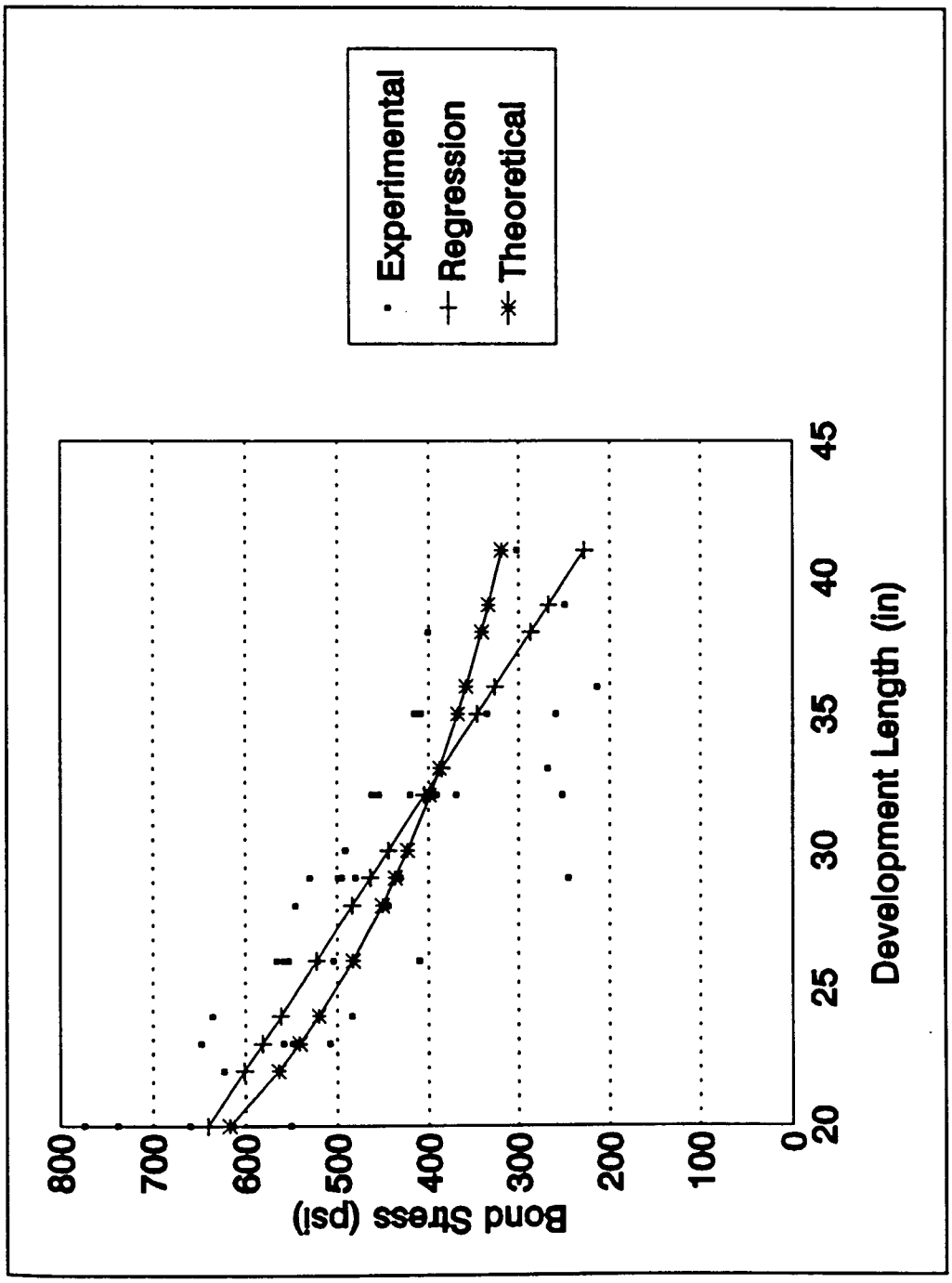


Figure 5.6. Development length versus bond stress, three-eighths-inch FCR, one-tenth-inch end slip criteria

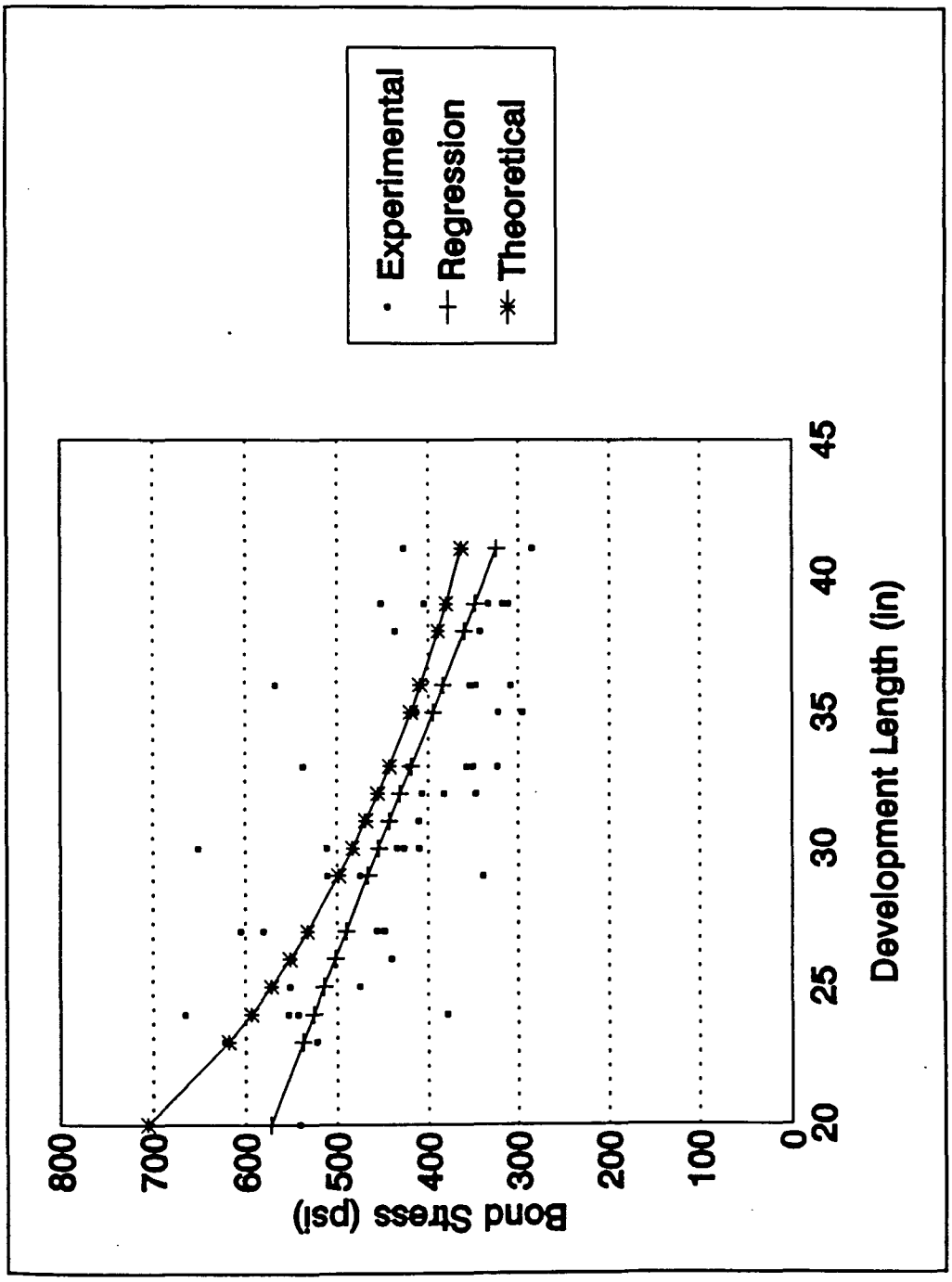


Figure 5.7. Development length versus bond stress, one-half-inch FCR, one-tenth-inch end slip criteria

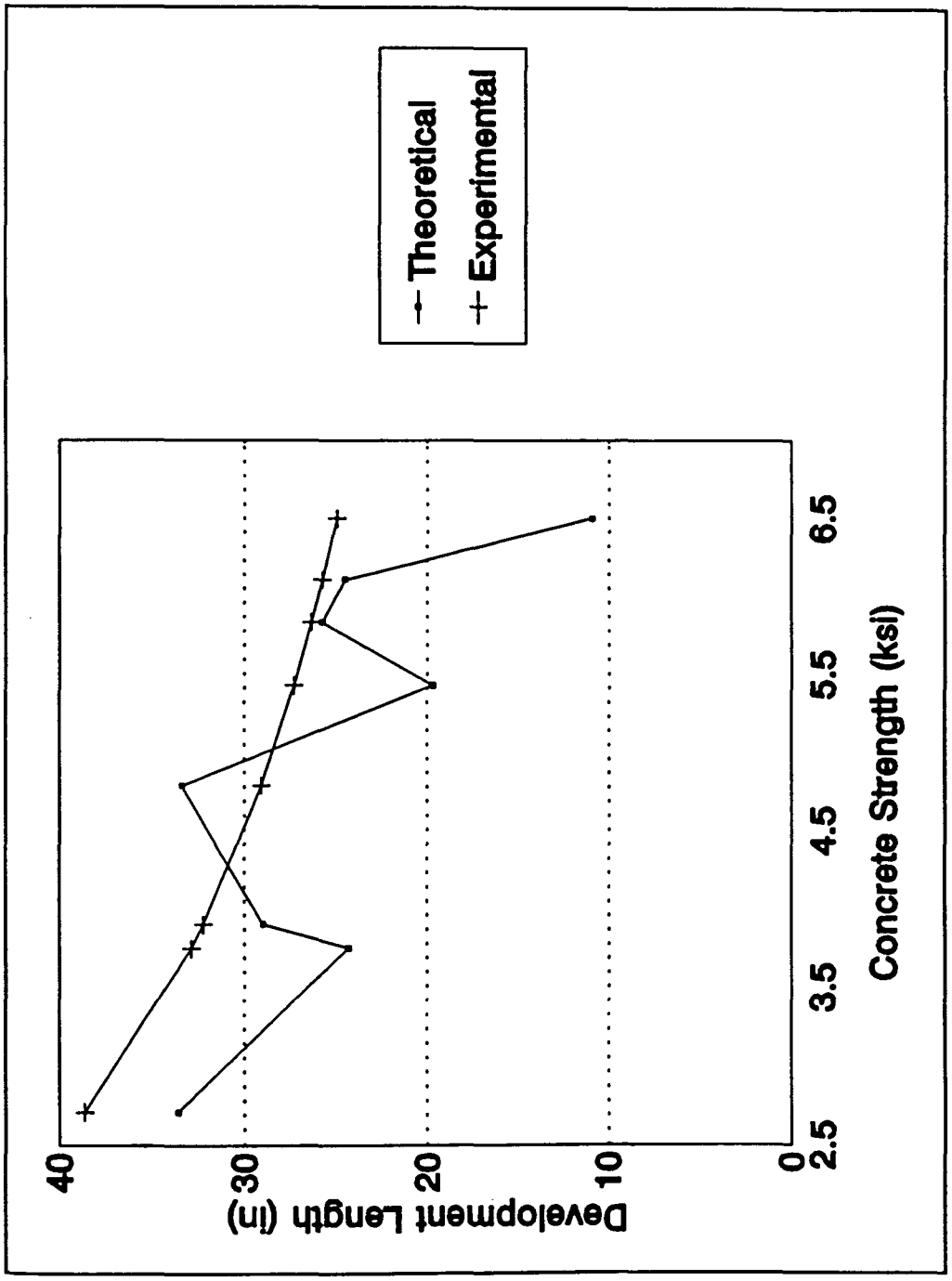


Figure 5.8. Concrete strength versus development length, three-eighths-inch FCR, one-tenth-inch end slip criteria

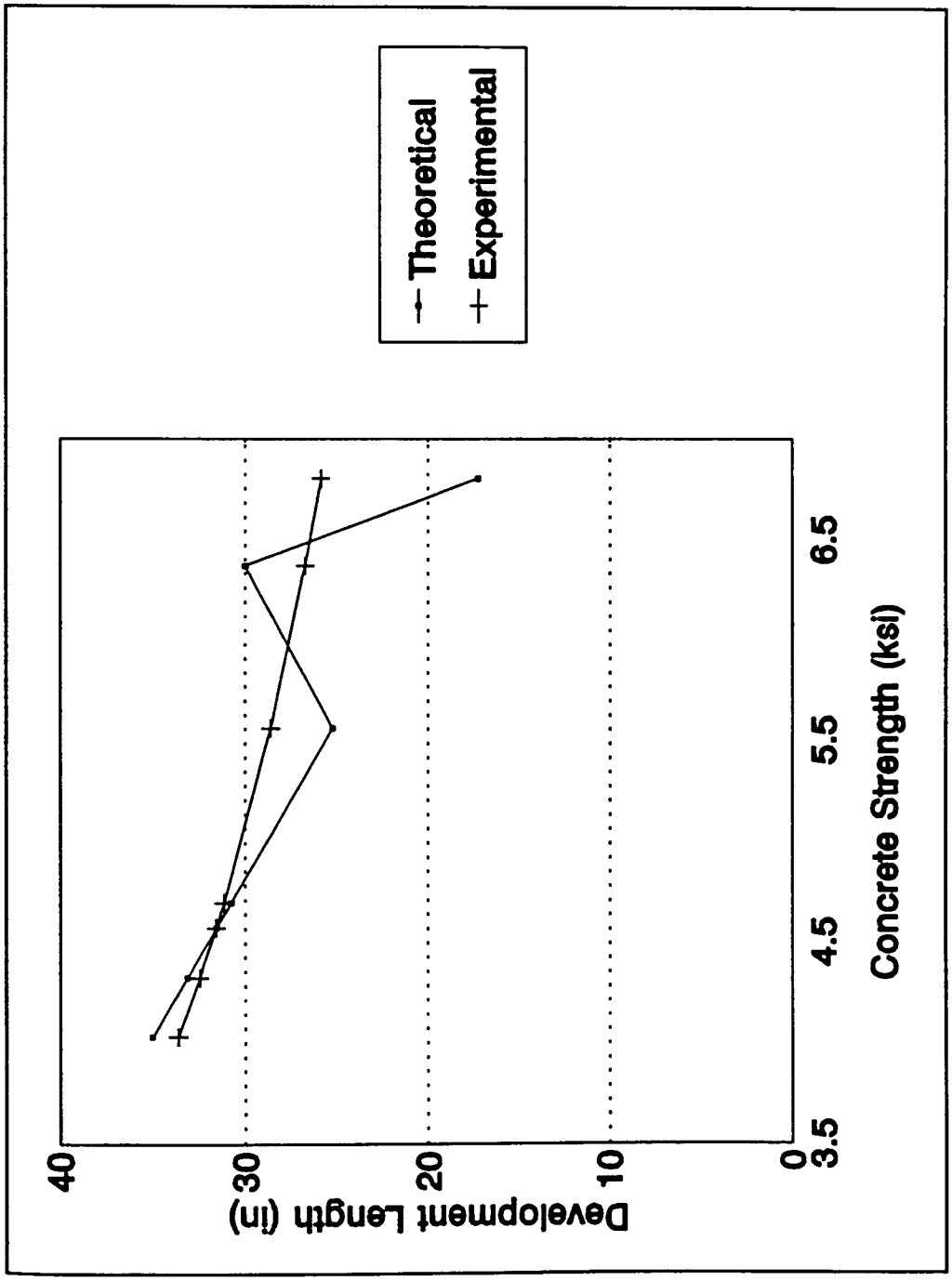


Figure 5.9. Concrete strength versus development length, one-half-inch FCR, one-tenth-inch end slip criteria

# 6 FLEXURAL TESTING

## 6.1 Test Frame

A test frame was designed and constructed at the beginning of the project. Originally the frame was to be designed for a fifty-kip load at each of the load points but because frame material was limited to material on hand, the frame was constructed stronger than the original design had required.

The lab that was used did not have a tie-down floor so the frame had to contain both the load points and the reaction points. The back reaction and the load members were fixed in position but the cantilever support was adjustable. Most of the steel framing members were either W24x76 or W21x73 steel. However, the cantilever support was made from W18x65 stock.

The beams were loaded into the test frame using a forklift with a long boom connected to the forks. A pin was placed under the first reaction point and a roller was placed under the cantilever section.

The beams were loaded with hydraulic loading rams which were both connected to the same pump to insure that the pressures in the rams were the same at each load point. The load was transferred from the rams to the beam through a loading member which straddled the beam and rested on both

sides of the dogbone. Neoprene was placed between the loading member and the dogbones so as to provide uniform pressure bearing to the concrete surfaces of the dogbones. A diagram of the test frame and loaded member is shown in Figure 6.1.

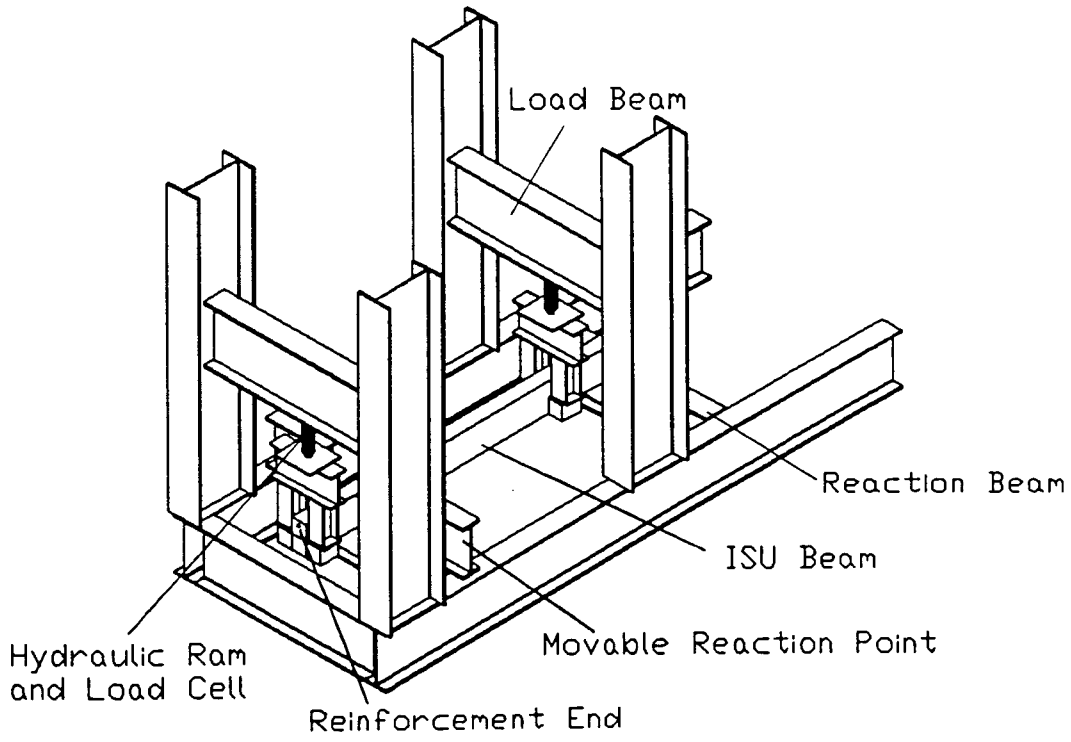


**Figure 6.1. Frame with ISU Beam loaded**

All deflections and bar movements were first monitored using dial gages. This created problems because the load would drop slightly while the readings were being recorded by the workers. Also the load was monitored using a voltmeter which had readings that varied while the pump operator tried to keep the load steady. For this reason, electronic measuring devices were used to achieve more consistent readings. The dial gages were replaced with direct current displacement transducers (DCDT's), and the load cell was read directly into the computer. Not only did this electronic equipment yield more accurate data but it also reduced testing time. All electronic devices were calibrated before testing of the beams started.

### 6.2 Results of Simply Supported Beam Tests

A comparison of simply supported beams versus ISU beams was desired so six simply supported beams were cast. Both steel and FCR were used for reinforcement. Two of the beams were cast with a single reinforcing bar and the other four beams were cast with two reinforcing bars. One-half-inch FCR and number-three reinforcing bars were used for the reinforcement. The beams cast were fourteen-feet long, six-inches wide, and twelve-inches high.

The test frame was modified to allow for the loading of the beams at the quarter points, so as to approximate a uniform loading. Deflections at the load points and the center of the beam were measured. Complete ultimate failure of some beams could not be achieved due to the large displacement which exceeded the six-inch stroke capacity of the rams. The load-deflection curves are plotted in Figures 6.2 and 6.3. These deflections were measured at midspan. These figures show the difference in deflection behavior between the steel and the FCR.

The beams reinforced with FCR obtained a higher load than the beams reinforced with steel. This fact is due to the slightly larger cross-sectional area and tensile strength of the FCR. The beam tested with steel reinforcement deflected less up to the yield point of the steel. At this point, because the steel is more ductile than FCR, the beam did not fail but continued deflecting. When the FCR reached it's ultimate tensile load the beam failed.

The lower deflection of the beams reinforced with steel was a result of two differences in the materials. Steel has a higher modulus of elasticity than FCR therefore less deflection was expected. Deformed steel also has greater bond strength than FCR, therefore less of the steel bar was being elongated which resulted in a lower deflection of the beams reinforced with steel.

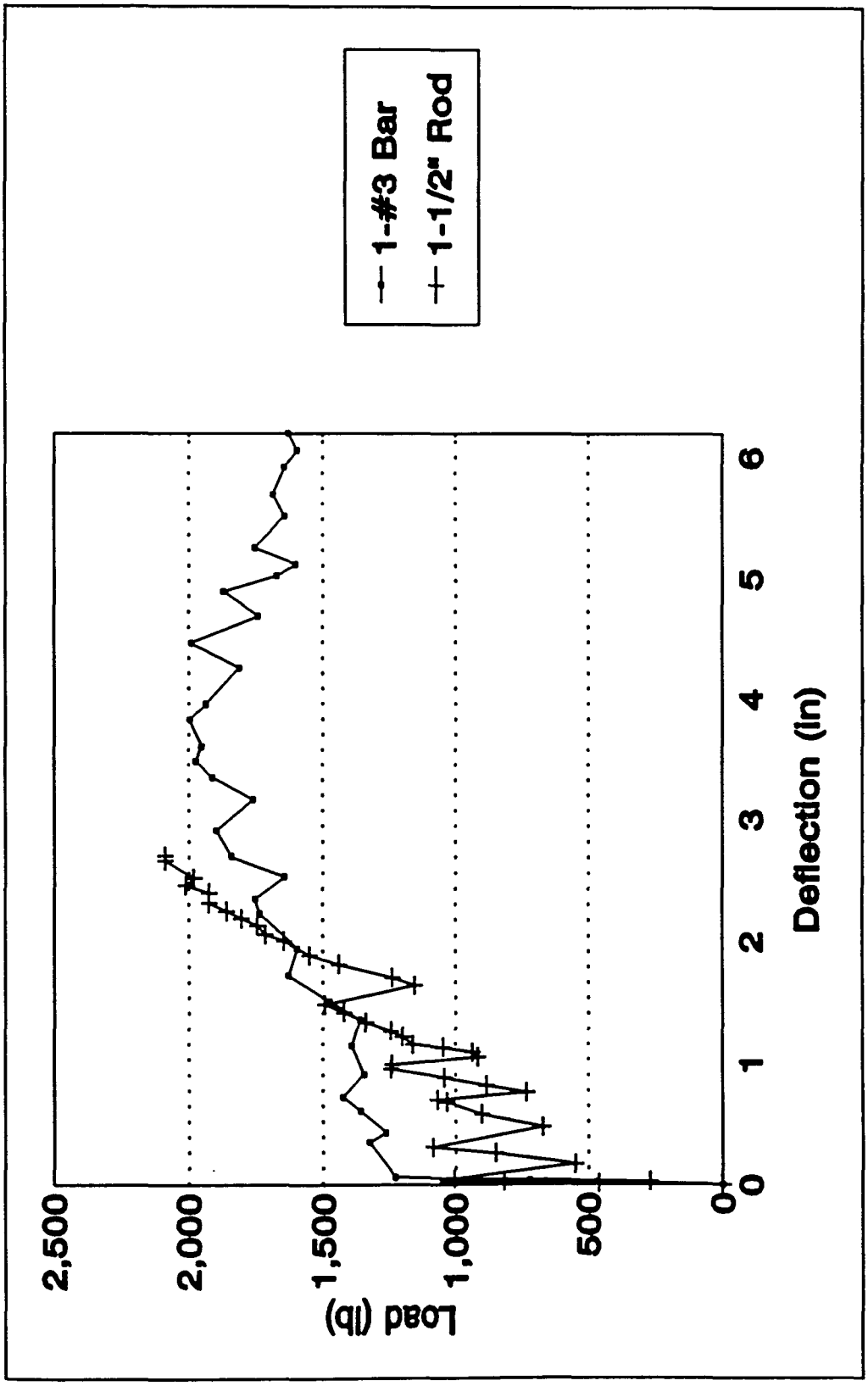


Figure 6.2. Load-deflection curves for simply supported beams, one number-three rebar versus one, one-half-inch FCR

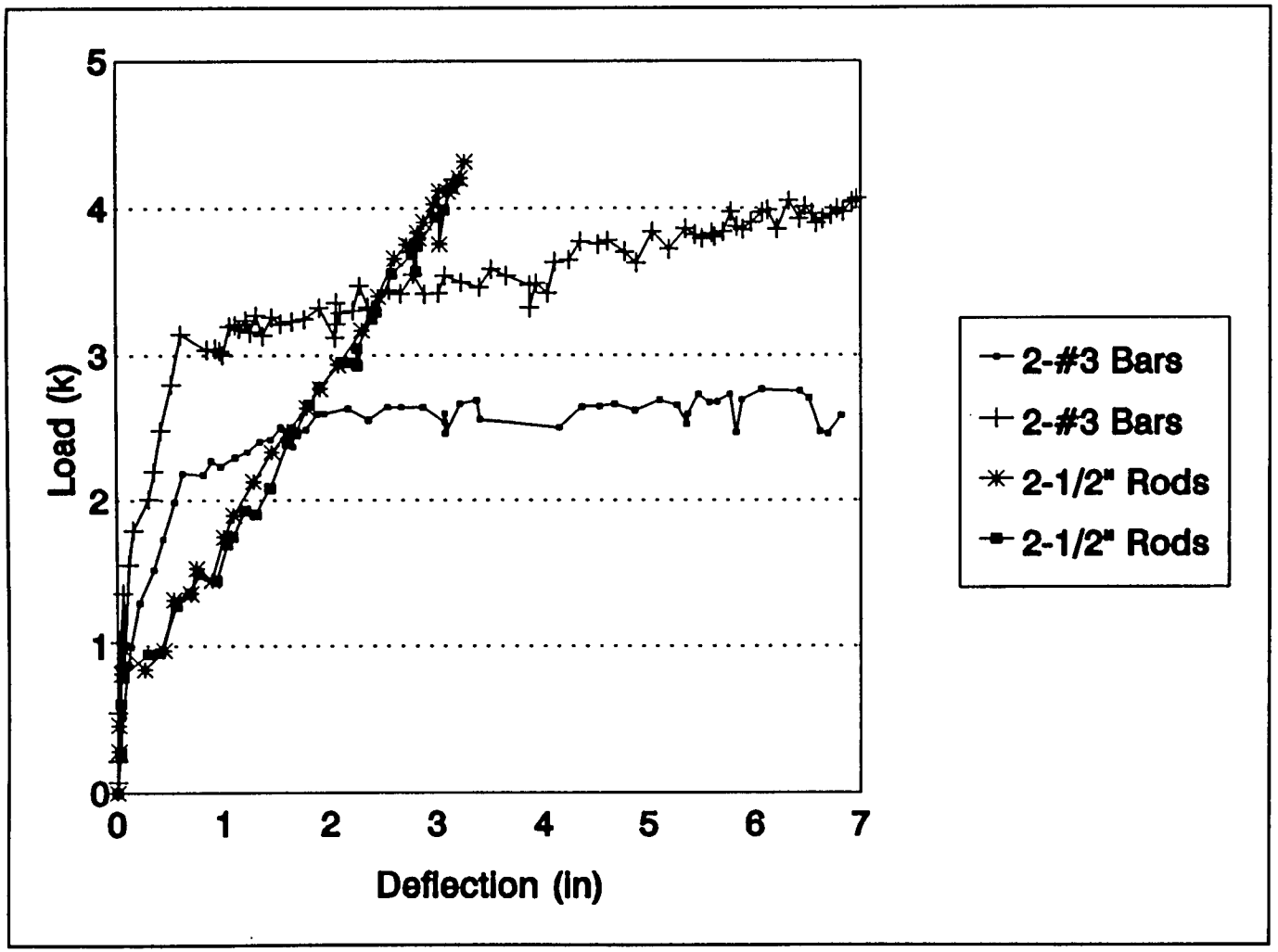


Figure 6.3. Load-deflection curves for simply supported beams, two number-three rebars versus two, one-half-inch FCRs

## 6.3 Results of the ISU Beam Tests

### 6.3.1 Load-Deflection Behavior

ISU Beams exhibited four distinct phases when tested. These phases are shown in Figures 6.4a and 6.4b.

Phase A shows the beam characteristics before the concrete cracked. During this phase the load-deflection curves for beams reinforced with FCR was similar to the load-deflection curves for the beams reinforced with steel.

After the first major crack occurred, the deflection of the beam reinforced with FCR increased sharply and the load was reduced because of the softening of the hydraulic loading system. This phenomena is shown in Phase B.

After this point the deflection increased with load but at a decreasing rate until the rod reached its ultimate strength as shown by Phase C. When the deflections increase without a corresponding increase in load, the rod will pull out. This phenomena is shown in Phase D of Figure 6.4b.

Phase D of Figure 6.4a can be explained by the fact that some of the strands in the rod are failing while others are not. Normally, when the rod failed, the fracturing of each of the individual strands could be heard as the rod was failing. FCR exhibited a less ductile failure than that of beams reinforced with steel rods. The tangential straight line demonstrates a perfectly elastic load-deflection curve.

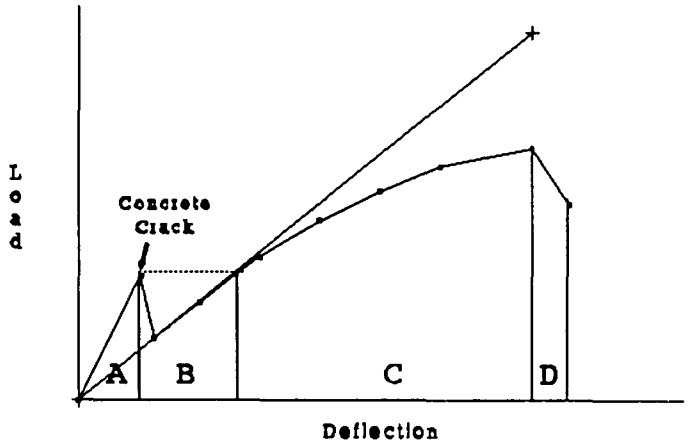


Figure 6.4a. Typical load-deflection curve for thermoset FCR

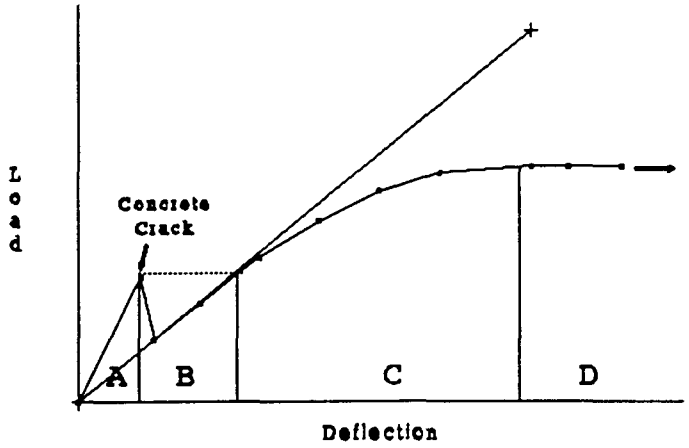


Figure 6.4b. Typical load-deflection curve for thermoplastic FCR

### 6.3.2 Steel Reinforcing Bars versus FCR

Two ISU beams were cast with number-three reinforcing bars to compare with FCR-reinforced beams. The deflection of the FCR-reinforced beams was greater than that of the beams reinforced with steel. This larger deflection was caused by a combination of two properties: development length and modulus of elasticity. The modulus of elasticity was lower in the FCR than in steel but this was only part of the problem. Because a longer development length was required to develop the FCR, more of the rod was in tension and was being allowed to elongate.

The longer development length and lower modulus of elasticity of FCR, when compared to steel, were also the reasons that the load dropped off substantially when the concrete cracked as the beam was loaded. The load dropped off slightly when the concrete cracked when steel reinforcement was tested but not nearly as much as with the FCR. When the tensile load was transferred from the concrete to the FCR, the rod elongated and the adhesive bond between the concrete and the rod was lost for around six inches from the loaded end of the rod in each direction. This loss of bond increased the elongation of the FCR when compared to a similar steel rod and allowed the cantilever section of the beam to deflect with a corresponding drop in load. Figure

6.5 shows a schematic of the bond stress distribution for steel reinforcement and FCR. The beams reinforced with steel develop a higher peak bond stress with a correspondingly shorter development length than beams reinforced with FCR. The above-mentioned behavior is shown by the load-deflection curves for a twenty-four and twenty-eight-inch embedment length. These curves are shown in Figures 6.6 and 6.7. Deflections were measured at the free end of the cantilever section.

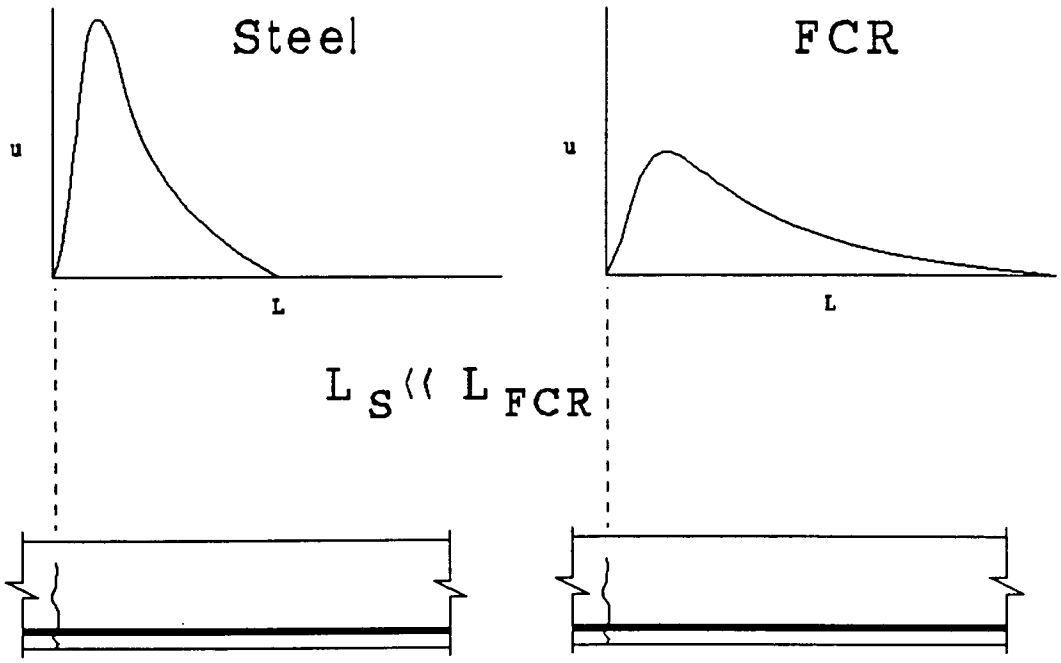


Figure 6.5. Stress distribution for steel and FCR

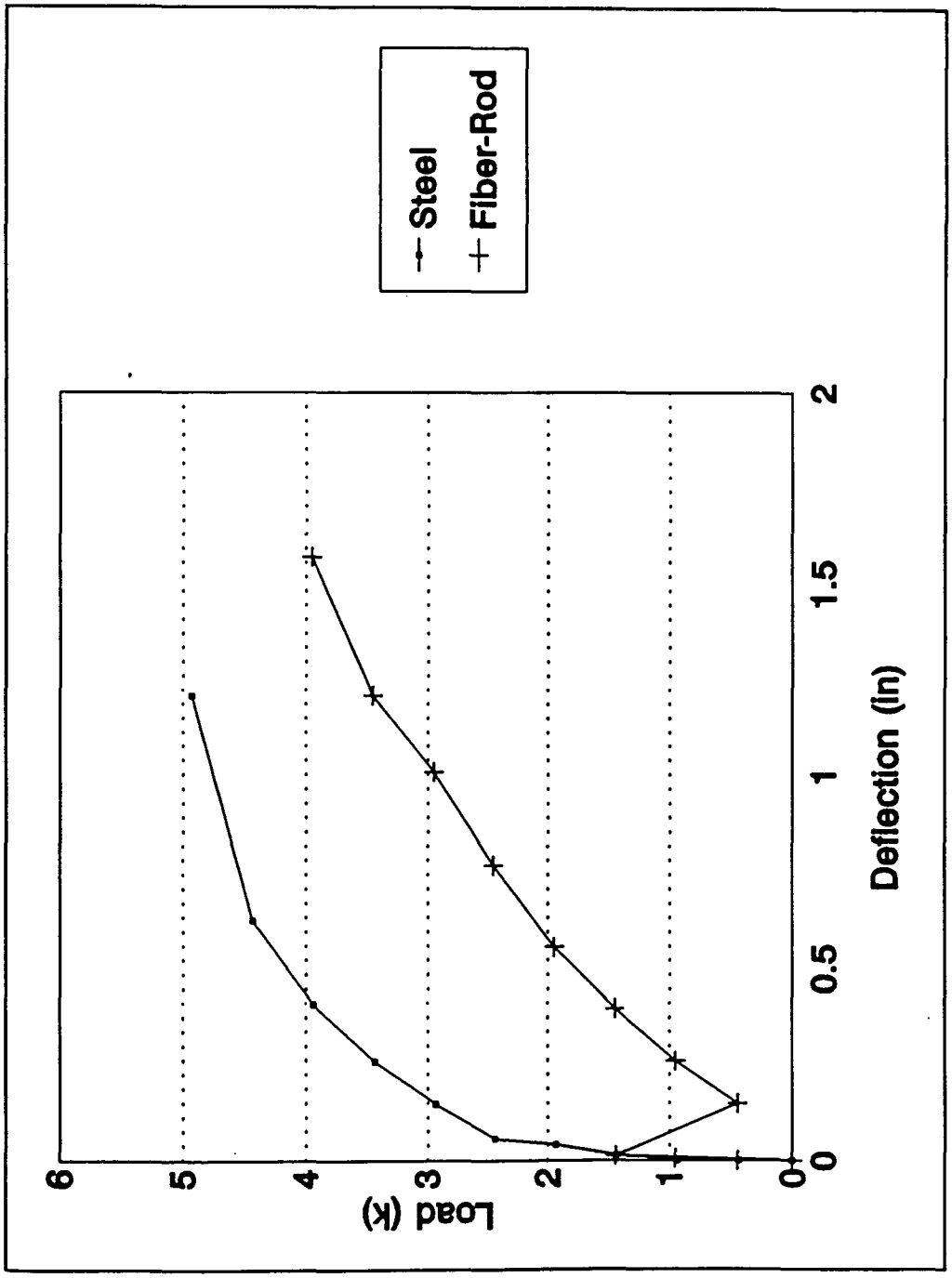


Figure 6.6. Load-deflection curves, ISU Beams, number-three rebar versus three-eighths-inch FCR, twenty-four-inch embedment length

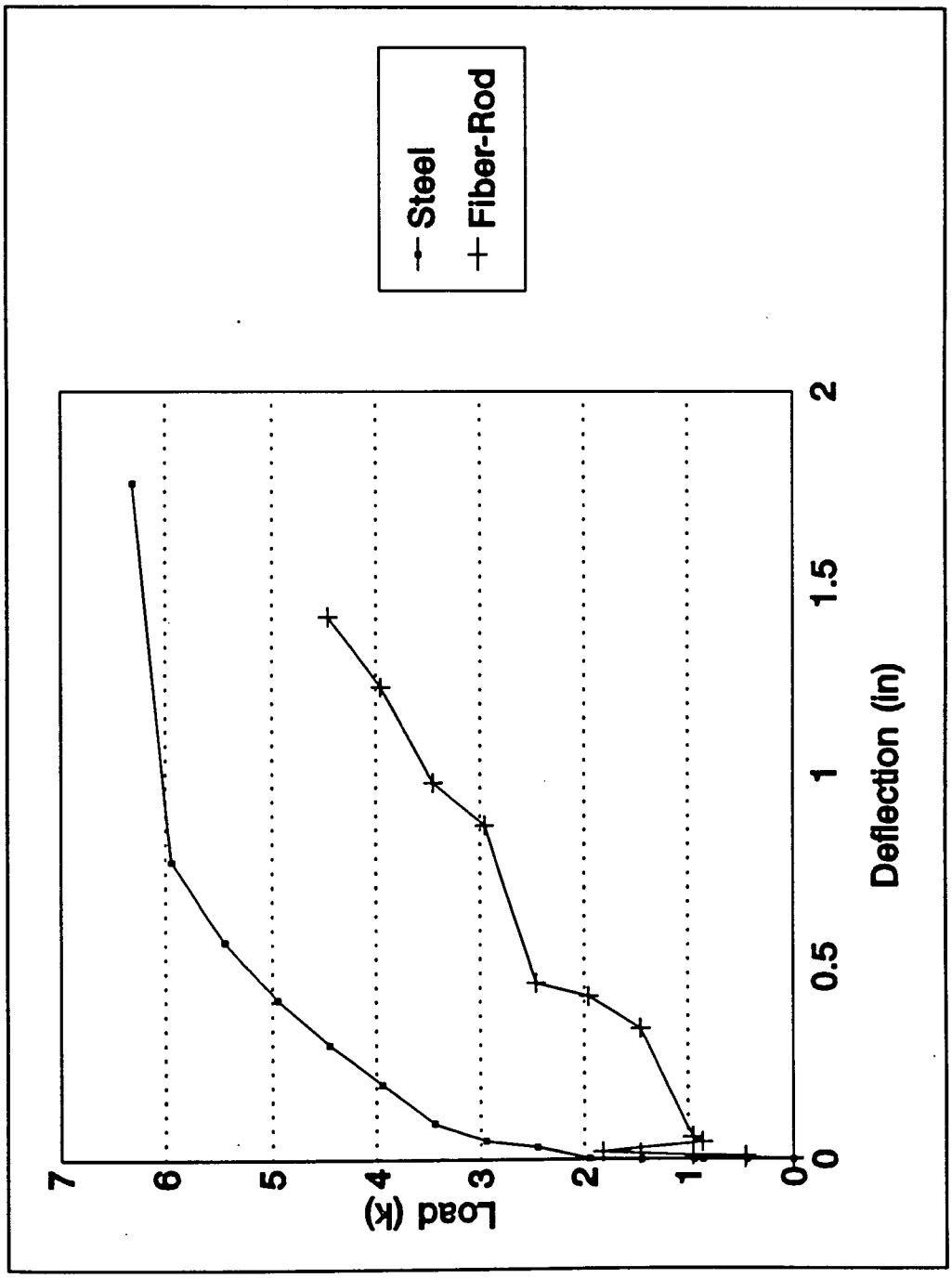


Figure 6.7. Load-deflection curves, ISU Beams, number-three rebar versus three-eighths-inch FCR, twenty-eight-inch embedment length

### 6.3.3 Prestressing Strands versus FCR

The cross-sectional shape of a prestressing strand is similar to the cross-sectional shape of FCR. For this reason, beams were also cast with prestressing strands. The data from these tests was then compared to FCR beams cast with the same embedment length and concrete strength. One test series of six beams was cast with two of the beams having FCR, two of the beams having five-eighths-inch prestressing strands, and the last two having two five-eighths-inch epoxy-coated prestressing strands. The embedment lengths tested were twenty-five and thirty-one inches.

The beams with prestressing strands withstood a larger load than those with the FCR. For this reason, the beams could not be taken to failure of the strands. These beams failed either by shear in the concrete or by a fracture of the dogbones. Shear reinforcement was used after this point for specimens that could withstand the larger loads.

Deflection of the beams reinforced with the prestressing strands was smaller than that of the beams reinforced with FCR. The beams cast with epoxy-coated prestressing strands exhibited a similar drop in load when the concrete cracked as the beams cast with FCR showed. The drop in load was not, however, as large as the drop in load with the FCR beams.

The prestressing strand without epoxy coating lost very little load when the concrete cracked and also exhibited less deflection than both the epoxy-coated prestressing strand and the FCR. The results of these tests are shown in Figures 6.8 and 6.9. Deflections were measured at the free end of the cantilever section.

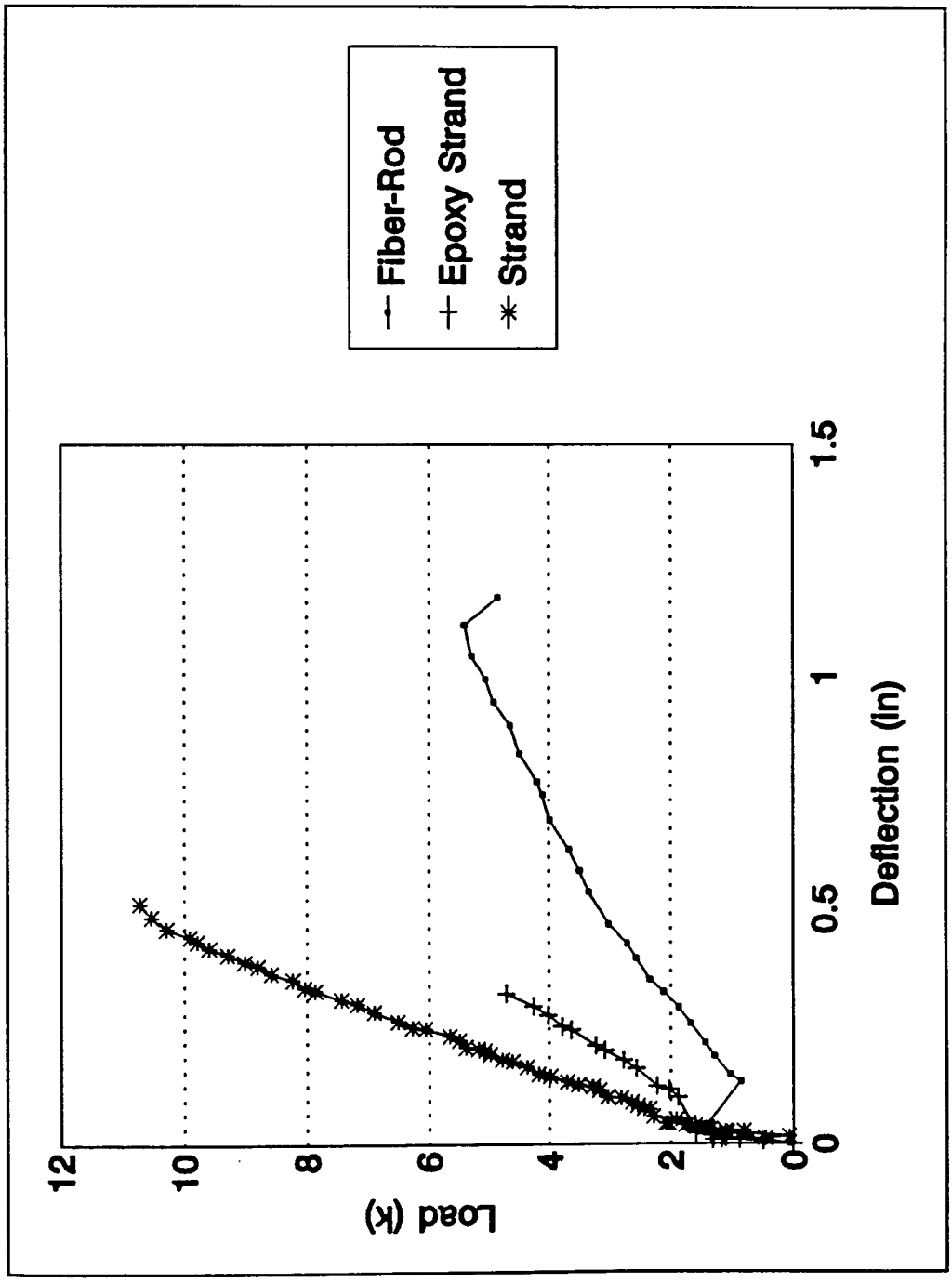


Figure 6.8. Load-deflection curves, ISU Beams, prestressing strands versus one-half-inch FCR, twenty-five-inch embedment length

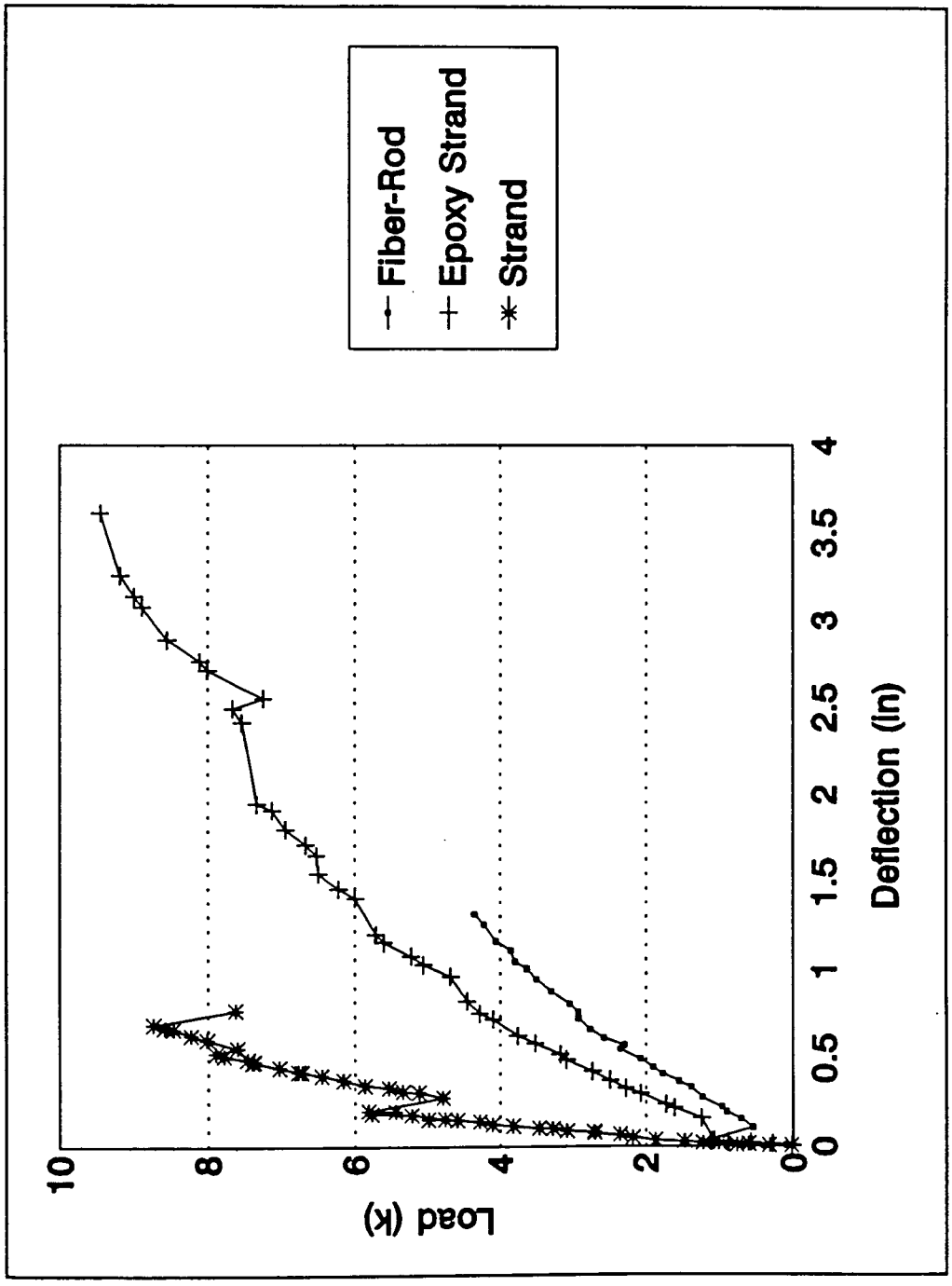


Figure 6.9. Load-deflection curves, ISU Beams, prestressing strands versus one-half-inch FCR, thirty-one-inch embedment length

### 6.3.4 Oiled versus Unoiled FCRs

A knowledge of the adhesive bond strength and frictional bond strength was desired so one test series consisted of six test beams in which one-half of the beams had the FCR coated with oil prior to casting. The oil broke the adhesive bond between the bar and the concrete. The reinforcing that was used for these tests was one-half-inch FCR. The embedment lengths used were twenty-four, twenty-eight, and thirty-two inches.

The oil did not effect the ultimate strength of the beams but did make the point of first end slip occur at a lower load, thus verifying that the adhesive bond had only a small effect on the total bond stress. The oiled FCR slipped sooner and slipped more than the unoiled FCR. A small reduction in frictional bond stress could also be assumed with the addition of oil. This reduction was considered to be negligible because only a small amount of oil was applied and this oil probably dissipated into the concrete. The results of these tests are presented in Figures 6.10, 6.11, and 6.12. Deflections were measured at the free end of the cantilever section.

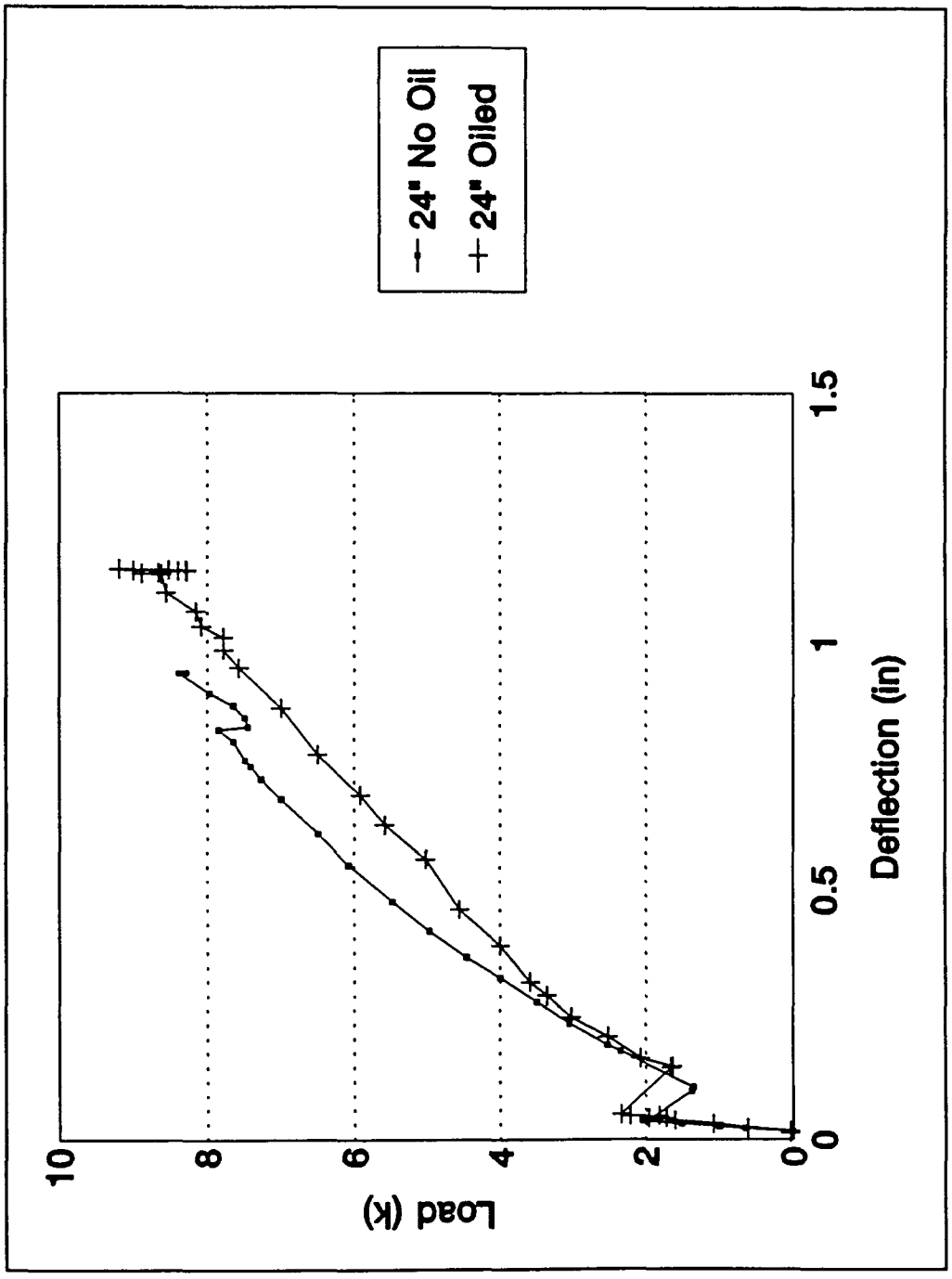


Figure 6.10. Load-deflection curves, ISU Beams, oiled versus unoiled, one-half-inch FCR, twenty-four-inch embedment length

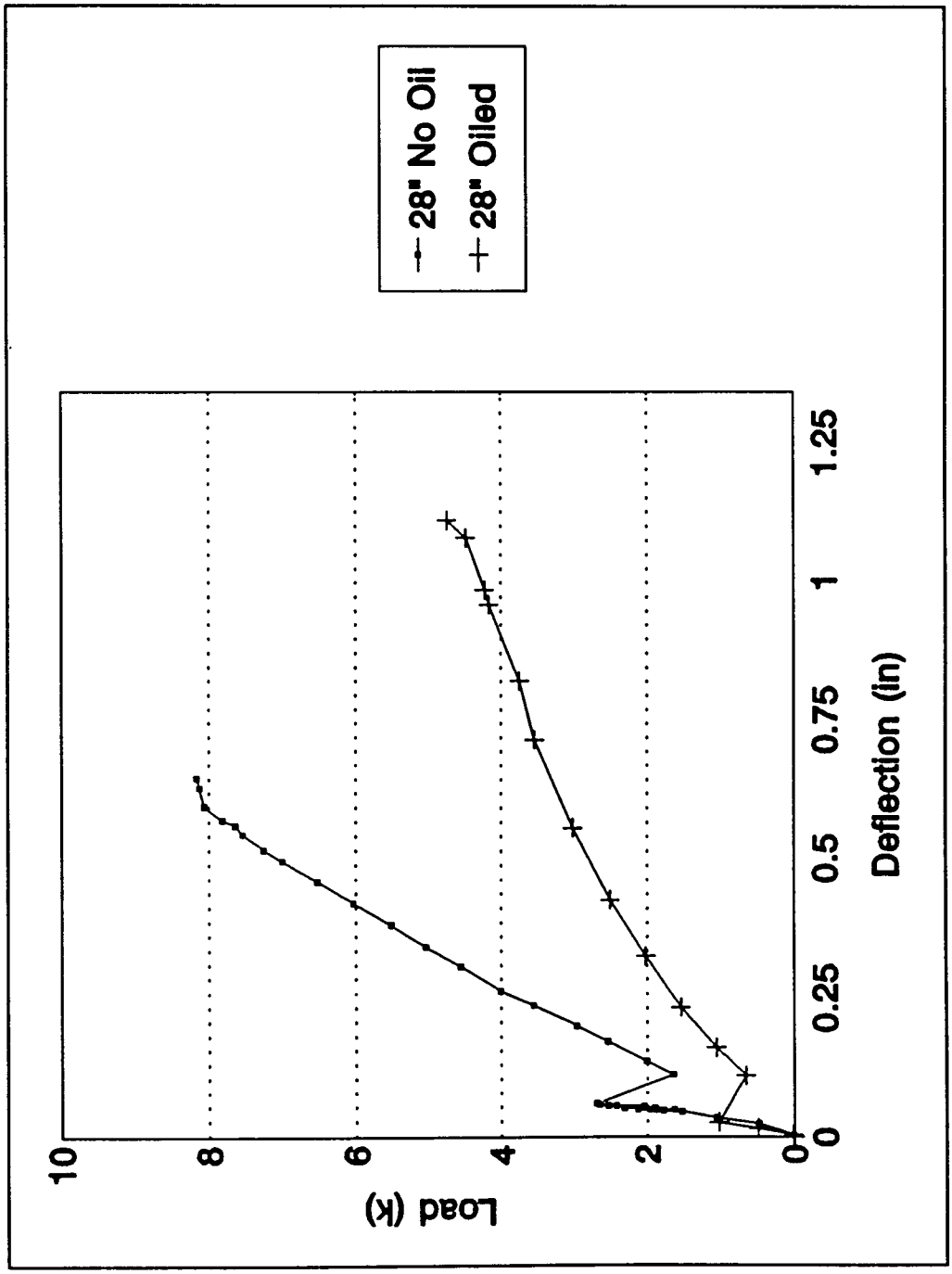


Figure 6.11. Load-deflection curves, ISU Beams, oiled versus unoiled, one-half-inch FCR, twenty-eight-inch embedment length

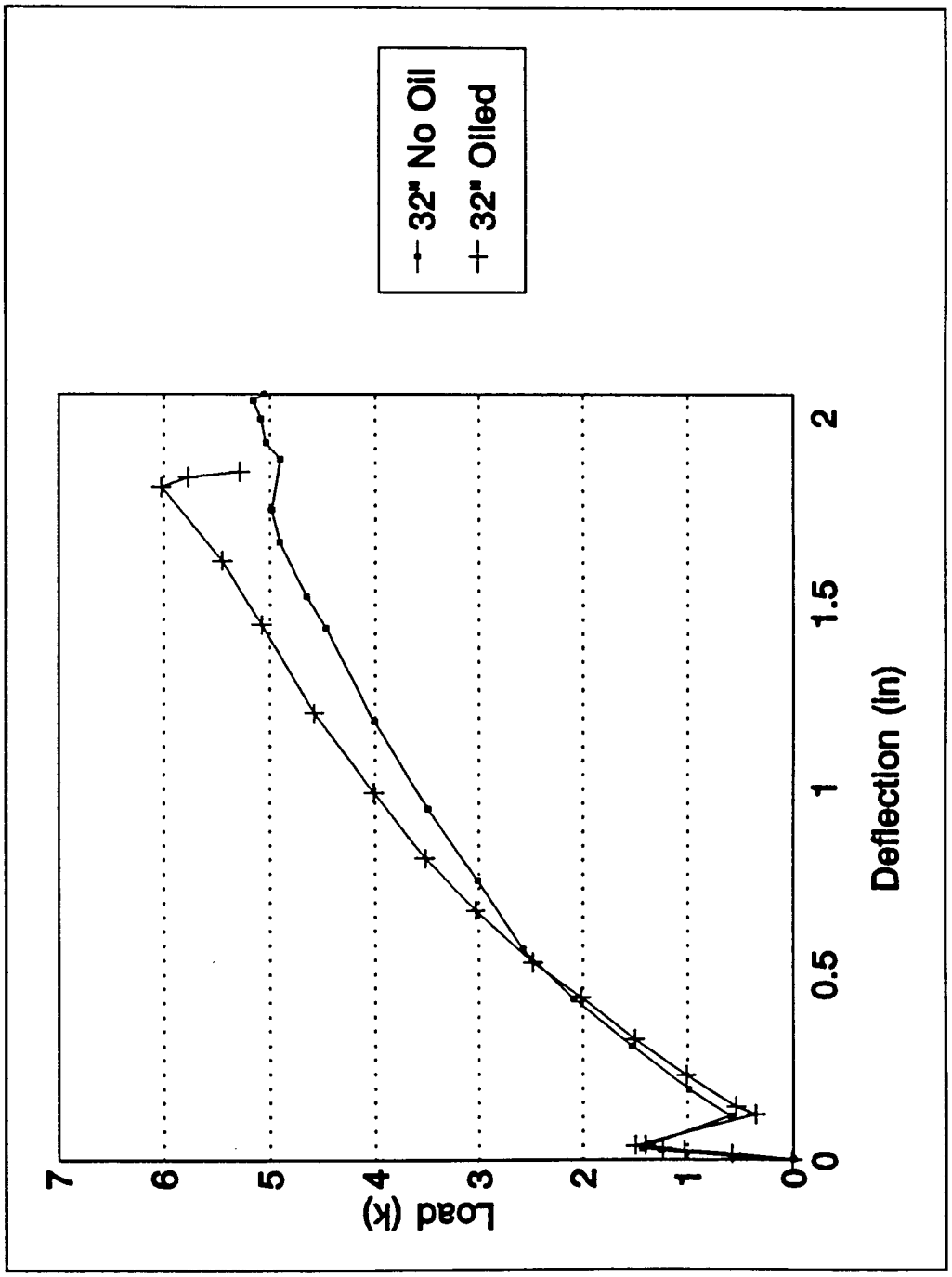


Figure 6.12. Load-deflection curves, ISU Beams, oiled versus unoiled, one-half-inch FCR, thirty-two-inch embedment length

### 6.3.5 Results of the ISU Beam Tests: Three-Eighths-Inch FCR

Forty-seven beams were tested using the three-eighths-inch FCR. Of these forty seven, seven of the beams had slip wires installed. The slip-wiring technique had not been perfected when these beams were cast therefore the slip wire data was poor. For this reason no useful slip wire data was collected for three-eighths-inch FCR. Embedment lengths of twenty to thirty-five inches were tested with concrete strengths ranging from 2500 psi to 6500 psi.

All of the beams cast with FCR exhibited a decrease in load when the concrete cracked. Beams reinforced with steel reinforcing bars or prestressing strands did not lose as much load as the FCR. The larger drop in load was caused by the lower modulus of elasticity of FCR when compared with steel and the lower bond strength of FCR when compared to steel. The lower modulus of elasticity allowed the cantilever section of the beam to deflect more than beams reinforced with steel which in turn, allowed the load to decline. Also with the lower bond strength of the FCR, more of the rod was placed in tension which allowed more of the FCR to elongate thus producing more deflection than beams that were cast with steel reinforcement. Load versus end deflection plots are shown in Figures 6.13 through 6.18.

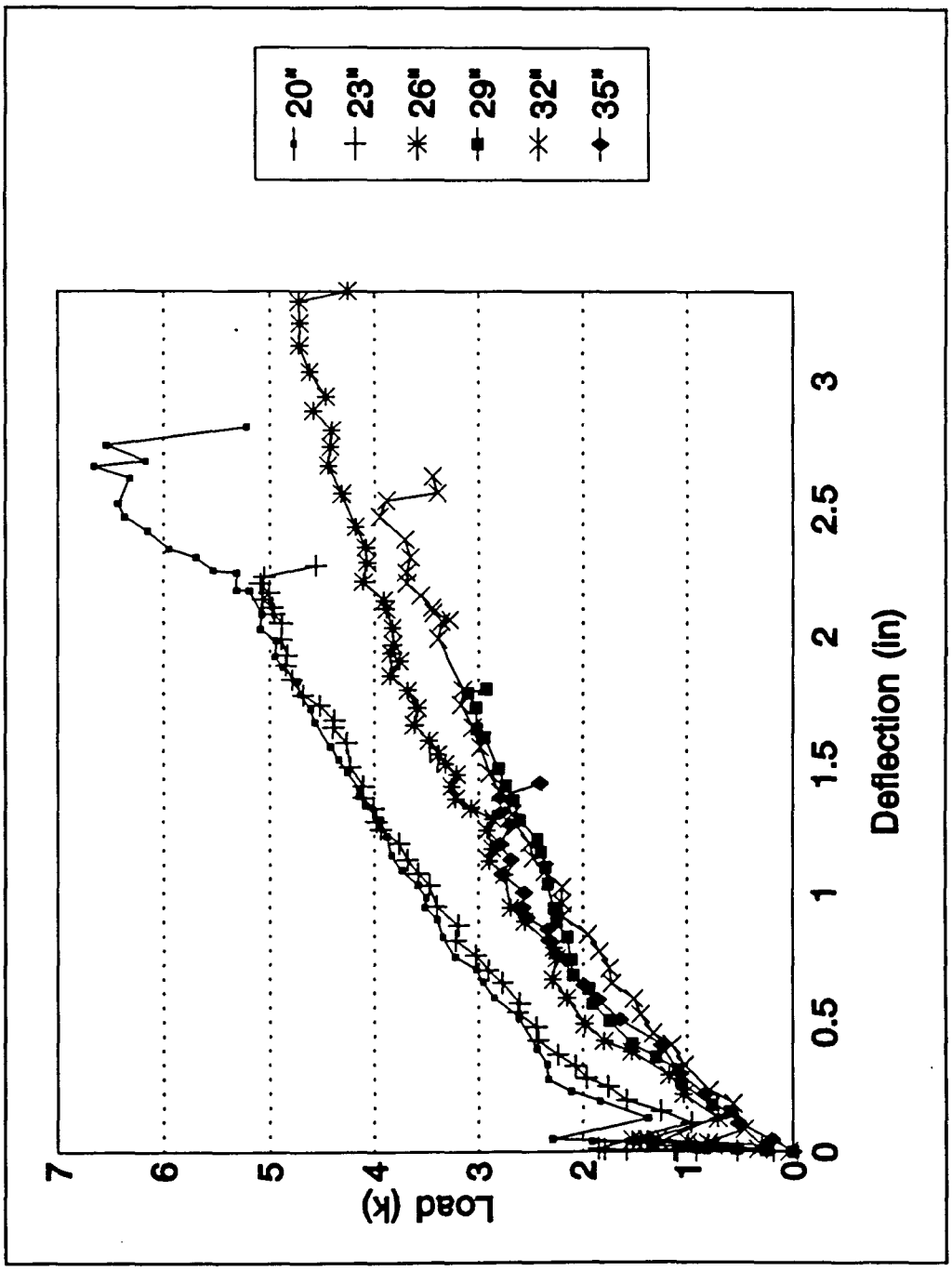


Figure 6.13. Load-deflection curves, ISU Beams, three-eighths-inch FCR, 2707-psi concrete strength, 20-35 inch embedment

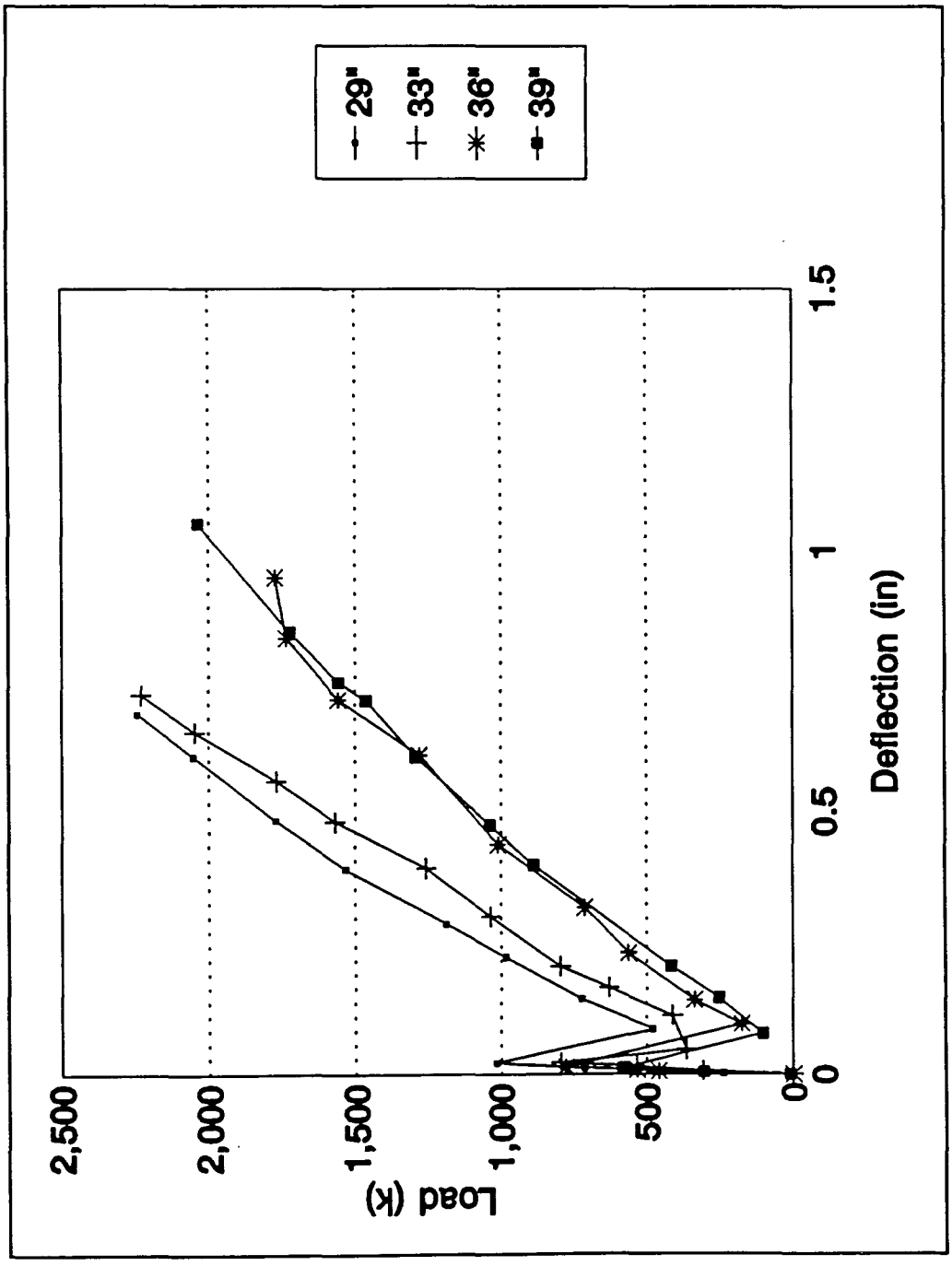


Figure 6.14. Load-deflection curves, ISU Beams, three-eighths-inch FCR, 3902-psi concrete strength, 29-39 inch embedment

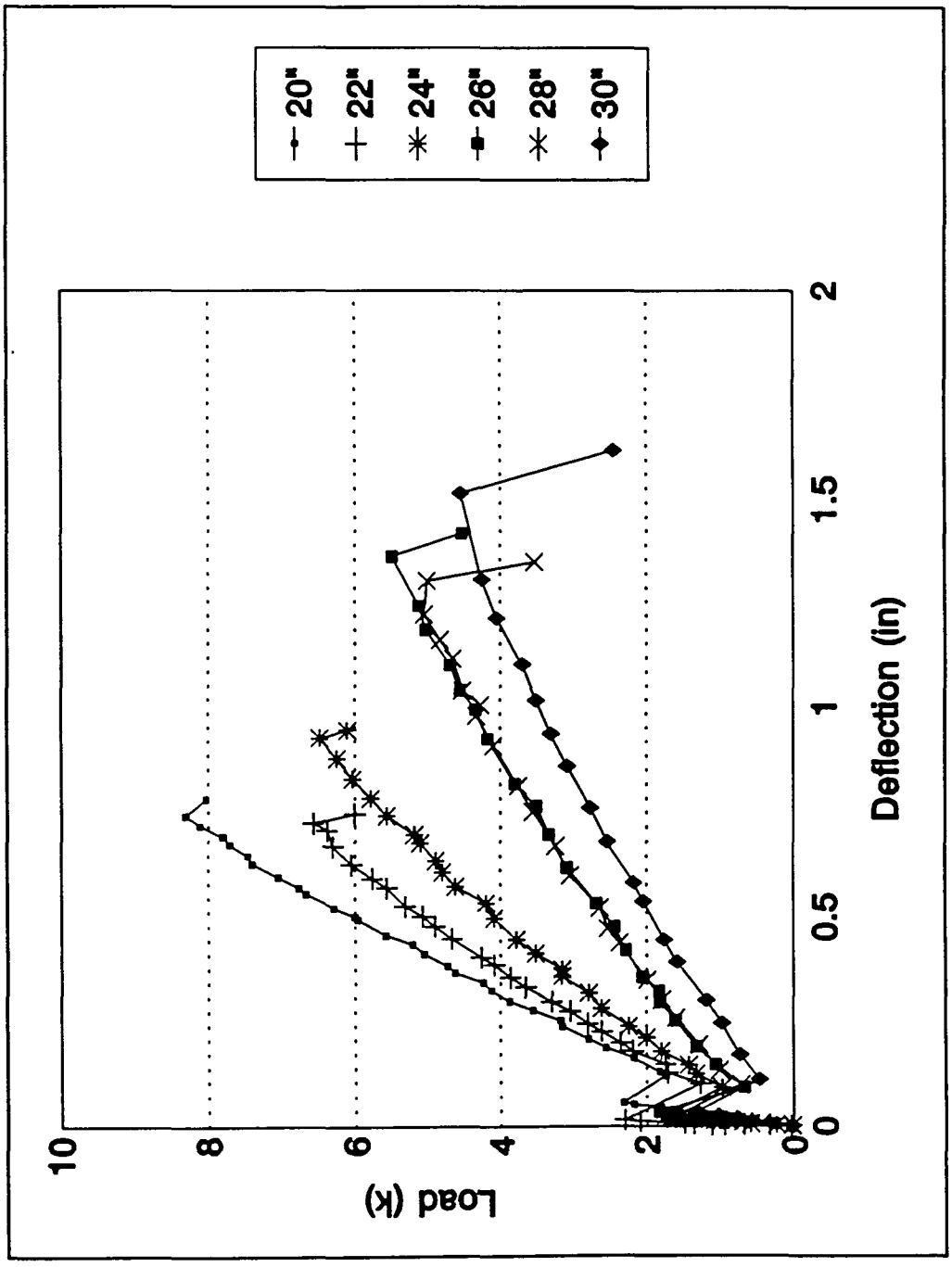


Figure 6.15. Load-deflection curves, ISU Beams, three-eighths-inch FCR, 6497-psi concrete strength, 20-30 inch embedment

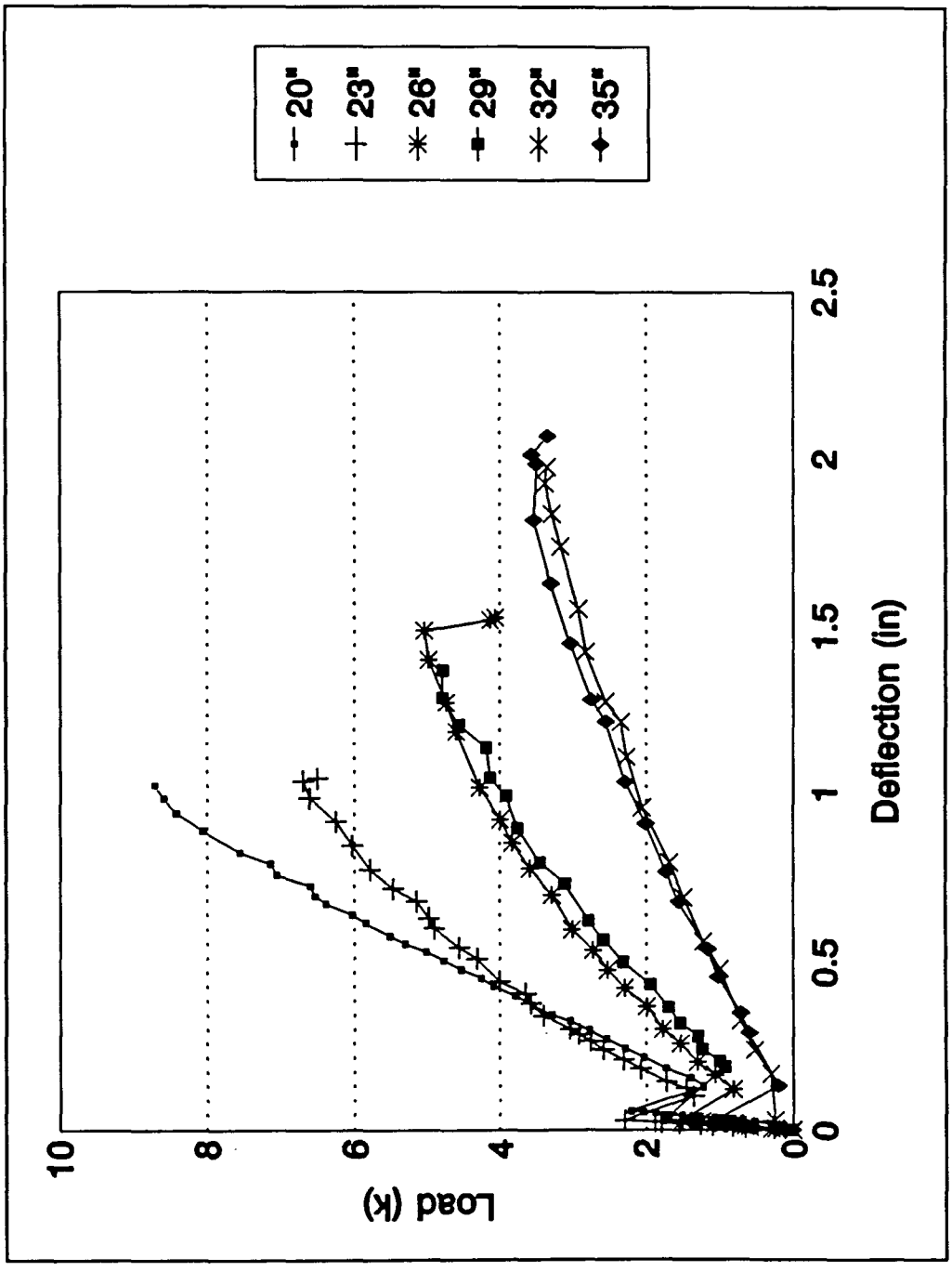


Figure 6.16. Load-deflection curves, ISU Beams, three-eighths-inch FCR, 5830-psi concrete strength, 20-35 inch embedment

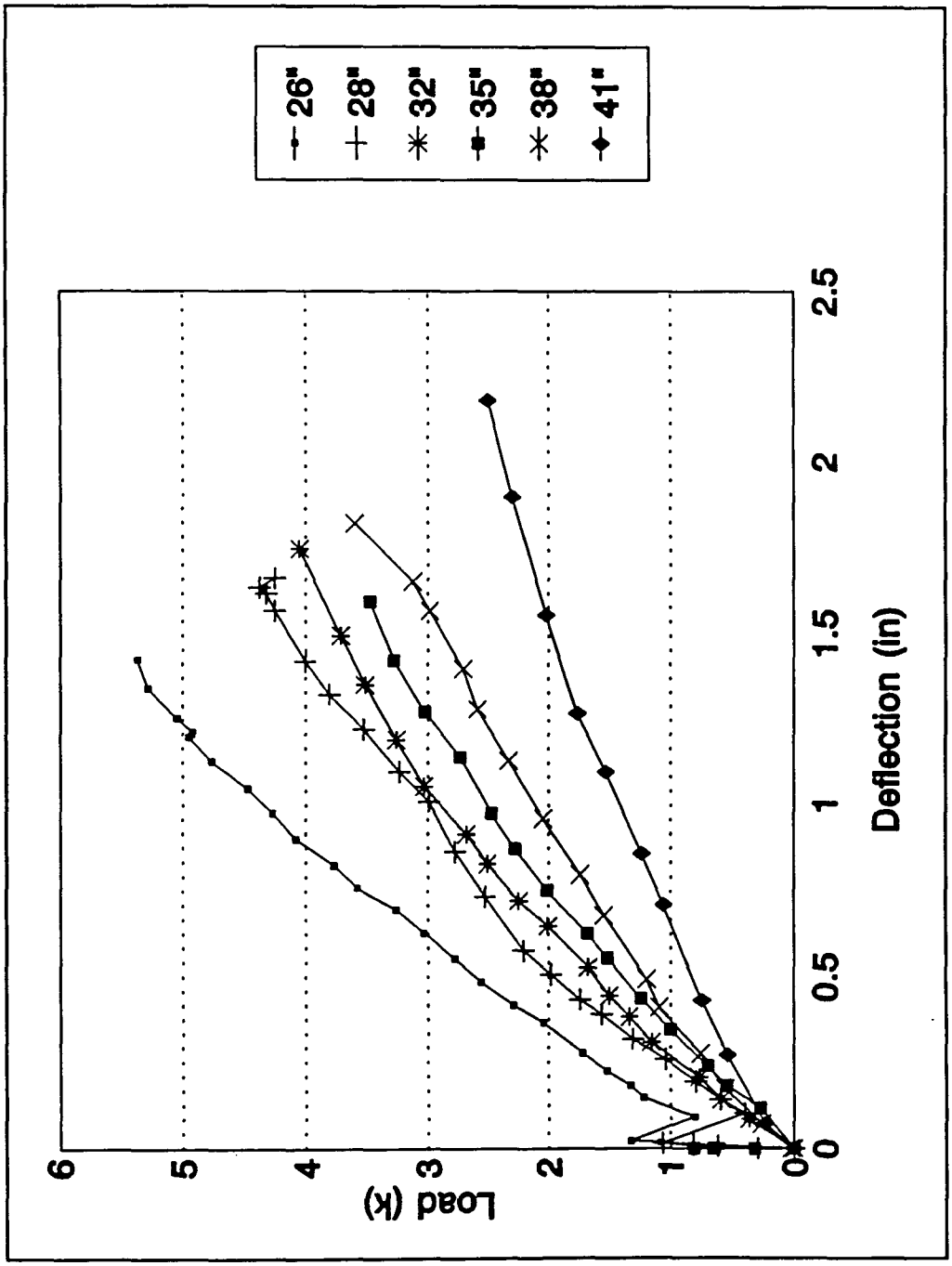


Figure 6.17. Load-deflection curves, ISU Beams, three-eighths-inch FCR, 3749-psi concrete strength, 26-41 inch embedment

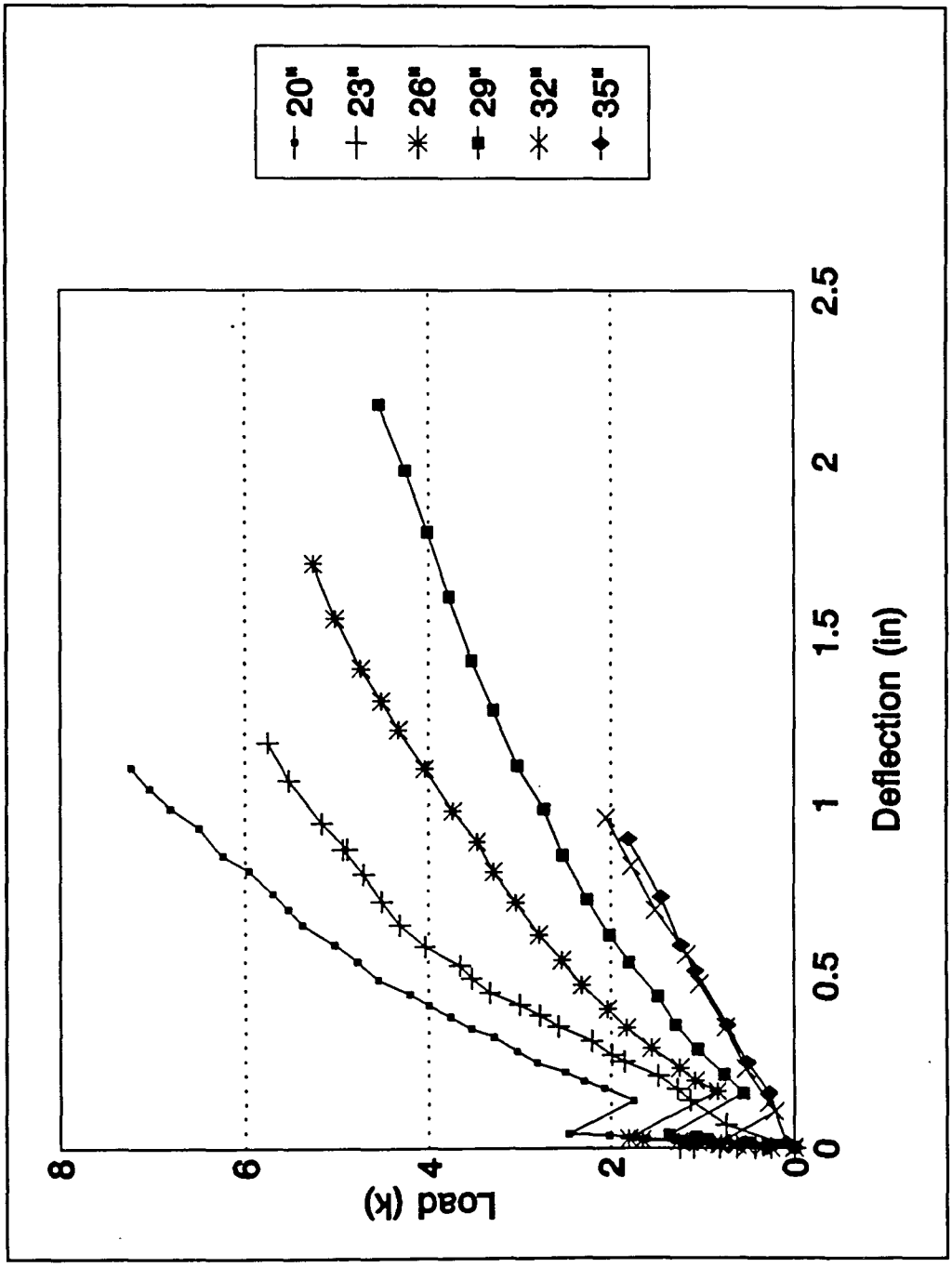


Figure 6.18. Load-deflection curves, ISU Beams, three-eighths-inch FCR, 4783-psi concrete strength, 20-35 inch embedment

### 6.3.6 Results of the ISU Beam Tests: One-Half-Inch FCR

Seventy-four ISU beams were cast with one-half-inch FCR. Of the seventy-four beams, thirty of the beams were cast with slip wires. Some of the slip wiring data proved to be useful. The addition of the slip wires, the epoxy used to attach the slip wires, and the tubing used to bring the wire out of the concrete, caused the end slip and deflection data to be inconsistent with that of the beams cast without slip wires. For this reason, the beams with the slip wires will be presented in a separate section.

#### 6.3.6.1 Beams Cast Without Slip Wires

Forty-four beams were cast using one-half-inch FCR with no slip wires. Embedment lengths varied from twenty inches to forty-one inches. Concrete strengths varied from 3500 to 7000 psi.

As was shown with three-eighths-inch FCR, the load declined when the concrete cracked. A discussion of this phenomena can be found in Section 6.3.4. A presentation of the results from these tests is shown in Figures 6.19 to 6.25. Deflections were measured at the free end of the cantilever section.

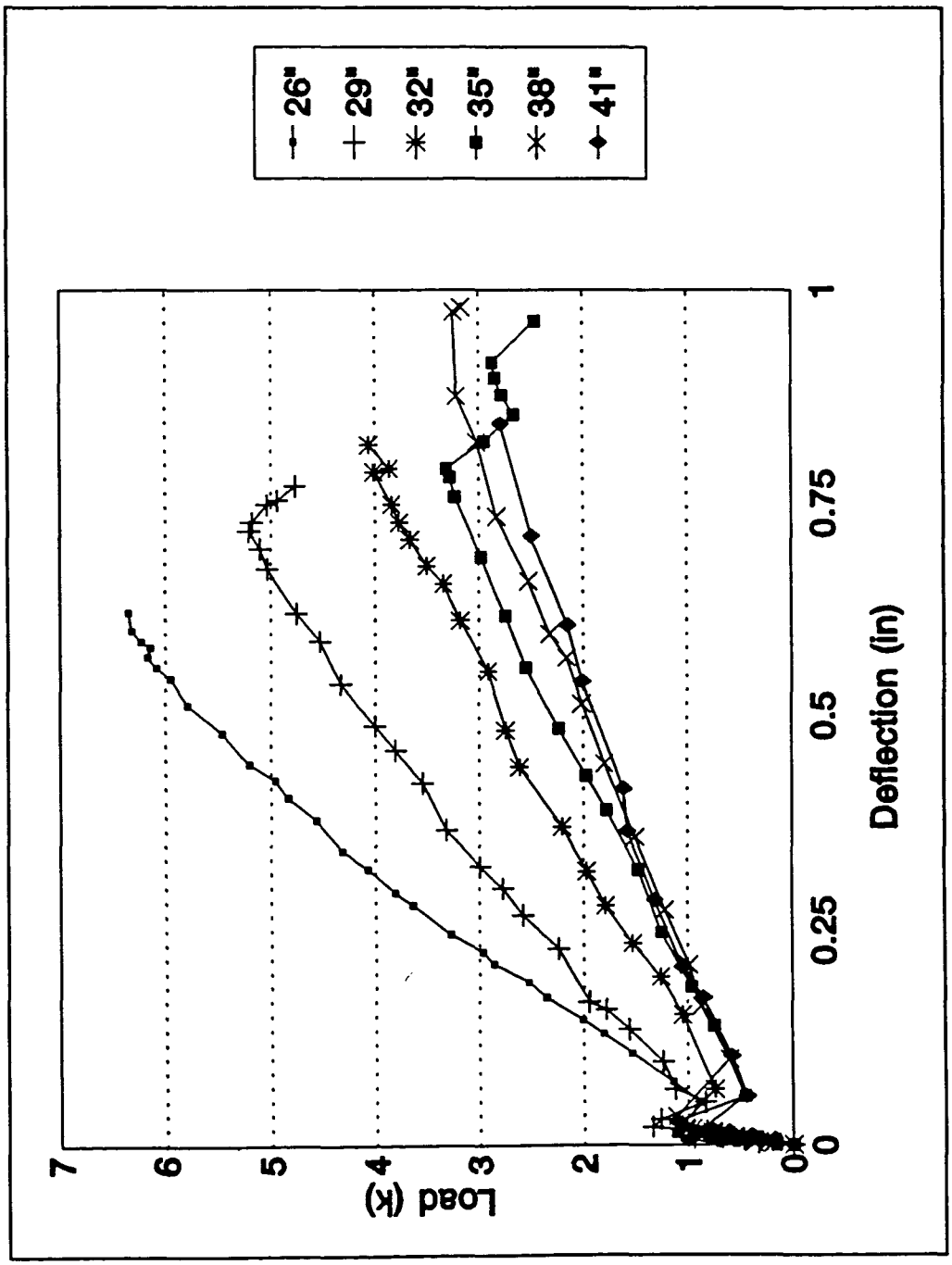


Figure 6.19. Load-deflection curves, ISU Beams, one-half-inch FCR, 6802-psi concrete strength, 26-41 inch embedment

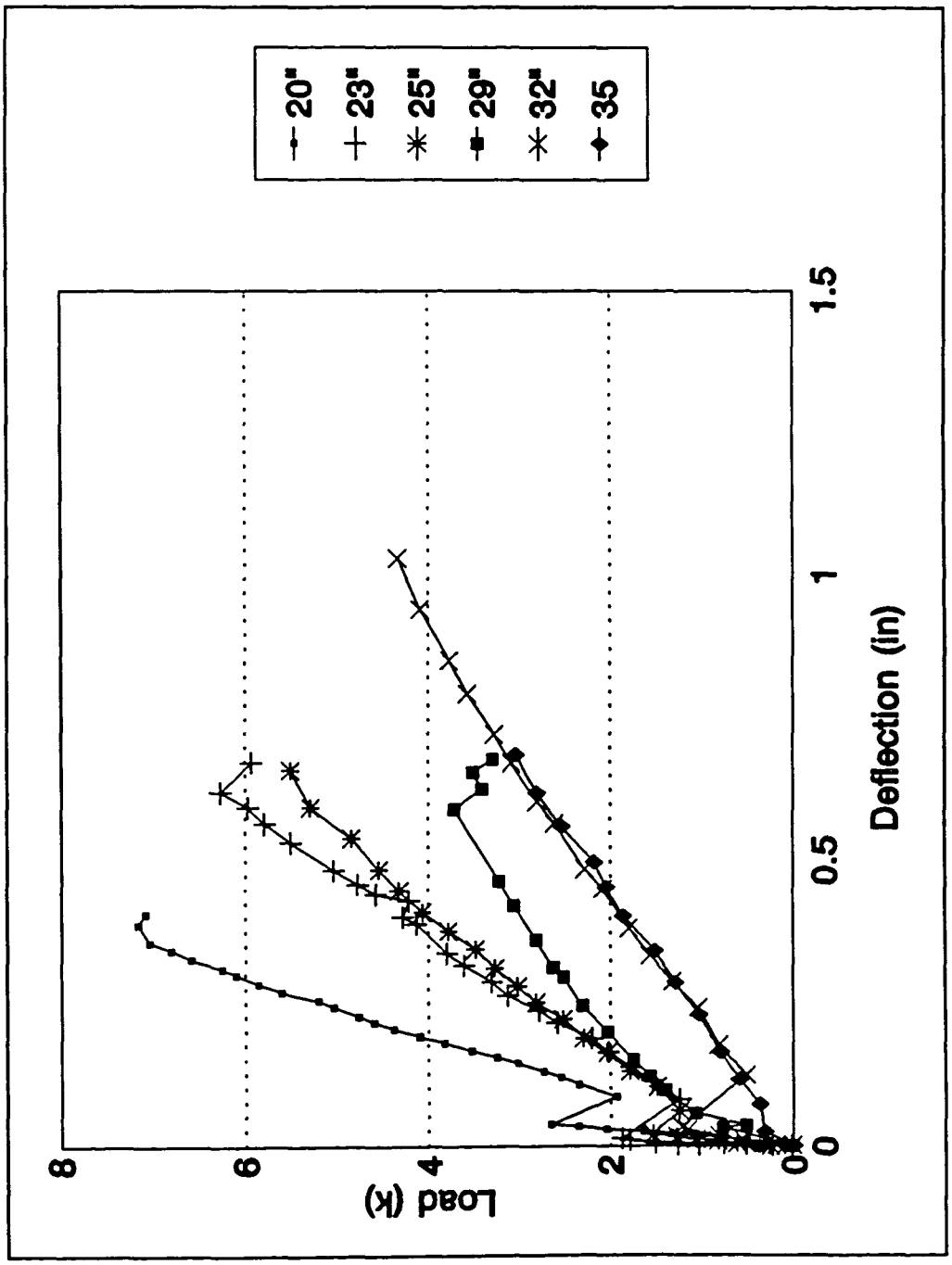


Figure 6.20. Load-deflection curves, ISU Beams, one-half-inch FCR, 6369-psi concrete strength, 20-35 inch embedment

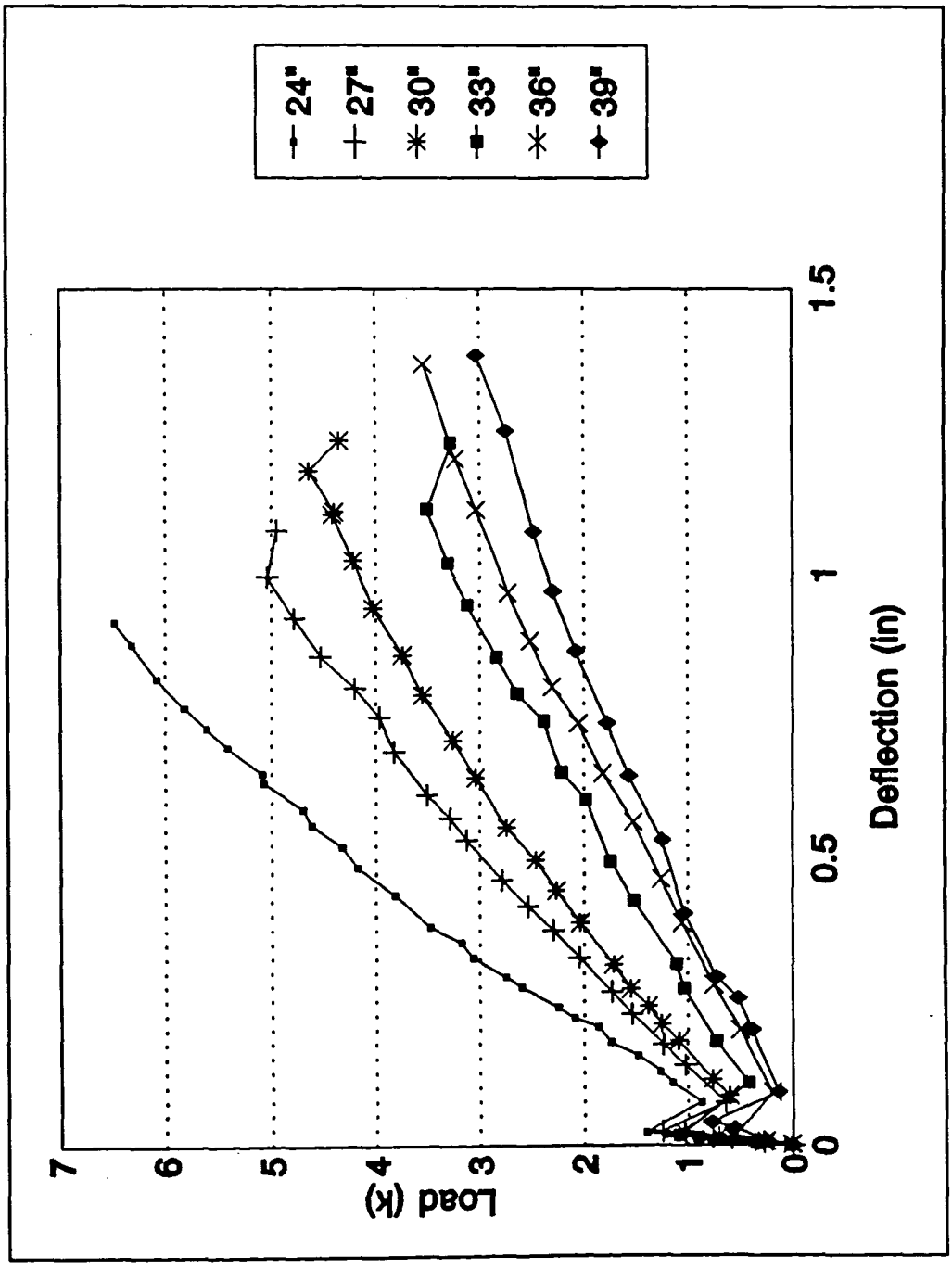


Figure 6.21. Load-deflection curves, ISU Beams, one-half-inch FCR, 4030-psi concrete strength, 24-39 inch embedment

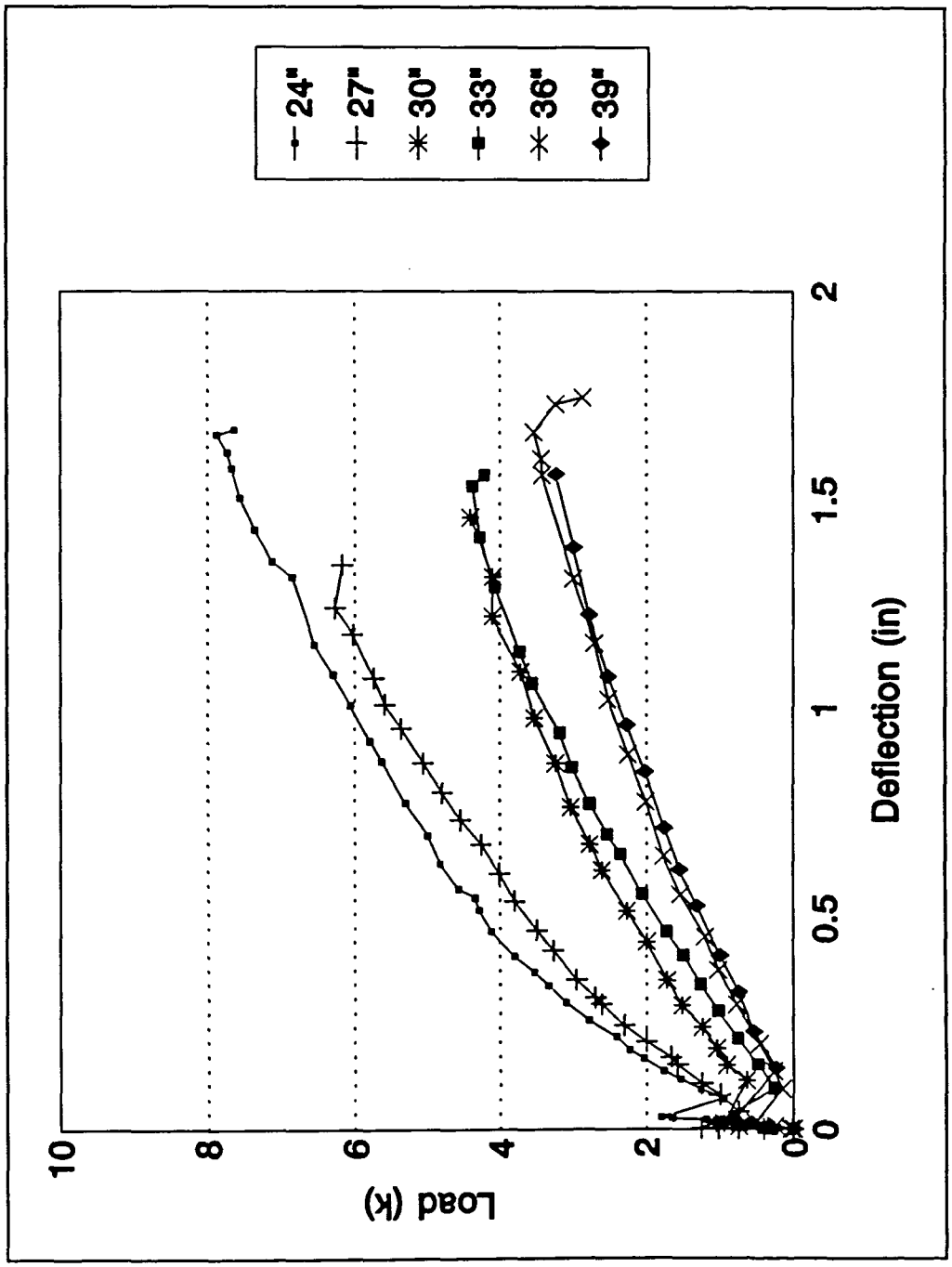


Figure 6.22. Load-deflection curves, ISU Beams, one-half-inch FCR, 4572-psi concrete strength, 24-39 inch embedment

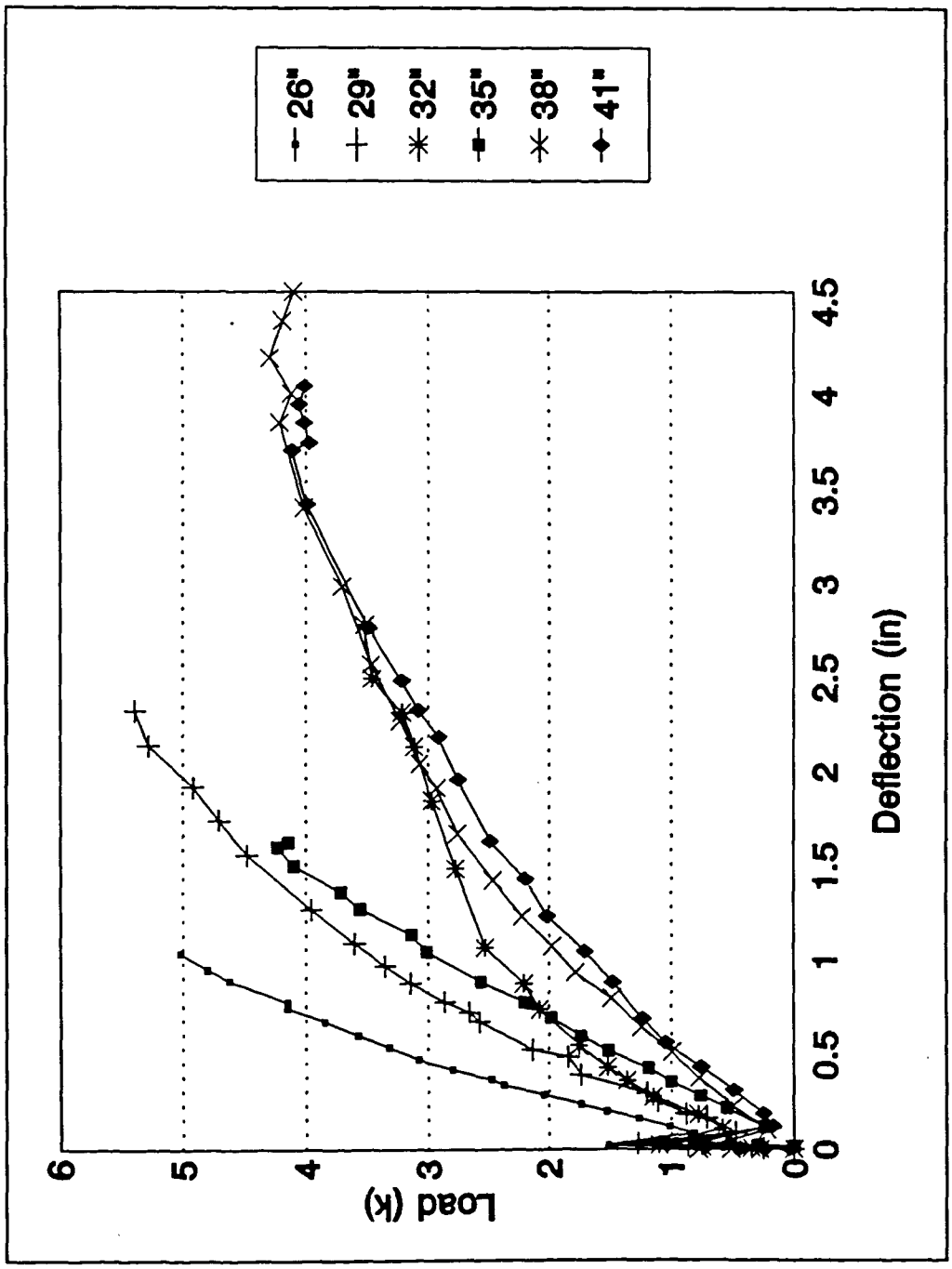


Figure 6.23. Load-deflection curves, ISU Beams, one-half-inch FCR, 4694-psi concrete strength, 26-41 inch embedment

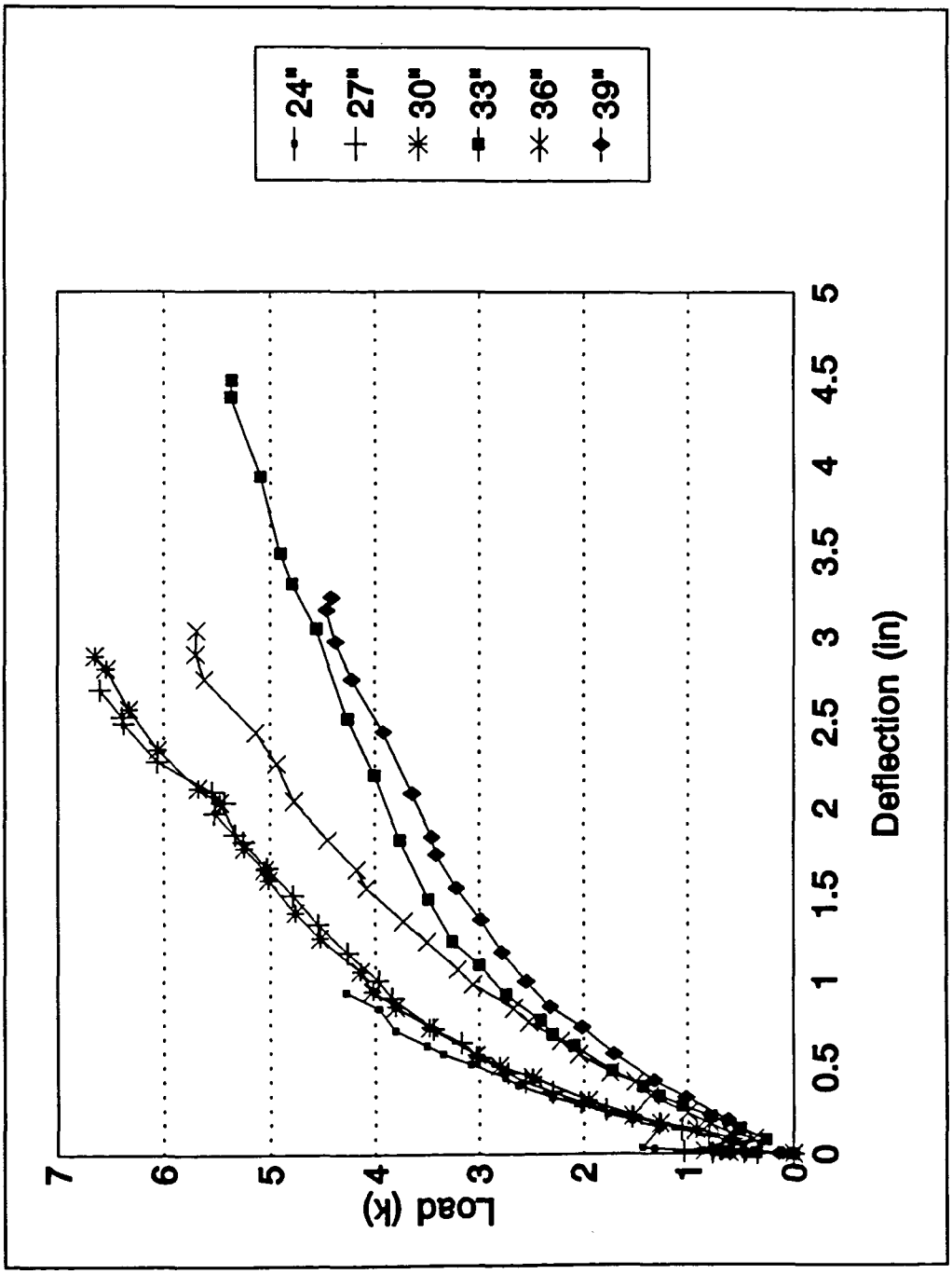


Figure 6.24. Load-deflection curves, ISU Beams, one-half-inch FCR, 4324-psi concrete strength, 24-39 inch embedment

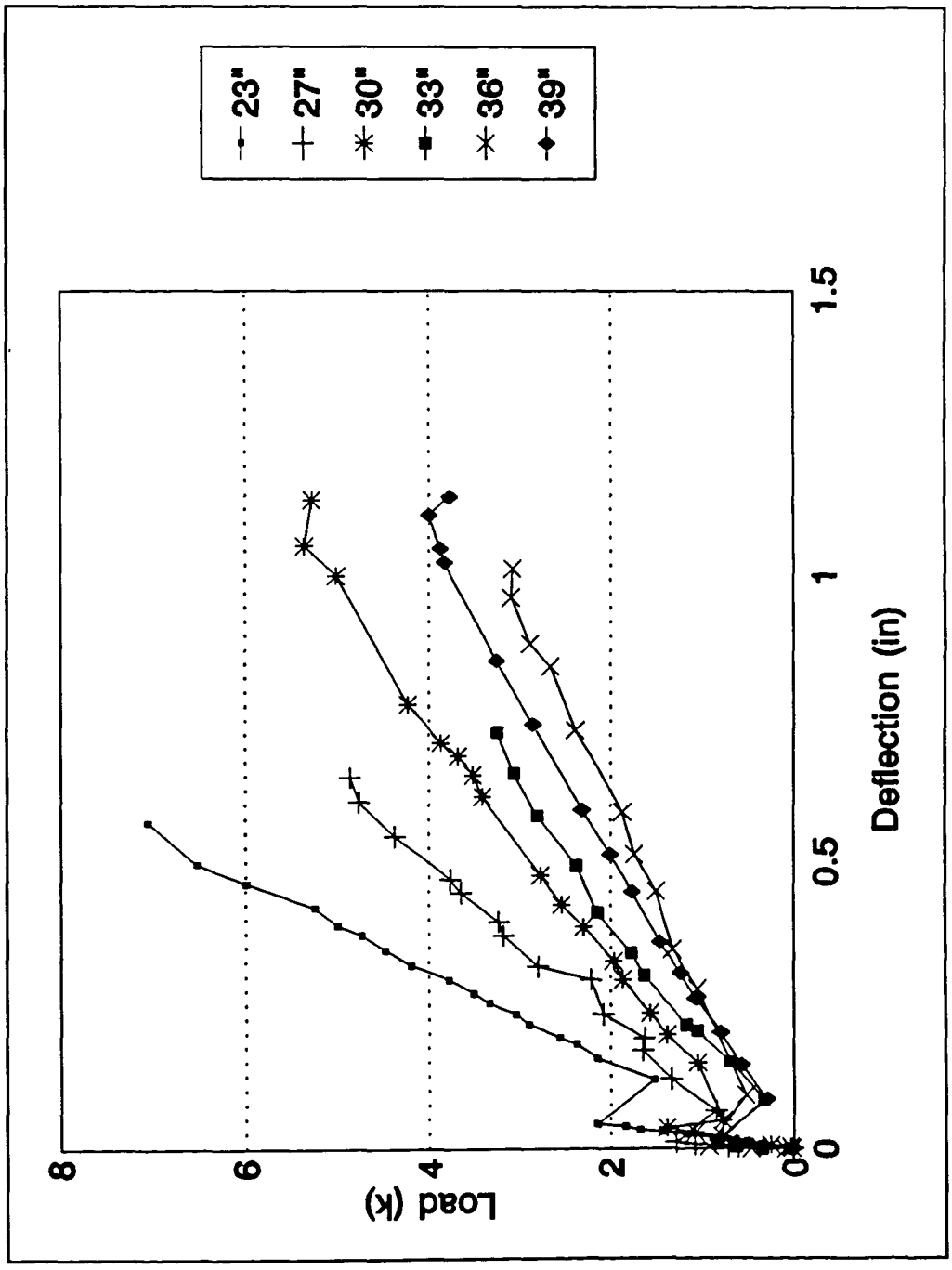


Figure 6.25. Load-deflection curves, ISU Beams, one-half-inch FCR, 5556-psi concrete strength, 23-39 inch embedment

#### 6.3.6.2 Beams Cast With Slip Wires

Thirty of the beams cast with one-half-inch FCR were also cast with slip wires. Embedment lengths ranged from twenty to thirty-eight inches. Concrete strengths varied from 3500 to 6500 psi.

End slips of beams cast with slip wires were larger than end slips of beams cast without slip wires. The attachment of the slip wires to the fiber-rod created a void where the concrete could not contact the FCR. This void reduced the surface area for frictional and mechanical anchorage thus increasing the embedment length required to develop the rod. A diagram of the slip wiring apparatus can be found in Figure 4.2.

The end slip data collected for slip wired beams varied considerably. One set of test beams exhibited 0.045 inches of end slip at ultimate load for a twenty-eight-inch embedment length and 0.267 inches of end slip for a beam with a thirty-eight-inch embedment length. Every beam cast with slip wires exhibited some end slip, even at a forty-eight-inch embedment length. Because of the inconsistent data and the increased development length, the use of slip wires was terminated. A presentation of the test results is shown in Figures 6.26 to 6.28. Deflections were measured at the free end of the cantilever section.

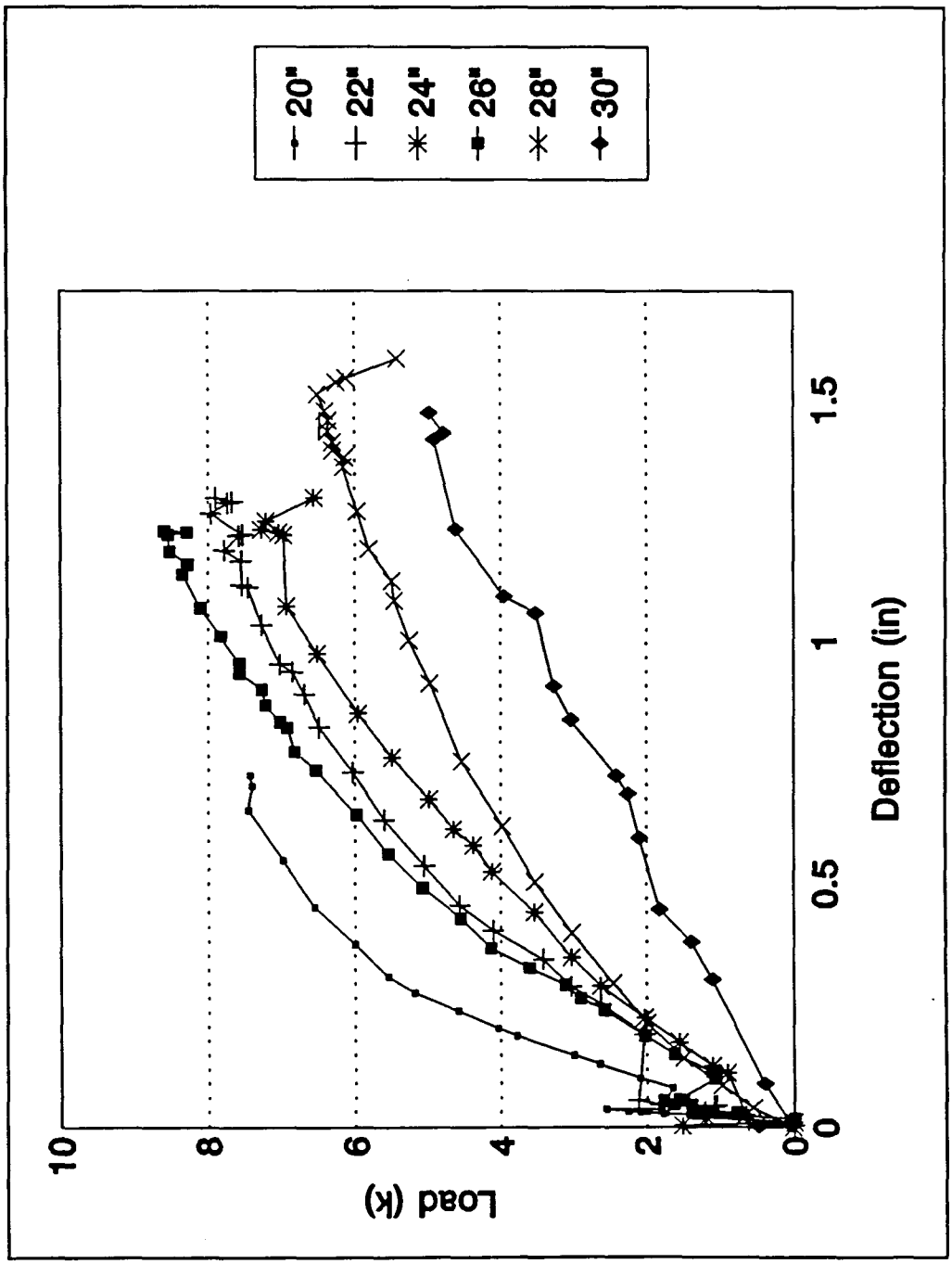


Figure 6.26. Load-deflection curves, ISU Beams, one-half-inch FCR, slip wired, 4690-psi concrete strength, 20-30 inch embedment

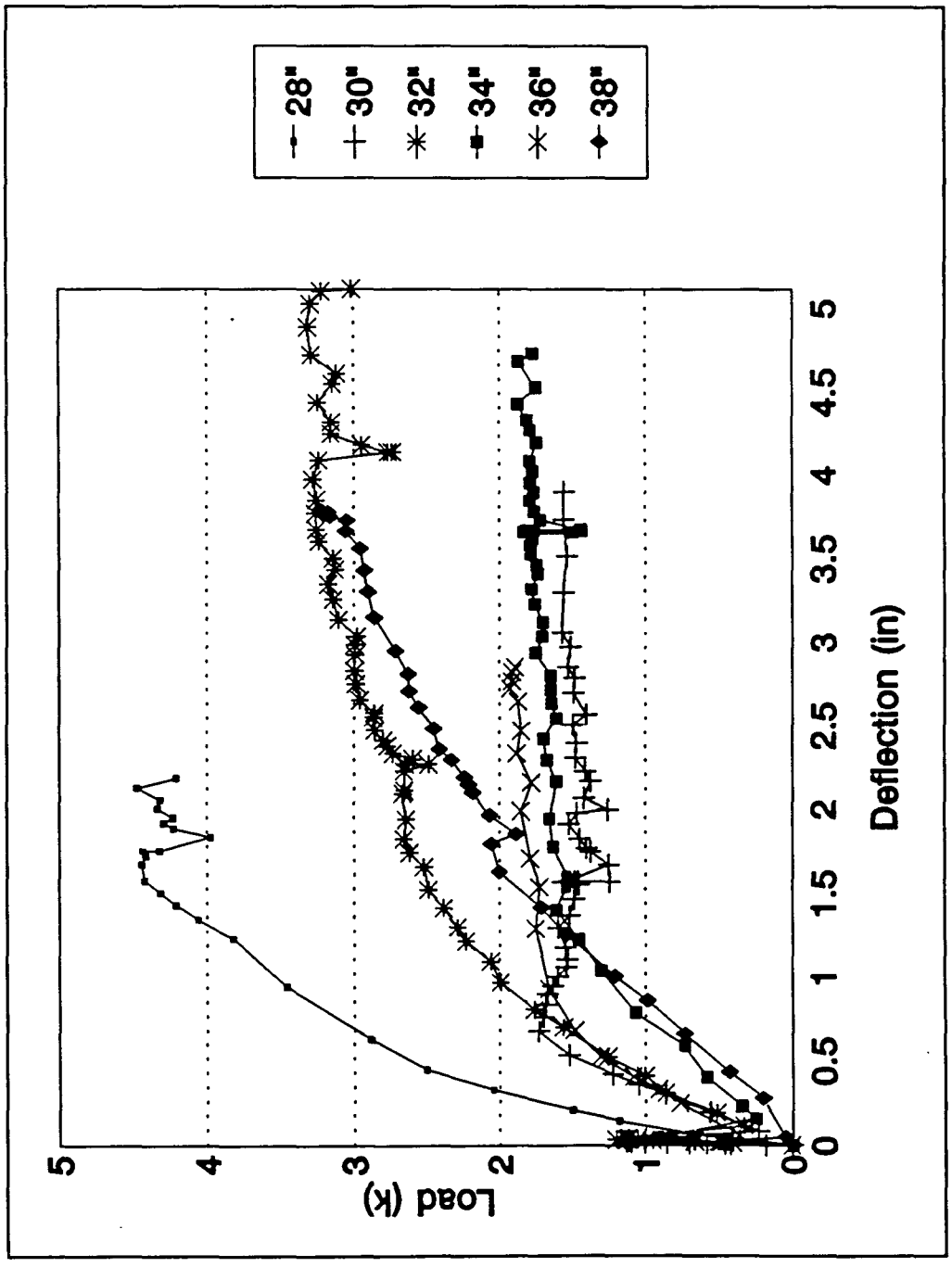


Figure 6.27. Load-deflection curves, ISU Beams, one-half-inch FCR, slip wired, 3591-psi concrete strength, 28-38 inch embedment

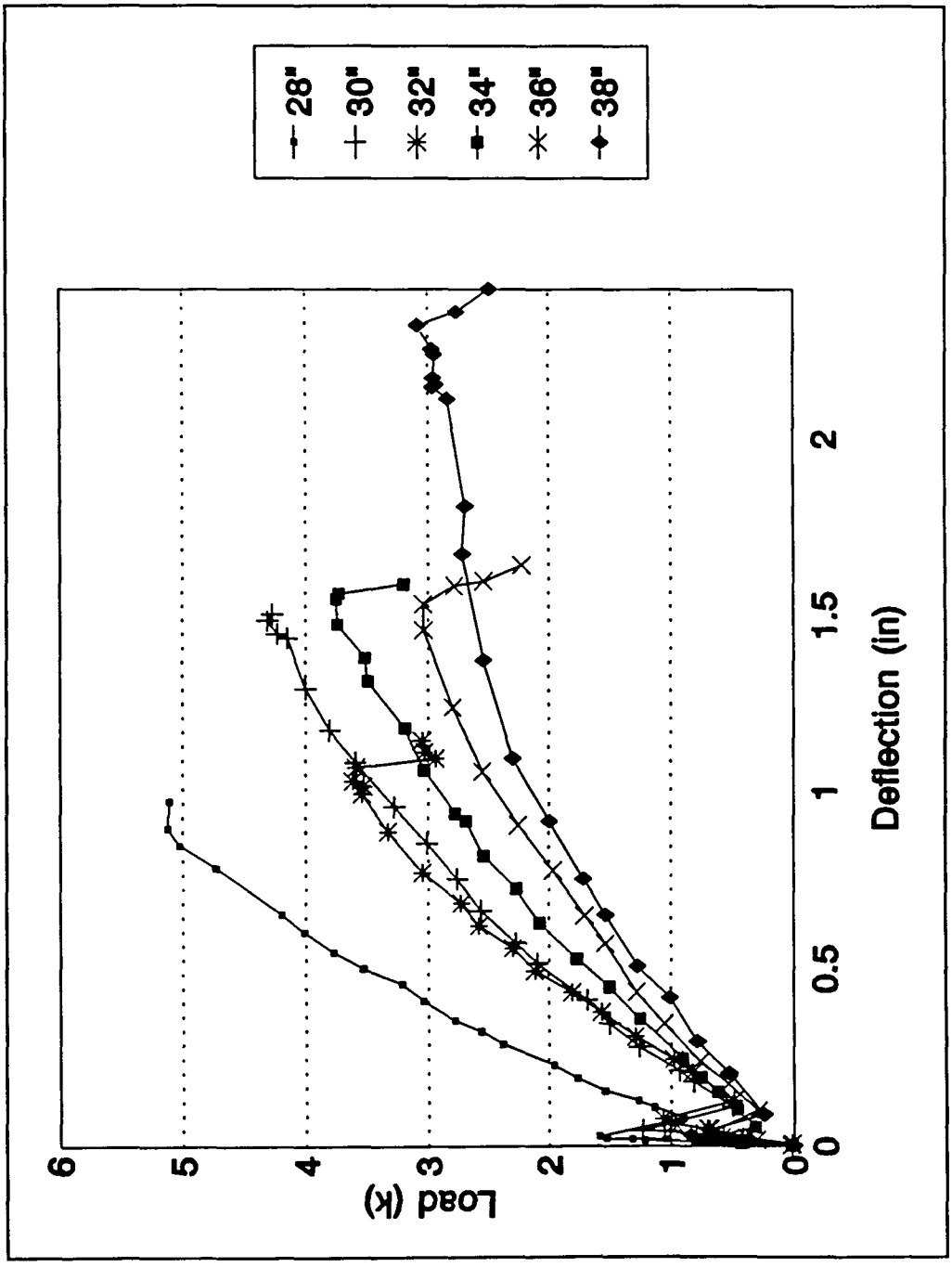


Figure 6.28. Load-deflection curves, ISU Beams, one-half-inch FCR, slip wired, 3646-psi concrete strength, 28-38 inch embedment

# 7 SUMMARY AND CONCLUSIONS

## 7.1 Summary

FCR has many applications in reinforced concrete construction, especially for areas where corrosion of steel is a problem. Applications where corrosion is of particular concern are structures in a salt water environment, highway and bridge structures, exterior buildings and other structures exposed to the environment or to corrosive surroundings.

There are many places where steel cannot be used. Steel reinforcement can generate a magnetic field which can cause problems with computers and other electronic equipment. For this reason an alternative source of reinforcement is needed. FCR can be used in these cases and also in areas of extremely high corrosion and structures where deflection is of a lessor concern.

FCR would make a good reinforcing material for use in footings and other underground reinforced concrete structures. FCR would also have applications in pavement slabs and bridge abutments.

Because of the fact that there were only small spiral undulations on the rod, splitting of the concrete will not be as great of a concern as with deformed steel reinforcement. Reduced splitting means that the bars could be placed closer

together without adverse effects. However, a determination of how close the bars can be placed together needs to be researched further before a minimum bar spacing can be specified. As in all reinforced concrete design, care should be taken by the designer not to over-reinforce the structure.

The advantages and disadvantages of FCR, when compared with steel reinforcement, are listed below:

Advantages:

- High tensile strength
- High corrosion resistance
- Lightweight, therefore easily shipped and handled
- Creates fewer concrete splitting problems
- FCR does not generate magnetic fields

Disadvantages:

- Low modulus of elasticity
- Long development length
- Brittle tensile failure
- Low compressive strength
- Low dowel shear strength

Because FCR is a very flexible material it could also, possibly have applications in flexible pavement.

## 7.2 Conclusions

Deflections of beams reinforced with FCR are larger than with beams reinforced with steel for similar bar areas. Part of this behavior was due to the lower modulus of elasticity of the FCR when compared with steel. The lower modulus leads to a lower stiffness of the FCR reinforced concrete when compared with steel reinforced concrete. Research is being conducted on high modulus, high tensile strength fibers which could be used in making fiber-composite reinforcing bars. The higher modulus would decrease deflections, but until better mechanical anchorage can be achieved, a higher tensile strength will probably not improve the bar significantly.

Bond stress distribution for FCR was similar to that for deformed bars, however the peak bond stress was considerably lower and the length required to resist a similar tensile force in the rods was longer for beams reinforced with FCR. Also, crack widths were larger for beams reinforced with FCR than they were for beams reinforced with steel reinforcement.

The plot of stress versus strain for FCR increases linearly, similar to steel in the elastic range, but instead of reaching a plateau, the plot continues to rise linearly until fracture of the rod occurs. This fact indicates that the FCR will exhibit a brittle fracture.

The ISU beam test procedure proved to be a valuable tool for determining bond stress and development length data. The offset loading points did not confine the reinforcement and, unlike pullout specimens, the ISU beam allowed the development length to be determined in a region of shear and moment.

This investigation indicated that conventional reinforced concrete analysis techniques could be utilized for FCR-reinforced beams.

Development length analysis was based on two different criteria; namely, zero end slip and one-tenth-inch end slip. The conclusions and results from the analysis for development length and material properties are summarized in Section 9.0.

FCR has many uses in the reinforced concrete industry as well as other industries. It is a lightweight, high tensile strength, highly durable material which is a viable substitute for steel reinforcement in many places.

# 8 RECOMMENDATIONS

Possible techniques for improving the mechanical bond anchorage capabilities of the rod would be to put a sand coating on the rods similar to that used in the epoxy coated prestressing strand industry. Wrapping an additional strand opposite the original strands could also improve the mechanical bond anchorage. Also, undulations of various types would serve to improve mechanical bonding. FCR, in its present design, is a useful product but it could be improved upon with the changes listed above.

More tests should be performed on beams with shorter embedment lengths than the twenty inch minimum that was used for this project. This testing could possibly prove that the development length could be reduced even more than with the one-tenth-inch end slip criteria. Testing for development length in high-strength concrete should also be performed.

An investigation of a new flexural design standard should be performed. Analysis techniques are needed to provide a criterion for a maximum strain limit state including the effects of slip and strain compatibility. Also, the strain compatibility and the equilibrium of forces should consider the maximum strain and the associated stress development on the compression zone of the concrete.

The ISU beam proved to be a valuable tool for determining bond strength and development length values. The test could, however, be improved by casting the beams upside down so that the reinforcement that is being tested is cast as bottom reinforcement. Also, the ISU beam test should be developed into a standard.

Additional work should be done to perfect the slip wiring techniques. The slip wires could help to determine the bond stress distribution of fiber composite materials without damaging the integrity of the rod.

Care should be taken not to design for the ultimate strength of the FCR because when the FCR reaches the ultimate load it will fracture instead of yield such as steel does.

# 9 SUMMARY OF ENGINEERING PROPERTIES

A summary of the engineering properties is provided in Table 9.1. No factors of safety have been used and note that the material fails catastrophically at the ultimate loads. Also note that FCR was cast as top reinforcement for the development length tests. Therefore, a smaller development length could possibly be used for FCR cast as bottom bars but further research needs to be performed to determine how much smaller.

Table 9.1. Summary of Engineering Properties

| | 3/8" FCR | 1/2" FCR |
|---|---|---|
| **Area** ($A_b$) | 0.12 $in^2$ | 0.14 $in^2$ |
| **Circumference** ($C_b$) | 1.45 in | 1.57 in |
| **Young's Modulus** (E) | $3.43 \times 10^6$ psi | $4.91 \times 10^6$ psi |
| **Ultimate Stress** ($f_u$) | | |
| Flexural | 68 ksi | 75 ksi |
| Theoretical | 81 ksi | 139 ksi |
| Direct Tension | 81 ksi | 120 ksi |
| **Development Length** (ld) | | |
| Zero End Slip | $l_d = \frac{0.59 f_u A_b}{C_b^2 \sqrt{f_c'}}$ | $l_d = \frac{0.59 f_u A_b}{C_b^2 \sqrt{f_c'}}$ |
| $1/10^{th}$ Inch End Slip | $l_d = \frac{0.42 f_u A_b}{C_b^2 \sqrt{f_c'}}$ | $l_d = \frac{0.42 f_u A_b}{C_b^2 \sqrt{f_c'}}$ |

# 10 APPENDIX

| Number Cast | Rod Size (in) | Concrete Strength (psi) | Slip Wires (Y/N) | Embedment Length (in) |
|---|---|---|---|---|
| 2 | 3/8 | 6316 | Y | 18 |
| 5 | 3/8 and #3 | 6516 | Y | 24-32 |
| 6 | 1/2 | 6462 | Y | 24-32 |
| 6 | 1/2 | 4686 | Y | 20-30 |
| 6 | 1/2 | 3591 | Y | 28-38 |
| 6 | 1/2 | 3646 | Y | 28-38 |
| 6 | 1/2 | 3574 | Y | 38-48 |
| 6 | 1/2 | 6802 | N | 26-41 |
| 6 | 1/2 and #3 | 4301 | N | Simply Supported |
| 6 | 3/8 | 2707 | N | 20-35 |
| 6 | 3/8 | 5425 | N | 20-35 |
| 6 | 1/2 and Prestress | 4654 | N | 25-31 |
| 6 | 3/8 | 6497 | N | 20-30 |
| 6 | 3/8 | 5830 | N | 20-35 |
| 6 | 1/2 | 6369 | N | 20-35 |
| 6 | 1/2 | 4030 | N | 24-39 |
| 6 | 3/8 | 3749 | N | 26-41 |
| 6 | 3/8 | 4783 | N | 20-35 |
| 6 | 3/8 and Prestress | 3902 | N | 24-39 |
| 6 | 1/2 | 4572 | N | 24-39 |
| 6 | 1/2 | 4694 | N | 24-39 |
| 6 | 1/2 | 4324 | N | 24-39 |

**BIBLIOGRAPHY**

1. Wang, Chu-Kia, and Salmon, Charles G., Reinforced Concrete Design. Fourth Edition. New York: Harper and Row, Publishers, 1985. 198-250.

2. American Concrete Institute. Building Code Requirements of Reinforced Concrete (ACI 318-89). American Concrete Institute, Detroit, 1989.

3. P. M. Ferguson. "Bond Stress-The State of the Art." Journal of the American Concrete Institute Proceedings 63, No. 11 (November 1966): 1161-1190.

4. R. C. Mathey and D. Watstein. "Investigation of Bond Strength in Beam and Pull-Out Specimens with High-Yield-Strength Deformed Bars." Journal of the American Concrete Institute Proceedings 57, No. 9 (March 1961): 1071-1090.

5. ACI Committee 408. "A Guide for Determination of Bond Strength in Beam Specimens." Journal of the American Concrete Institute Proceedings 61, No. 2 (February 1964): 129-136.

6. P. M. Ferguson and J. N. Thompson. "Development Length of High Strength Reinforcing Bars in Bond." Journal of the American Concrete Institute Proceedings 59, No. 7 (July 1962): 887-922.

7. L. A. Lutz and P. Gergely. "Mechanics of Bond and Slip of Deformed Bars in Concrete." Journal of the American Concrete Institute Proceedings 64, (November 1967): 711-721.

8. ACI Committee 408. "Opportunities in Bond Research." Journal of the American Concrete Institute Proceedings 67, (November 1970): 857-869.

9. T. D. Mylrea. "Bond and Anchorage." Journal of the American Concrete Institute Proceedings 44, (March 1948): 521-552.

10. E. S. Perry and J. N. Thompson. "Bond Stress Distribution on Reinforcing Steel in Beams and Pullout Specimens." Journal of the American Concrete Institute Proceedings 63, (August 1966): 865-875.

11. J. O. Jirsa, L. A. Lutz, and P. Gergely. "Rationale for Suggested Development, Splice, and Standard Hook

Provisions for Deformed Bars in Tension." Concrete International 1, (July 1979): 47-61.

12. R. E. Untrauer and R. L. Henry. "Influence of Normal Pressure on Bond Strength." Journal of the American Concrete Institute Proceedings 62, (May 1965): 577-586.

13. K. R. Peattie and J. A. Pope. "Effects of Age of Concrete on Bond Resistance." Journal of the American Concrete Institute Proceedings 52, No. 6 (February 1956): 661-672.

14. N. W. Hanson and P. H. Kaar. "Flexural Bond Tests of Pretensioned Prestressed Beams." Journal of the American Concrete Institute Proceedings 55, (January 1955): 783-802.

15. J. R. Janney. "Nature of Bond in Pre-Tensioned Prestressed Concrete" Journal of the American Concrete Institute Proceedings 50, (May 1954): 717-736.

16. J. R. Salmons and T. E. McCrate. "Bond Characteristics of Untensioned Prestressing Strands." PCI Journal 22, (September/October 1977): 54-65.

17. J. P. Moehle, J. W. Wallace, and S. J. Hwang. "Anchorage Lengths for Straight Bars in Tension." American Concrete Institute Structural Journal 88, No. 5 (September/October 1991): 531-537.

18. A. E. Naaman, G. G. Namur, J. M. Alwan, and H. S. Najm. "Fiber Pullout and Bond Slip. I: Analytical Study." Journal of Structural Engineering 117, No. 9 (September 1991): 2769-2789.

19. R. M. Mains. "Measurement of the Distribution of Tensile and Bond Stresses Along Reinforcing Bars." Journal of the American Concrete Institute Proceedings 48, No. 2 (November 1951) 225-252.

20. G. E. Warren. Anchorage Strength of Tensile Steel in Reinforced Concrete Beams. Ph.D. Dissertation. Iowa State University, Ames, Iowa, 1969.

21. B. A. Barnes. Bond and Low Cycle Fatigue Behavior of Thermoset Composite Reinforcing for the Concrete Industry. M.S. Thesis. Iowa State University, Ames, Iowa, 1990.

22. American Society for Testing and Materials. Annual Book of ASTM Standards. American Society for Testing and Materials. Volume 4.02. ASTM: Philadelphia, PA, 1984.

23. B. A. Barnes. Oral conversation with Bruce A. Barnes of Iowa State University, Ames, Iowa, November 15, 1991.

24. M. L. Porter and B. A. Barnes. "Tensile Testing of Glass Fiber Composite Rod." Advanced Composites Materials in Civil Engineering Structures New York, NY, (February 1, 1991): 123-131.

25. G. T. Wade, M. L. Porter, and D. R. Jacobs. Glass-Fiber Composite Connectors for Insulated Concrete Sandwich Walls. Civil and Construction Engineering Department Report. Engineering Research Institute, Iowa State University, Ames, Iowa, March 1988.

26. R. Long. Oral conversation with Robert Long of Composite Technologies Incorporated, Ames, Iowa, December 2, 1991.

27. G. L. Krupicka. The Behavior and Analysis of Steel-Deck-Reinforced Concrete Slabs With End-Span Studs. M. S. Thesis. Iowa State University, Ames, Iowa, 1979.

28. G. M. Smith and L. E. Young. "Ultimate Flexural Analysis Based on Stress-Strain Curves of Cylinders." Journal of the American Concrete Institute Proceedings 53, (December 1956), 597-609.